CENTRAL RESEARCH LIBRARY
DOCUMENT COLLECTION

OAK RIDGE NATIONAL LABORATORY
operated by
UNION CARBIDE CORPORATION
NUCLEAR DIVISION
for the
U.S. ATOMIC ENERGY COMMISSION

MARTIN MARIETTA ENERGY SYSTEMS LIBRARIES
3 4456 0059938 7

ORNL-TM-1465

3

WASTE TREATMENT AND DISPOSAL SEMIANNUAL PROGRESS REPORT

JULY-DECEMBER 1965

OAK RIDGE NATIONAL LABORATORY
CENTRAL RESEARCH LIBRARY
DOCUMENT COLLECTION
LIBRARY LOAN COPY
DO NOT TRANSFER TO ANOTHER PERSON
If you wish someone else to see this document, send in name with document and the library will arrange a loan.
UCN-7969
(3 3-67)

NOTICE This document contains information of a preliminary nature and was prepared primarily for internal use at the Oak Ridge National Laboratory. It is subject to revision or correction and therefore does not represent a final report.

LEGAL NOTICE

This report was prepared as an account of Government sponsored work. Neither the United States, nor the Commission, nor any person acting on behalf of the Commission:

A. Makes any warranty or representation, expressed or implied, with respect to the accuracy, completeness, or usefulness of the information contained in this report, or that the use of any information, apparatus, method, or process disclosed in this report may not infringe privately owned rights; or

B. Assumes any liabilities with respect to the use of, or for damages resulting from the use of any information, apparatus, method, or process disclosed in this report.

As used in the above, "person acting on behalf of the Commission" includes any employee or contractor of the Commission, or employee of such contractor, to the extent that such employee or contractor of the Commission, or employee of such contractor prepares, disseminates, or provides access to, any information pursuant to his employment or contract with the Commission, or his employment with such contractor.

ORNL-TM-1465

CHEMICAL TECHNOLOGY DIVISION

HEALTH PHYSICS DIVISION

WASTE TREATMENT AND DISPOSAL SEMIANNUAL PROGRESS REPORT

JULY-DECEMBER 1965

R. E. Blanco F. L. Parker

JUNE 1966

MARTIN MARIETTA ENERGY SYSTEMS LIBRARIES

3 4456 0059938 7

OAK RIDGE NATIONAL LABORATORY
Oak Ridge, Tennessee
operated by
UNION CARBIDE CORPORATION
for the
U. S. ATOMIC ENERGY COMMISSION

ABSTRACT

Solidification of High-Level Wastes: Engineering Development.--Four rising-level potglass tests were made in this report period, two (R-89, -90) with FTW-65 Purex (with sulfate) waste and two with PW 1 Purex waste (R-91, -92). Particular emphasis was placed determining the best method of adding the glass-making additives and evaluating the pot-corrosion problem. Test R-89, in an 8-in.-diam pot at 900°C, showed an excessively high corrosion rate on the pot; but a duplicate test, R-90, at 850°C, was completely successful, with negligible corrosion. A similar test in a 8-in.-diam pot at Pacific Northwest Laboratory also showed negligible corrosion. Test R-91, in an 8-in.-diam pot at 900°C, was also successful, with low corrosion. A similar test in a 12-in. diam pot showed excessive corrosion, up to 239 mils. The proportional feeding of a solution of glass-making additives (LiOH, NaOH, and H_3PO_4) to the waste feed-line is recommended as preferable to mixing directly with the waste in the feed tank.

Solidification of High-Level Wastes: Laboratory Development.--The ORNL work on waste solidification by the pot-calcination and rising-level glass processes was summarized in the ORNL section of the Operating Manual for the Waste Solidification Engineering Prototype (WSEP). Phosphate melts were developed for fixation of Purex-1 and Purex-2 waste types in glassy solids. Fixation in these melts was successfully demonstrated in semiengineering-scale experiments with solutions containing elements simulating the fission products resulting from a burnup of 20,000 Mwd/metric ton of uranium. The solid products obtained had volumes that varied from 11.1 to 17.5 gal per metric ton of uranium processed for Purex-1 waste. The best Purex-2 melt produced 14.3 gal of solid per metric ton. Low-melting-point lead silicate compositions developed for fixation of Purex-1 waste gave solid volumes as low as 9 gal of solid per metric ton of uranium.

Scoping experiments indicated the feasibility of fixing solid alumina wastes from fluidized-bed fuel processing in either phosphate or lead borate glasses at temperatures $\lesssim$900°C.

Incorporation of Intermediate-Level Waste in Asphalt.--Considerable interest has been shown throughout the world in the use of asphalt as a medium in which waste having an intermediate level of radioactivity can be incorporated. In the process being developed at ORNL, evaporator wastes are introduced into an emulsified asphalt, which contains about 35% water, and the water volatilized by heating to about 160°C to yield a product containing up to 60 wt % salts from waste.

Products containing 60 wt % salts from simulated waste reach a steady-state leach rate for ^{137}Cs or sodium of 3×10^{-4} g cm^{-2} day^{-1}. Hot-cell tests with concentrated actual ORNL intermediate-level waste, containing 5 curies of aged mixed fission products per gallon, confirmed these nonradioactive and tracer tests. After 5 months of leaching, a product incorporating 60 wt % salts from actual waste approached a steady-state leach rate of 2×10^{-4} g cm^{-2} day^{-1}. No radiolytic gas was released from the asphalt product over this period (an internal radiation dose of about 1.2×10^{7} rads).

Initial results with small samples, 1 or 2 g, indicate that the flash point of unirradiated asphalt, approximately 280°C, is not lowered significantly--about 50°C--when the mixture contains 35 wt % nitrate and a total of 60% salts. Further tests are continuing to determine the effect of sample size and radiation dose level.

Water-Recycle Process.--A large inventory of decontaminated and demineralized water is being accumulated from the treatment of low-radioactivity-level waste (LLW) in order to demonstrate the recycle portion of the water-recycle process. During this period, the effects of several variations in the process flowsheet are being studied. In one run, where the nitrate concentration in LLW was 20 times that normally present, low pH (4.9) resulted in poor alum flocculation, and, consequently, there was a 35-fold decrease in the overall decontamination factor (DF) for ^{60}Co. In a second run, another activated-carbon column was added to the system and located between the cation and anion exchangers. This activated carbon altered the chemistry of the ^{60}Co in the cation exchange effluent and resulted in a greater than 100-fold

decrease in the overall DF for ^{60}Co. These runs show that the pH of the raw waste must be in the range of 7 to 8 before treating it in a system that includes activated-carbon treatment after anion exchange.

Engineering, Economic, and Safety Evaluations.--The costs of "perpetual" tank storage of both acid and alkaline wastes were estimated as a function of tank size, tank life, and fission product concentration in the waste for three representative types of financing. For acid wastes, the optimum tank capacity is about a million gallons, and minimum total costs range from 0.0165 to 0.0272 mill/kwhr. For alkaline wastes, the optimum tank capacity is 2.5 million gallons, and minimum total costs range from 0.0177 to 0.0294 mill/kwhr. Reducing the volume of wastes, as stored, by doubling the concentration of fission products reduces the total costs between 15 and 30%.

The total costs for storing cladding wastes ranged from 0.0215 to 0.0398 mill/kwhr. These costs were greater than those for raffinate wastes because of the greater volumes of cladding wastes.

In a study of the safety of tank storage, consideration of the nature and extent of tank failure indicates that the most likely mechanism of release would be through loss of cooling, and that the atmosphere would constitute the major exposure pathway. Two incidents leading to major releases were postulated, and total radiation exposures to neighboring populations at various distances downwind were estimated based on dosage to the lungs resulting from inhalation, subsequent exposure to the fallout from the passing cloud, and exposure to direct radiation from the passing cloud. Exposure due to direct radiation from the passing cloud was found to be only a few percent of that from the other two sources and may be considered to be of negligible importance.

Disposal by Hydrofracturing.--The seventh experimental injection was made in the slot used for the sixth injection. The clumpiness of the solid blend used in the sixth injection was traced to the fly-ash source. The injection proceeded smoothly in spite of several changes in mix ratios demanded by differences in the waste composition. The slurry was too low

in solids, resulting in phase separation of the grout. The injection required 6-1/2 hr to complete and dispose of 78,000 gal of liquid waste.

A theoretical analysis of the uplift due to the injections of the waste-cement matrix has been developed, based on the analysis extraction mining theory.

Disposal in Natural Salt Formations.--All experimental equipment (except for the floor array) for Project Salt Vault was installed and checked out. A number of waste-handling operations were performed with dummy canisters to verify the procedures. Two canisters were loaded with 500 curies each of ^{60}Co each and transferred to Lyons, Kansas, in the shipping carrier. The canisters were lowered into the mine and removed a number of times to obtain experience in handling radioactive canisters and to test the effectiveness of the shielding.

Fourteen fuel assemblies from ETR cycle 73 were selected. The assemblies were sawed to length, loaded into the seven canisters, the canisters welded shut, leak tested, loaded into the carrier, and shipped to Lyons. On November 17-19, the seven cans, containing about one million curies of fission products, were placed in the mine. The maximum radiation dosage received by those involved in the transfers was about 200 millirads. Radiation levels immediately above the array holes are generally less than 10 mr/hr, and unlimited access is allowable everywhere except immediately over the holes.

The rise in salt temperature and the temperatures of the fuel elements are in reasonable agreement with theoretical calculations, although generally running somewhat below the predictions. Thermal expansion of the floor had reached about 1/2 in. in the center of the arrays at the end of the second week. Thermal stresses (but not yet temperature rises) have also been transmitted to the supporting pillars, as indicated by the increased flow rates of the salt in the pillars and in the roof. There have been no indications of any differences in behavior between the radioactive and control arrays, and no indications of chlorine release.

Soil Studies.--Measurement of losses of ^{137}Cs from field plots has been extended to cover 1 year of operation. Comparisons of losses among the three different cover plots are made, and the factors affecting ^{137}Cs loss are discussed.

Unusual desorption of radiocesium from three soils of Southeastern United States was reported in the Health Physics Division Annual Progress Report for 1965. It was shown that 1 M sodium acetate released radiocesium from these soils but that with increasing length of solution:soil contact time, the amount released decreased. The tests were extended to evaluate different desorbing salts and to include reference clay minerals for comparisons.

Behavior of Radionuclides in the Ground.--A computer program was written to describe the transient behavior of radionuclides in the ground when the transporting solution is of a different concentration than the original ground water. Experimental data, obtained on a Berea sandstone for different sets of conditions, confirm the model. The program is based on Glueckauf's model for the passage of a wide band of solute through a chromatographic column, modified for changes in the adsorptive capacity due to changes in the total electrolyte concentration.

Disposal of Gases into Permeable Formations.--In a nuclear incident involving fuel-element meltdown, ^{131}I appears to present the most serious short-term hazard. If the radioactive gases could be pumped underground, the delay time afforded by absorption and physical movement through the soil would allow a reduction in the relative hazard by a few orders of magnitude. Strontium-90 would present the most serious potential for contaminating ground water near the site of discharge.

Laboratory studies have been conducted on the sorption of iodine by clays. The activation energy for the desorption of iodine increases from 14.2 kcal/mole at a loading of 10^{-10} mole of I_2 per square centimeter to 54 kcal/mole at a loading of 10^{-11} mole per square centimeter for Clinch River floodplain sediment. Iodine has a heat of sublimation of 14.66 kcal/mole.

Safety Evaluation.--An age-dependent metabolic model developed by Kulp was used to estimate dose to the skeleton of males from ingestion of Clinch River water. This model yields a slightly larger estimate of dose than the adjusted ICRP model.

CONTENTS

Page

Abstract iii

1. Introduction 1

2. Solidification of High-Level Wastes 3

2.1 Engineering Development 3

2.1.1 FTW-65 Purex Waste 3

2.1.2 PW 1 Purex Waste 5

2.1.3 Conclusions 12

2.2 Laboratory Development 15

2.2.1 Preparation of Operating Manual for WSEP 15

2.2.2 Melt Development Studies 15

2.2.3 Semiengineering-Scale Fixation Tests 15

2.2.4 Ruthenium Volatility Studies 18

2.2.5 Corrosion with Phosphate Melts 20

2.2.6 Conclusions 22

2.2.7 Fixation of Fluidized-Bed Waste in Glass 23

3. Low- and Intermediate-Level Waste Treatment 23

3.1 Incorporation of Intermediate Level Waste in Asphalt . . . 23

3.2 Water-Recycle Process 26

4. Engineering, Economics, and Safety Evaluations 31

4.1 The Cost of Perpetual Tank Storage 31

4.1.1 Raffinate Wastes 31

4.1.2 Cladding Wastes 32

4.2 A Safety Analysis of Tank Storage 35

5. Disposal by Hydrofracturing 42

5.1 Objectives 42

5.2 Plant Modification and Preparation 42

CONTENTS (cont'd)

Page

5.2.1 Plant Modifications 42
5.2.2 Solids Blending 43

5.3 Injection 44

5.4 Analysis of Data 45

5.5 Mechanical Effects of Hydrofracturing on Nearby Rocks . . 48

6. Disposal in Natural Salt Formations 51

6.1 Preparation for Project Salt Vault 51
6.1.1 Prototype Test 51
6.1.2 Safety Analysis 51
6.1.3 Equipment Installation 52
6.1.4 Preoperational Tests 52

6.2 Startup of Project Salt Vault 54
6.2.1 ETR Fuel Assemblies 54
6.2.2 Startup 55
6.2.3 Preliminary Results 57

6.3 Pillar-Model Studies 59
6.3.1 Effects of Shale Partings 59
6.3.2 Deformational Behavior 63

7. Soil Studies 65

7.1 Desorption of Cesium-137 from Clays and Soils 65

7.2 Movement of Cesium-137 by Runoff, Erosion, and Infiltration 70

8. Behavior of Radionuclides in the Ground 73

8.1 Nonequilibrium Ion Exchange 73

8.2 Hydroxide Consumption by Conasauga Shale 76

CONTENTS (cont'd)

Page

9. Disposal of Gases into Permeable Formations 76

9.1 Estimation of the Behavior of Radionuclides Discharged to the Ground in a Gas 76

9.2 Adsorption of Iodine by Minerals 82

9.3 Nuclear Safety Pilot Plant Runs 86

10. Safety Evaluation 87

10.1 Clinch River Safety Studies 87

11. References 90

1. INTRODUCTION

This report is the fifteenth of a series* of reports on progress in the ORNL development program, the objective of which is to develop and demonstrate on a pilot plant scale integrated processes for treatment and ultimate disposal of radioactive wastes resulting from reactor operations and reactor fuel processing in the forthcoming nuclear power industry. The wastes include those of high, intermediate, and low levels of radioactivity in liquid, solid, or gaseous states.

Under the integrated plan, low-activity wastes, consisting of very dilute salt solution, such as cooling water and canal water, would be treated by scavenging and ion exchange processes or foam separation to remove radioactive constituents, and the water would be discharged to the environment. The retained waste solids or slurries would be combined with the high-activity wastes or incorporated into asphalt or concrete before disposal in concrete vaults, salt mines, or burial pits. Alternatively, the retained solids or the untreated waste could be discharged to the environment in deep geologic formations. The high-activity wastes could be stored at their sites of origin for economic periods to allow for radioactive decay and artificial cooling.

Methods investigated for the permanent disposal of high-activity liquid wastes include conversion to solids by high-temperature "pot" calcination or glass formation in the final storage container (pot) and formation of a glass or ceramic in a continuous melter. High-activity solid wastes from nonaqueous fuel processing method, such as the fluid bed-fluoride volatility process, could be packaged directly as solids or incorporated in a glassy matrix. The solids from either process would be stored in a permanently dry place such as a salt mine. This is undoubtedly the safest method because control of radioactivity can be ensured within present technology during treatment, shipping, and storage.

---

*ORNL-CF-61-7-3, ORNL-TM-15, ORNL-TM-49, ORNL-TM-133, ORNL-TM-169, ORNL-TM-252, ORNL-TM-376, ORNL-TM-396, ORNL-TM-482, ORNL-TM-516, ORNL-TM-603, ORNL-TM-757, ORNL-TM-830, and ORNL-TM-1081; see also annual reports for 1962-1965, ORNL-3452, ORNL-3492, ORNL-3672, ORNL-3697, ORNL-3830, and ORNL-3849, from the Chemical Technology and Health Physics Divisions.

Tank storage or high-temperature calcination of intermediate-activity wastes may be unattractive because of their large volumes, and other disposal methods will be studied. One method, for example, the addition of solidifying agents prior to direct disposal into impermeable shale by hydrofracturing, has been investigated. Particular attention was given to the engineering design and construction of an experimental fracturing plant to dispose of ORNL intermediate—activity wastes by this method. A second method is incorporation (and dehydration) of intermediate-level wastes in asphalt.

Environmental research on the Clinch River, motivated by the need for safe and realistic permissible limits of waste releases, is included in this program. The objective is to obtain a detailed characterization of fission product distribution, transport, and accumulation in the physical, chemical, and biological segments of the environment.

2. SOLIDIFICATION OF HIGH-LEVEL WASTES

The development programs were principally concerned with making the final tests in the development of the rising-level (RL) potglass process, using two new prototype waste compositions, PW 1 and PW 2. These compositions, to be used as new standard wastes for the development program in the U.S., were proposed early in 1965 at a meeting in Washington. These wastes differ considerably from the previous standard waste, FTW-65, because of the high iron content of PW 1 and the increase in the fission product concentration of both wastes to that equivalent to a burnup of 20,000 Mwd/metric ton. This necessitated additional melt-development studies and small-scale rising-level tests in the laboratory to develop a melt with a suitably low melting point and low corrosivity. Additional large-scale tests were also required to define pumping, heat transfer, corrosion, and other engineering variables in 8- and 12-in.-diam pots.

Previous work on high-level wastes has been confined to processing aqueous wastes. A new program was started to develop suitable treatment methods for the solids (alumina, etc.) from the Fluidized-Bed Fluoride-Volatility process. An engineering economic survey is being made to define the parameters for this work, and a topical report will be issued when the survey is completed. It will also be summarized in the 1966 annual report for the Chemical Technology Division (ORNL-3945).

2.1 Engineering Development

J. C. Suddath C. W. Hancher

2.1.1 FTW-65 Purex Waste

A final test (test 90) of the RL potglass process with FTW-65 Purex waste was made in an 8-in.-diam x 96-in.-high pot (Tables 1,2,3). The operating temperature was limited to 850°C since laboratory studies had indicated that the viscosity and corrosivity of the melt were satisfactorily low at this temperature. Also, a previous test at 900°C (test 89) in an 8-in.-diam pot had shown that the corrosion rate was excessive (Table 3). Test R-90 proceeded smoothly, and the corrosion was negligible--

Table 1. Composition of FTW-65-X3 Waste, Tests R-89, R-90
Expressed in moles/liter

Constituent	Type of Waste: FTW-65-X3[a]
H^+	1.5
Na^+	0.9
Al^{3+}	0.15
Fe^{3+}	0.30
Cr^{3+}	0.06
Ni^{2+}	0.03
Hg^{2+}	0.0105
SO_4^{2-}	0.45
PO_4^{3-}	0.015
SiO_3^{2-}	0.03
F^-	0.0015
NO_3^-	~3.1
Fission Products	0.5

[a]The FTW-65-X3 represents the highest concentration of this waste type that can be conveniently simulated by direct makeup from laboratory reagents without heating the solution.

Table 2. Composition of FTW-65-X3 Purex Glass, Tests R-89, R-90
Concentration of additives expressed as g-moles per liter of waste.

Additives	
H_3PO_4	3.6
LiOH	2.4
NaOH	2.7
$Al(NO_3)_3$	0.75
Wt % waste oxides (theoretical)	
10,000 Mwd/metric ton FP's[a]	30
Approximate mp, °C	
10,000 Mwd/metric ton FP's	800

[a]Hanford-BNL simulated-fission-product composition.

Table 3. Corrosion Results in Rising-Level Potglass Engineering-Scale Test

Diameter of pot, 8-in.

Run	Waste Type	Equiv. Fission Product Level (Mwd per metric ton)	Additive[a] per of Liter Waste	Operation Temp. (°C)	Operation Time (hr)	Additive Addition Method	Maximum Corrosion Depth (mils)
R-89	FTW-65-3X	10,000	Type 1	900	45[b]	Pre-mix	320
R-90	FTW-65-3X	10,000	Type 1	850	97	Pre-mix	15[c]
R-91	PW-1	20,000	Type 2	900	67	Pre-mix	<5[d]
R-92[e]	PW-1	20,000	Type 2	900	100	Feed line	239

[a]Type 1: 2.7 moles NaOH, 2.4 moles LiOH, 0.75 mole $Al(NO_3)_3$, and 3.6 moles H_3PO_4.
Type 2: 1.27 moles NaOH, 1.37 moles LiOH, 2.4 moles H_3PO_4, and 0.1 moles NaH_2PO_2.

[b]Failure occurred.

[c]Pot cooled and solids remelted and held at 700 to 800°C for 30 additional hours.

[d]Crushing and remelting caused failure of 28-mil-wall tubing.

[e]Pot diameter, 12-in.

a total of 15 mils. The original wall thickness of the pot was 320 mils. The same melt was also successfully tested at Pacific Northwest Laboratory in a 8-in.-diam pot. In this test, a dense solid product was formed, and there was no evidence of any corrosion.

2.1.2 PW 1 Purex Waste

Purex Waste 1 (PW 1) is a synthetic waste (Table 4) about 5 M in HNO_3 and 1 M in $Fe(NO_3)_3$; it contains simulated fission products equivalent to burnup of 20,000 Mwd/metric ton. Test R-91 was a rising-level potglass test made in an 8-in.-diam pot, using simulated PW 1 waste and lithium and sodium phosphates as glass-making additives (Tables 4 and 5). Phosphite was also added to provide a reductant to decrease corrosion (see Sect. 2.2.3). The waste, additives, and simulated fission products

Table 4. Composition of Purex Waste 1, Tests R-91, R-92

	Desired Molarity	Molarity Found by Analysis
Chemical Constituents		
H^+	5.0	4.9
Fe^{3+}	0.93	0.93
Na^+	0.14	0.16
H_3PO_4	0.003	0.004
NO_3^-	7.8	8.0
Ni^{2+}	0.005	NA[a]
Al^{3+}	0.001	NA
Cr^{3+}	0.012	NA
Fission Products		
Sr^{2+}	0.015	NA
Ba^{2+}	0.019	NA
Rare earths	0.118	NA
Zr^{4+}	0.065	NA
MoO_3	0.065	

[a]NA = no analysis.

Table 5. Composition of Glass-Making Additive Mixture, Tests R-91, R-92

Concentration Expressed as gram-moles of Additive per liter of Original Feed

Additive	Desired Makeup	Found by Analysis: Average of 3 Samples	Percentage Deviation of 3 Samples
NaOH	1.27	1.256	6.5
LiOH	1.37	1.09	11.3
H_3PO_4	2.40	2.105	9.2
NaH_2PO_2	0.10	NA[a]	NA[a]

[a]NA = no analysis.

were combined in the feed tank and fed to the pot as a single stream, as in all previous tests. A precipitate formed in the feed tank, making it difficult to control the flow rate of the resultant slurry to the pot. However, the test was completed, and a satisfactorily dense glassy product was formed. Corrosion was negligible; less than 5 mils (Table 3).

Test R-92 was a duplicate of R-91, with two exceptions: (1) a 12-in.-diam pot was used to determine the effect of pot diameter on processing rate, and (2) the glass-making additives and phosphite were added as a separate, proportionated stream to the waste feed line to the pot. Test R-92, which lasted for 100 hr, was carried out in a 12-in.-diam by 6-ft-high stainless-steel (304LC) pot. The pot was heated in an induction furnace having a 15-in.-diam susceptor.

The glass-forming additives (Table 5) were added to the pot as a separate liquid stream. In the 100-hr test, the total amount of liquid feed was 852 liters of waste and 294 liters of additive; the average feed rates were 8.5 liters/hr for waste and 3 liters/hr for additive. The condensate volume represented the sum of the waste feed, the additive feed, feed-line washings (to remove plugs), and condenser washings (to remove entrained solids). The contributions to the condensate were, in liters:

Feed	852
Additive	294
Washings	260
Total	1406 liters

The waste feed rate was controlled manually, starting at 15 to 20 liters/hr and then decreasing as the test progressed. After 68 hr of operation, the pot became filled with a mixture of glass at the bottom, solid above and on the walls, and a foam-liquid mixture in the center. After this condition was reached, the feed was stopped from time to time to prevent overfilling. The top thermocouples were used as level indicators. During the test, about 100 liters of feed overflowed from the pot to the condensing system as the result of inattention of the operators. The principal overflow occurred in the 44th and 45th hours and caused a general surging of liquid and foam from the pot. During this period,

the feed rate for the waste stream was 5 times that of the average and the ratio of additives flow to the waste flow as 0.1, not the desired ratio of 0.34 (Figs. 2.1 and 2.2).

The glass-making additives (Table 5) were fed through a line teed into the waste feed additive line. The flow rate of the additive was controlled by a volume-ratio feed controller, 0.34 volumes of additive per volume of waste feed.

Both the feed line and the additive line plugged occasionally, although these lines were equipped with water purges to prevent plugging. When either of the feed lines plugged, the plug was removed by applying high-pressure water. The liquid-level-probe line in the additive tank also plugged six or seven times during the test, resulting in a false indication of a high liquid-level in the additive tank. The controller then caused the outlet valve on the additive feed tank to open until the blockage of the dip tube was removed. This malfunction, coupled with the lack of manual control of the waste feed stream, caused the ratio of additive to waste stream to vary from 4.00 to 0 during the test (Fig. 2.2). About 26% too much additive solution was fed to the pot for the first 20 hr of operation. Not until the 44th hour did the additive-to-waste ratio in the pot reach the desired value of 0.34 (Fig. 2.3). This may have caused excessive corrosion in the bottom of the pot, since laboratory experience (Sect. 2.2.5) indicates that excessive phosphate additives of this type frequently lead to excessive corrosion.

Undoubtedly, these variations in flow rates can be controlled and prevented by suitable equipment modification. Otherwise, the feeding operation in test R-92 proceeded smoothly in the absence of significant amount of solid. Consequently, proportional addition of the additives is recommended for the rising-level Potglass process.

The material balance for test R-92 is shown in Table 3. The iron balance was high (151%), probable because of pot corrosion. If the iron from corrosion is included (calculated from corrosion penetration), the material balance for iron is 96%. The balance for phosphate was low (61%).

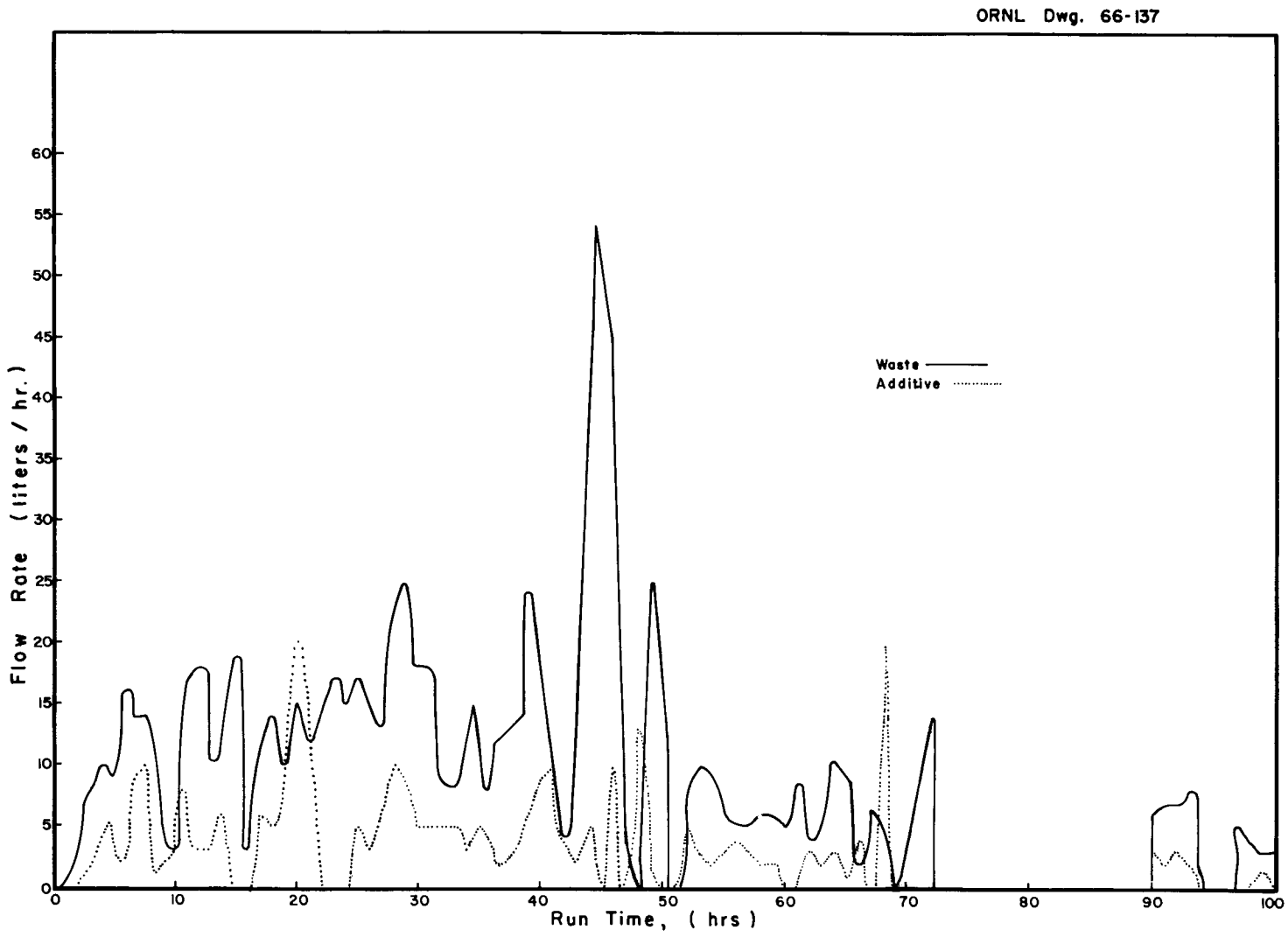

Fig. 2.1 Instantaneous Flow Rates of Additive and Waste Solutions for R-92.

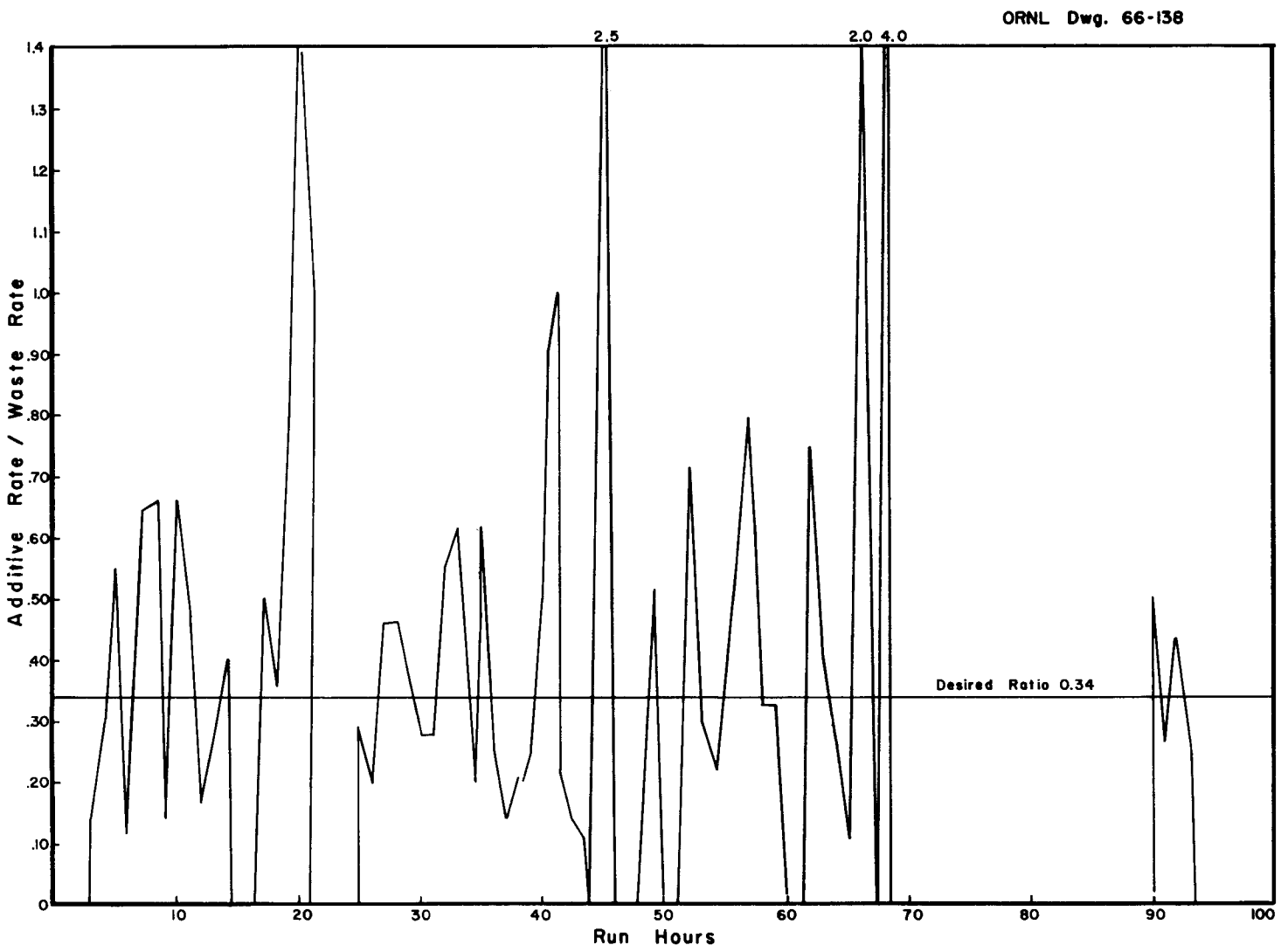

Fig. 2.2 Instantaneous Ratio of Flow Rates for Glass Additive and Waste Solution for R-92.

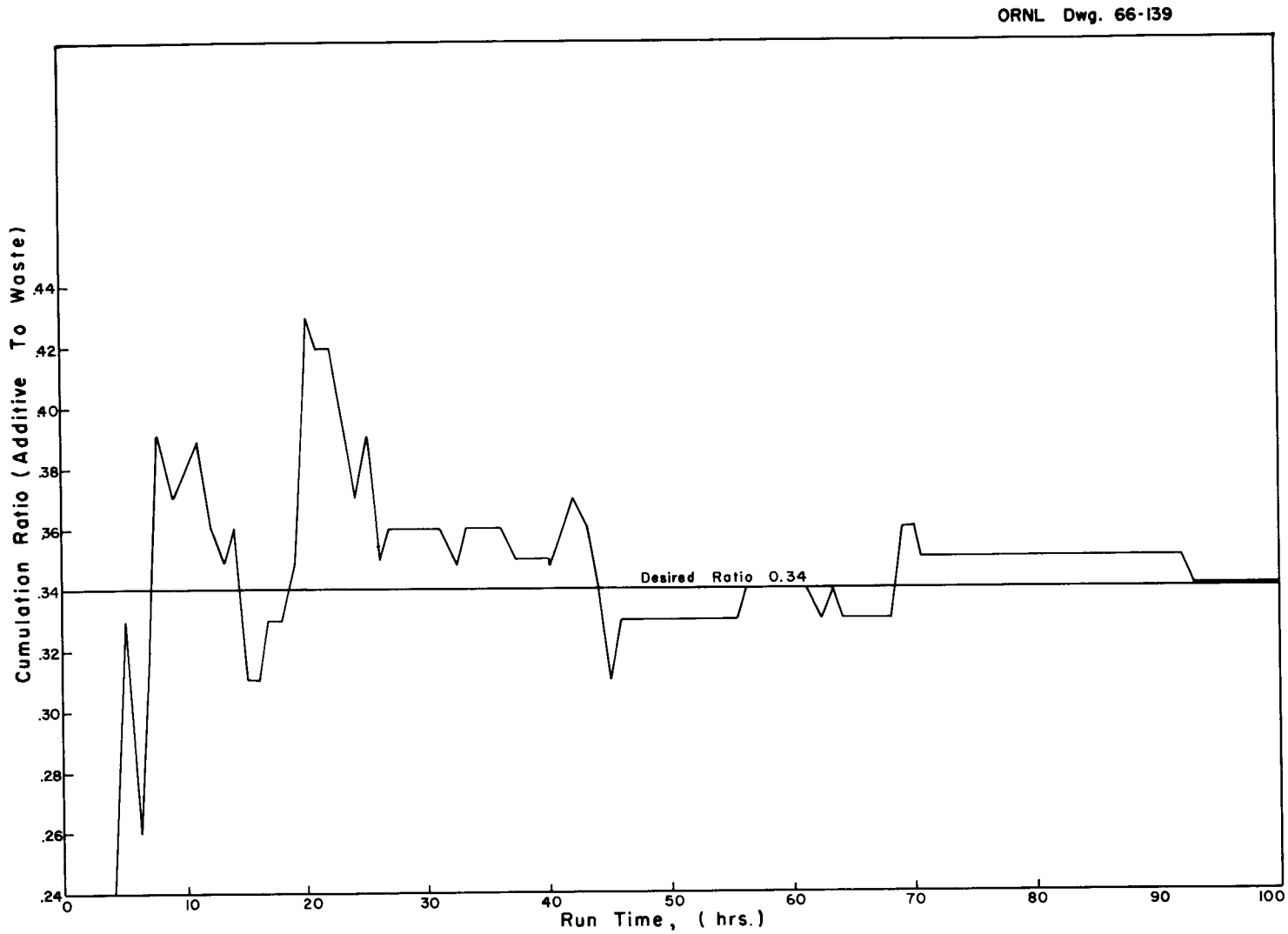

Fig. 2.3 Cumulative Ratio of Total Volumes of Glass Additive to Waste Solutions for R-92.

The large deviation in analyses for the phosphate concentration in the glass additives solution (Table 5) makes an accurate estimate of the amount of phosphate added difficult. Also, the large variation in the ratio of feed to additive solution (Fig. 2.1) makes the uniformity of the product glass suspect. Five samples of glass were taken and the analyses averaged in making the material balance (Table 6). The semi-glassy solid produced in the pot contained the following major ions (wt %):

Fe	Na	PO_4	Li
22.1	9.42	18.2	2.42

The residual nitrate concentration was 45 ppm.

The operating temperature of the pot was 900°C; the maximum temperature was 925°C, but for not over 30 min. After the feed was stopped, the contents were held for 9 hr at 900°C as part of the 100-hr test.

During the last half of the test, zone 1 produced additional heat to heat the overfilled pot. With zone 2 at its control temperature, the large heat output from zone 1 caused zone 2 to overheat. Hence, it was necessary to reduce the temperature of zone 1 to about 800°C.

The pot was 12-in. in diameter by 97-in. long and was made of 304L stainless-steel about 500 mils thick. Thickness was measured before and after the test at 30 places per heating zone by an ultrasonic thickness gauge. After the tests, the bottom zones of the pot were badly corroded (up to 239 mils), and the amount of corrosion decreased to very near zero at the top. Thus, the corrosion in this test appears to increase with the time that the area was covered. The center thermocouple well (109 mils) was completely corroded away at the zone-5 and -6 level (Table 7).

2.1.3 Conclusions

Only a limited number of large-scale tests (ten) have been made in the development of the rising-level process, two on PW 1 Purex waste, five on FTW-65 Purex waste, and three on TBP-25 aluminum waste. In

Table 6. Material Balance for Test R-92

Concentrations Expressed as gram-moles

	Nitrate	Iron	Sodium	Phosphate
Waste feed (852 liters)	6816	792	136	3
Additive (294 liters)	646	--	981	1780
Total	7462	792	1117	1783
Condensate (1404 liters)	8564	252	449	620
Solids (236 kg)	--	938	968	454
Total	8564	1190	1417	1074
Balance, %	115	151	127	61

Table 7. Wall Thickness of 12-in.-diam 304L Stainless-Steel Pot For Test R-92

Average Wall Thickness in inches, Measured Ultrasonically

Zone	Before Glass Test	After Glass Test
1	- 0.007 0.525 + 0.007	- 0.002 0.524 + 0.012
2	- 0.007 0.527 + 0.011	- 0.082 0.515 + 0.021
3	- 0.009 0.532 + 0.008	- 0.046 0.452 + 0.071
4	- 0.008 0.530 + 0.008	- 0.063 0.410 + 0.063
5	-0.007 0.524 + 0.011	- 0.039 0.349 + 0.134
6	- 0.008 0.529 + 0.011	- 0.040 0.338 + 0.072

Maximum penetration - 0.239 in. in zone 6.

addition, both 8-in.- and 12-in.-diam pots were used. Because of the large number of variables, it is difficult to draw firm conclusions or show a definite cause-and-effect relationship. The exact corrosion mechanism is unknown, and, more work, both in the laboratory and in large-scale tests, is required to definitely establish acceptable operating limits.

1. Corrosion: Test R-90 in an 8-in.-diam pot with FTW-65 waste (containing sulfate) and a maximum temperature of 850°C, and a similar run at Pacific Northwest Laboratory in an 8-in.-diam pot, were completely satisfactory. Corrosion was negligible. However, a duplicate run at ORNL, R-89, in an 8-in.-diam pot at 900°C was highly corrosive. This emphasizes the dependence of corrosion on the temperature and indicates the need for operating at the lowest possible temperature. Laboratory-scale tests have also shown a sharp relationship between corrosion and temperature.

Test R-91 with PW 1 waste (no sulfate, but high iron content) at 900°C in an 8-in.-diam pot showed a negligibly low corrosion rate. All glass-making additives were added to the waste feed tank, thus guaranteeing a uniform mixture. Test R-92, with the same chemical system, showed a high corrosion rate, up to 239 mils. The total times for the two tests were 67 and 100 hr, respectively. Operational problems in test R-92 caused a variation in the ratio of additive to waste solutions of 4.0 to 0, in contrast to a desired ratio of 0.34. The exact reason of the high corrosion rate in test R-92, compared with rate for R-91 is unknown but could have been caused by (1) improper mixing of waste and additives (see Sect. 2.2.5), (2) additional length of operating time, or (3) unpredictable corrosivity at high temperatures (see Sect. 2.2.5).

2. Addition of Glass Additives: The addition of phosphate and other glass-making additives can cause considerable precipitation in some kinds of waste. Although most wastes will contain solids as they come to the waste-treatment plant, it would be wise to limit the amount of slurry (solids) which must be pumped to a pot. Hence, the proportional feeding of the additive solution to the waste feed addition line is recommended.

2.2 Laboratory Development

W. E. Clark H. W. Godbee C. L. Fitzgerald

2.2.1 Preparation of Operating Manual for WSEP

The ORNL work on waste solidification has been summarized in the ORNL section of the operating manual for the Waste Solidification Engineering Prototype (WSEP) at Pacific Northwest Laboratories (PNWL). With a few additions and alterations this will be issued as a final report summarizing the ORNL work on solidification of highly radioactive aqueous wastes.

2.2.2 Melt Development Studies

A series of studies was made in which the compositions of melts from FTW-65 Purex waste were varied systematically, and the leach rates of the products were determined. Correlation of this data has not been completed.

The designation by PNWL of two new standard compositions for Purex waste with and without sulfate and both containing simulated fission products from a burnup of 20,000 Mwd/metric ton of uranium (Table 8) necessitated development of modified melt compositions for those particular variations. Reasonably satisfactory phosphate-melt compositions were readily available as a result of past melt-development work recorded in the ORNL melt catalog[1] (Table 9). Some difficulty was encountered with corrosion from Purex-1 waste, which is high in iron (see following paragraph). Lead silicate melts were also developed for this waste type. These were more homogeneous in appearance, had lower softening and operating temperatures, and gave higher volume reductions than the phosphate melts. They have not, however, been tested on a semiengineering scale.

2.2.3 Semiengineering-Scale Fixation Tests

Seven semiengineering-scale rising-level experiments were made, five with Purex-1 and two with Purex-2 waste types. The most satisfactory compositions tested are listed in Table 9.

Table 8. Simulated Purex Waste Types, Including Fission Products

For a burnup of 20,000 Mwd/metric ton at 15 Mw/metric ton, a cooling time of 6 years and a waste volume of 100 gal/metric ton.

Constituent (g-moles/l)	Purex-1	Purex-2	Simulated Fission Products (g-mole/l) Identical for Both Waste Types	
H^+	5.00	5.00	Rb	0.71×10^{-2}
Fe^{3+}	0.93	0.445	Cs	3.45×10^{-2}
Cr^{3+}	0.012	0.024	Sr	1.55×10^{-2}
Ni^{2+}	0.005	0.010	Ba	1.95×10^{-2}
Al^{3+}	0.001	0.001	Rare earths (total)	11.85×10^{-2}
Na^+	0.138	0.930		
Hg^{2+}	<0.001	<0.001	Zr	6.50×10^{-2}
$NO_3^- - NO_2^-$	8.80	6.44	Mo	7.9×10^{-2}
SO_4^{2-}	--	0.870	Ru	4.66×10^{-2}
PO_4^{3-}	0.003	0.006		
SiO_3^{2-}	0.010	0.010	Ag	0.80×10^{-2}
F^-	<0.001	<0.001	Total fission products	39.37×10^{-2} (0.394 M)

Fixation of Purex-1 waste in phosphate ceramics at reasonable rates required a slightly higher operating temperature (900 to 950°C) than the 900°C maximum, which is desirable in a stainless steel pot. At about 950°C, corrosion was fairly severe and resulted in loss of one or more thermocouples in times as little as 5 to 6 hr. Substitution of 0.1 M hypophosphite for an equivalent amount of phosphate in the melt decreased the corrosion markedly, perhaps by reducing Cr(VI) to Cr(III). The optimum amount of reductant to be added was not determined.

Volume reductions obtained from the Purex-1 waste type varied from 5.7 to 9 volumes of liquid waste per volume of solid product and corresponded to 11.1-17.5 gal of product per metric ton of uranium processed. Physical entrainment during operation (determined by lithium carryover

Table 9. Melt Compositions Currently Recommended for Fixation of Purex-1 and Purex-2 Waste Types

Additives (g-moles added to a liter of waste)	Purex-1 Melts A	Purex-1 Melts B	Purex-2 Melt
NaH_2PO_2	0.1	--	0.1
$Pb(NO_3)_2$ or	--		--
PbO	--	0.9	--
H_3PO_4	2.4	--	2.2
$LiOH \cdot H_2O$	1.37	--	1.37
NaOH	1.27	1.0	1.37
$Ca(NO_3)_2 \cdot 4H_2O$	--	--	0.2
H_3BO_3	--	0.8	--
SiO_2	--	0.8	--
Simulated fission products (g-moles/liter waste)	0.397	0.397	0.397
Wt % waste oxides	40.0	30.0	45.03
Approximate softening temperature, °C	750°	770°	750°
Operating temperature, °C	900°-950°	850°[a]	800-850°
Gal product/metric ton U	11.1	9.0	14.3

[a]Estimated. This melt has not been used in any semiengineering-scale test.

into the off-gas) was as low as 0.01% in one experiment. A figure of about 0.2% appears to be more realistic, however, since wide fluctuations in operating conditions during the course of an experiment often result in much higher entrainment values. Ruthenium volatility varied from 24 to 53% of the total present, the lower value representing the case in which a maximum of reductant was present. Molybdenum volatility varied from 0.4% to 1%.

Purex-2 was successfully converted to ceramic phosphate solids in two semiengineering-scale experiments. Previous small batch experiments had shown that volatilization of sulfate can be made almost negligible

if the equivalents of alkali and alkaline earths present overbalance the equivalents of nonvolatile anions (SO_4^{2-}, PO_3^-, BO_2^-, SiO_3^{2-}, etc.). The cation/anion ratio was too low, i.e., 0.95, in the first experimental melt, and 15.2% of the sulfate was volatilized, although the experiment was successful otherwise. Increasing the ratio to 1.05, as in the recommended melt shown in Table 9, resulted in a satisfactory experiment. Sulfate volatility was 11% of the total present vs about 2% for normally satisfactory experiments with other high-sulfate wastes. Both melts produced about 7 volumes of solid per volume of liquid waste, which corresponds to about 14.3 gal of solid per metric ton of uranium processed.

2.2.4 Ruthenium Volatility Studies

The flowsheets developed for all pot processes at ORNL assume that ruthenium volatility will be controlled by recycle of the pot off-gas to the evaporator. In the latter, the nitric acid is steam-stripped from the combined feed and pot condensate to yield a condensate containing very little ruthenium. Although this approach has been successfully tested on an engineering-scale,[2] controlled laboratory experiments were also desirable.

For this purpose, metered streams of water, simulated Purex-1 waste, and simulated pot condensate (9.68 M HNO_3) were fed into a glass distillation apparatus at volume ratios of 2:1:1, respectively. The volume ratio of evaporator condensate (about 3.2 M HNO_3) to evaporator bottoms (simulated pot feed) was 3:1 (Fig. 2.4). Temperatures in the solution and vapor phases were about 115-116° and 106°C, respectively. Ruthenium content of the simulated waste was 0.0566 M (about 5 mg/ml), and the ruthenium concentration of the simulated pot off-gas was varied from 0 to 1 mg/ml to resemble the possible buildup of ruthenium in the off-gas with time. Material balances for ruthenium for each of the three experiments were about 99%.

About 0.99, 0.59, and 0.40% of the ruthenium fed in was volatilized when the concentration of the ruthenium in the simulated pot off-gas was 0, 0.5, and 1.0 mg/ml, respectively. The value predicted from equilibrium-

ORNL Dwg. 66-140

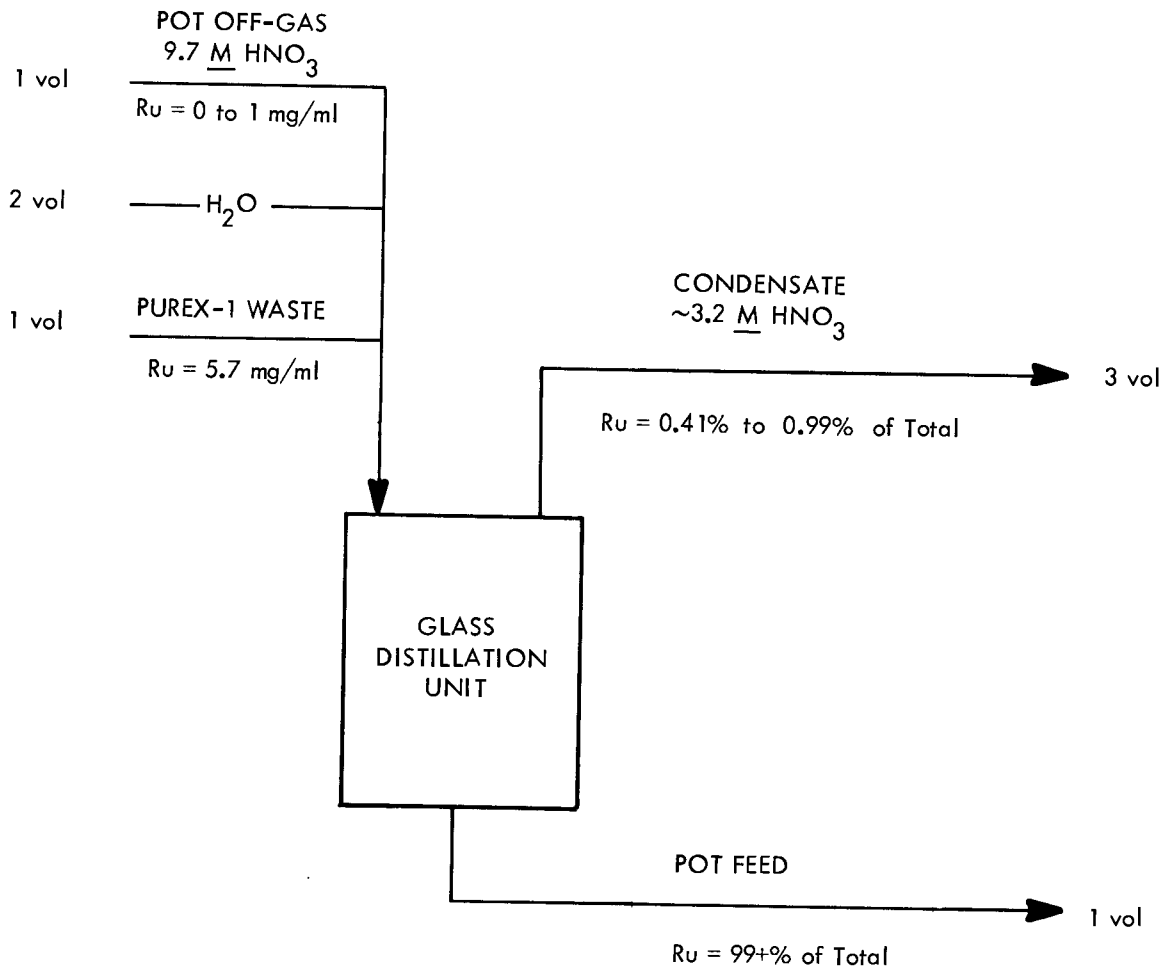

Fig. 2.4 Flowsheet for Laboratory-Scale Experiments Simulating Evaporator Operation.

still studies was $\geqq 2\%$.[3] The steam-stripping technique resulted in less ruthenium volatility than predicted. Also the apparently reversed trend of volatility with ruthenium content cannot be real and must be ascribed to either physical entrainment and/or analytical scatter. The results indicate that the ruthenium decontamination factor from the evaporator could be limited by physical entrainment. Small concentrations of a reductant (e.g., NaH_2PO_2) will reduce the "true volatility" of ruthenium by factors which vary between 38 and 2500 (ref 4), depending upon the waste type and the experimental conditions.

2.2.5 Corrosion with Phosphate Melts

The corrosion of test specimens and stainless steel beakers during batch studies on phosphate melts in the laboratory was somewhat erratic. However, there seemed to be some general trends. Usually, corrosivity of the melts increased with increasing ratio of phosphoric acid or phosphoric acid plus alkali metals to waste solution, and decreased with increasing amounts of calcium. Particular studies that lead to such generalizations include melts 398 through 421 (ref 1) with FTW-65 waste, and melts 466 through 477 with Purex-1 in which the additives (expressed as gram-moles added to a liter of waste) were H_3PO_4 (2.5 to 4), LiOH (1.4 to 2.2), NaOH (1.4-2.2), and $Ca(NO_3)_2$ (0 to 0.45).

Summarized below are observations from four laboratory experiments in which phosphate melts were much more corrosive than expected. Most of the glassy melts were taken from large-scale-test pots (see Sect. 2.1).

1. Long-Term Storage Test.--Material from Unit Operations (UNOP) run 91 — Purex-1 plus phosphate, lithium, and sodium (melt 478)[1]— was crushed and ground. A can (7-1/2-in.-OD and 25-in.-long) was filled with powder, and the temperature of the system raised to between 850 and 900°C. The temperature was held constant (for about 4 hr) until sufficient powder could be added to bring the level of molten material to within about 5 in. of the top of the pot. During this time at temperature, the eight thermocouple wells (1/4-in. 304L stainless steel tubing with 28-mil wall) in the can failed and filled with molten material.

2. Thermal Conductivity of Melt 478.--Material from UNOP run 91 — Purex-1 plus phosphate, lithium, and sodium — was crushed and ground. A can (4-in.-OD and 24-in.-long) was filled with powder, and the temperature of the system raised to between 850 and 900°C. The temperature was held constant (for about 2 hr) until sufficient powder could be added to bring the level of molten material to within 4 in. of the top of the pot. The pot was cooled to room temperature. Thermal conductivity measurements were made from 100 to 830°C. The material was at 830°C for about 24 hr. At the end of the tests, the can was taken apart. No severe corrosion was apparent. There was a 1/2- to 1-in. layer of snow-white crystals that had floated to the top of the material in the can.

3. Thermal Conductivity of Melt 2.--The thermal conductivity of a product (melt 2)[1] formed in the laboratory with Purex FTW-65 waste plus phosphate, lithium, aluminum, and calcium was measured *in situ*. The product was formed in a 4-in.-OD and 24-in.-long pot by the rising-level technique. Conductivity measurements were made from about 100 to 830°C. The material was at 830°C for about 24 hr. During the tests, the material in the pot had corroded through the inner 1-in. tube (1/16-in. wall) that accommodated a central heater. The material filled the tube and completely coated the central platinum heater.

4. Thermocouples as Level Detectors.--In a series of experiments to determine the response of pulse-heated thermocouples in various media, a product from a laboratory continuous-melter experiment was tested. The material was made with Purex FTW-65 waste plus phosphate, lithium, sodium, and aluminum (melt 358).[1] This product was crushed and ground. Sufficient material was put into a 4-in.-OD and 24-in.-long pot so that upon melting the pot was about half full. The material was held at 850°C for 3 or 4 hr on each of two successive days. The central heater (Nichrome) was lost during the second day. The pot was taken apart and it was discovered that the central 1-in. tube (1/16-in. wall) that accommodated the heater had been corroded through at the melt-air interface.

2.2.6 Conclusions

The corrosion observed in the above tests and in the large-scale engineering tests (Sect. 2.1) indicates a serious lack of knowledge regarding the mechanisms and control of corrosion of phosphate melts containing sulfate and multivalent metals such as iron and chromium. Previous work with aluminum—lead phosphate melts from TBP-25 waste had shown low corrosion rates on 304L stainless steel at temperatures up to 950-1000°C once the water and nitrate had been volatilized. Corrosion in the FTW-65 (sulfate) and PW 1 (high in iron) Purex systems in "neutral" glass (suitable balance of cations and anions) at low temperatures also has been negligible in many small- and large-scale tests. However, in other tests, corrosion has been unacceptably high. Comparison of small and large scale tests at 825 to 850°C and 900°C (1 and 2 above) and R-89, R-90, and the PNWL test (see Sect. 2.1) shows a significant decrease in corrosion at lower temperatures. However, excessive corrosion was noted at 830 to 850°C in tests 3 and 4 above. The fact that the material in tests 1, 2, and 4 was ground in air and added to the melt containers may have increased corrosion due to the presence of moisture or as the result of a change in valence of the iron and chromium. The effect of these variables is not known at present but is being determined in additional tests.

Recommendations and conclusions at the present time are:

1. The corrosion mechanism in Purex glassy melts is not sufficiently known at present. Consequently, tests in the radioactive pilot plant at Hanford are not recommended at temperatures above 850°C. A test using FTW-65 Purex waste and the conditions successfully tested at ORNL and PNWL could be considered. A test with TBP-25 aluminum waste could also be considered.

2. The corrosion and other data obtained in small-scale tests (4-in.-diam x 24-in.-high cans) cannot be used to accurately predict the results in large-scale tests. Additional research and development is required on both a laboratory and engineering scale if a dependable and successful rising-glass process is to be developed for Purex wastes. The total of

ten large-scale tests involving three waste types, in addition to other variables, has been too small to provide adequate data for process evaluation or to serve as a guide to laboratory research.

2.2.7 Fixation of Fluidized-Bed Waste in Glass

Preliminary scoping experiments show that the alumina bed plus the fission products that collect in the bed during fluidized-bed volatility processing can be readily incorporated in glass compositions developed for TBP-25 waste. Borophosphate glasses were prepared which contained about 33% by weight (about 29 mole %) of waste oxides (Al_2O_3 plus simulated fission-product oxides). Four different grades of alumina were investigated, and the effects of oxides from cladding materials (e.g., stainless steel, zirconium) were also studied. The 33% melts were sufficiently fluid for fixation at 900°C, although there was some cracking of the glass on cooling, probably caused by entrapped air bubbles. Pouring the glass melts appeared to minimize this problem.

Lead borate glasses provide a second possible type of matrix. One such melt was prepared which contained 37.3 mole % of Al_2O_3 and was completely molten, although very viscous, at 850°C.

The alumina bed was completely dissolved in these initial tests; that is, visual examination indicated only one phase. Further definition of the effects of constituents of the bed, for example, H_2O, F^-, etc., is also required. Dissolution of the alumina may not be required, however, and may be undesirable since the presence of solid alumina would increase the thermal conductivity of the product. Further tests are planned using melts to encapsulate, but not dissolve, the alumina.

3. LOW- AND INTERMEDIATE-LEVEL-WASTE TREATMENT

3.1 Incorporation of Intermediate-Level Waste in Asphalt

H. W. Godbee W. E. Clark J. H. Goode J. R. Flanary

Intermediate-level wastes (ILW's) are generally stored in tanks or incorporated in concrete since their high salt or solids content prevents

efficient treatment by normal water-treatment methods. Incorporation in concrete has not proved entirely satisfactory for several reasons: The operation is dusty, good mixing is difficult to achieve, the product generally represents a volume increase over that of the original waste, and radioactivity can be leached from the product at an unacceptably high rate. Considerable interest has been shown throughout the world in the use of asphalt as a medium in which ILW can be incorporated. Asphalt has good adhesive and coating properties and is insoluble in water, but its sensitivity toward radiation limits the radioactivity of wastes to be treated, and its organic nature limits the temperatures at which it can be used. Plants for incorporating ILW waste in asphalt have been constructed in Belgium and in France.

At ORNL, emphasis is placed on developing a process which can handle both liquid (including nitrates) and solid wastes. Details of the development program at ORNL are reported in refs 5, 6, and 7. In this process, evaporator wastes are introduced into an emulsified asphalt, which contains about 35% water, and the water is volatilized by heating to about 160°C to yield a product containing up to 60 wt % salts from waste (Table 10). Attractive features of the process include: use of emulsified asphalt which flows readily at room temperature; evaporation at low temperatures (120 to 160°C) to minimize entrainment of activity and degradation of the asphalt; low agitation rates (100 to 300 rpm), which provide adequate mixing and keep the heated surfaces of the evaporator clean; operation in batch or continuous manner; and incorporation of soluble as well as insoluble solids with equal effectiveness.

Probably the best measure of how well the waste particles have been coated with asphalt is how resistant the product is to leaching by water. Samples of asphalt products containing 20 to 60 wt % salts from simulated waste were leached with water in the laboratory for periods of up to 16 months. Products containing 20 and 60 wt % salts reach steady-state leach rates for ^{137}Cs (as well as sodium) of 1.5×10^{-4} and 3×10^{-4} g cm^{-2} day^{-1}, respectively. Hot-cell tests with concentrated actual ORNL ILW, containing 5 curies of aged mixed fission products per gallon, confirmed these nonradioactive and tracer tests. After 5 months of

leaching, a product incorporating 60 wt % salts from actual waste approached a steady-state leach rate of 2×10^{-4} g cm^{-2} day^{-1}.

Samples of product containing 60 wt % salts from simulated waste (Table 10) were prepared from an emulsified hard-base asphalt and were irradiated to absorbed doses ranging from 10^6 to 10^8 rads. A dose of 10^6 rads had negligible effect. A dose of 10^7 rads caused the asphalt to swell very slightly, while a dose of 10^8 rads caused the material to increase about 36% in volume. In contrast, similar samples prepared from a soft-base asphalt and irradiated to a dose of 10^8 rads showed only a slight increase in volume. Calculations have shown that the maximum dose absorbed by an asphalt product made from waste containing 5 curies of mixed fission products per gallon will be 10^8 rads. Thus, a product made with this soft-base asphalt will be satisfactory from the standpoint of radiation stability. Leach tests on the irradiated samples indicated that irradiation to a dose of 10^8 rads has no effect on the leach rate. As mentioned above, a product incorporating actual ORNL waste with 5 curies per gallon of mixed fission products had a leach rate after 5 months (an internal radiation dose of about 1.2×10^7 rads) essentially the same as that obtained with nonradioactive products. No radiolytic gas was released during this time.

In addition to the laboratory-scale tests with nonradioactive and radioactive waste in a 4-in.-diam x 6-in.-high evaporator, tests on a pilot-plant scale were carried out with a 12-in.-diam x 16-in.-high Pfaudler wiped-film evaporator with 4 ft^2 of heat transfer surface. The processing rate in the large unit was about 4 gal/hr of nonradioactive product containing 60 wt % salts from waste (Table 10). In all, eight 30-gal drums of asphalt products were prepared with the Pfaudler unit.

The incorporation of inert solids in asphalt does not appear to present any additional hazard to that normally present when processing, storing, or shipping an organic material with a high flash point. However, the hazards involved in incorporating nitrate salts in asphalt are being studied intensively. Specifically, the objectives are to

Table 10. Compositions of Simulated ORNL Intermediate-Level Waste (ILW) Solution and an Asphalt Product Incorporating Solids from ILW

Component	ILW Solution (M)	Asphalt Product[a] (wt %)
Sodium	6.61	18.5
Nitrate	4.64	34.9
Hydroxide	2.06	3.8
Sulfate	0.35	4.1
Aluminum	0.22	0.7
Ammonium	0.19	--
Chloride	0.056	0.2
Asphalt	--	37.8
Density at 25°C	1.34 g/ml	1.5 g/ml

[a]Volume reduction = $\frac{\text{volumes ILW}}{\text{volumes product}} = 2.$

determine the change in burning rate or flash point with increasing nitrate content and to determine whether the mixture will sustain combustion in the absence of external oxygen. Initial results with small samples, 1 to 2 g, indicate that the flash point of irradiated asphalt, approximately 280°C, is not lowered significantly--about 50°C--when the mixture contains 35 wt % nitrate and a total of 60% salts. The flame was easily extinguished when the air was replaced by nitrogen, even though the solid-phase temperature was in the range of 400 to 500°C. Tests are continuing to determine the effect of radiation-dose level. Further standard safety tests are being carried out by a subcontractor. These tests include drop weight, autoignition, shock sensitivity, and flame propagation tests with small samples, and fire tests with 30-gal drum samples.

3.2 Water-Recycle Process

W. C. Yee W. E. Clark

The conservation of water resources and the minimization of waste pollution of water streams have been the subjects of increasing national concern. The resulting penchant for water reuse has served as the

motivation for developing the water-recycle process for treating low-level-radioactivity waste (LLW). In this process, the waste water of a nuclear installation, containing a low concentration of bulk ions, is completely decontaminated and completely demineralized; the product water is returned to the plant for reuse, thus providing a closed circuit. Fresh water is demineralized before entering the circuit. This approach contrasts with the more traditional "treat and discharge" method, which allows "tolerable" amounts of radioactivity to leak into natural streams and relies on dilution by the stream to maintain radionuclide concentrations at levels below Federal (MPC_w) requirements. Speaking out on stream pollution in general, however, the U.S. Public Health Service maintains that "dilution is no solution."[8]

Promising results have been reported[9,10] for micro-pilot plant tests of the process. Overall decontamination factors (DF's) range from 100 to 10,000 — in the hundreds for ^{144}Ce, ^{131}I, ^{106}Ru, ^{125}Sb, and ^{95}Zr-Nb; in the thousands for ^{137}Cs and ^{90}Sr; and in the ten-thousand range for ^{60}Co and total rare earths (Table 11). The DF's for ^{106}Ru and ^{60}Co were 10 to 1000 times as high as previous values obtained in the ORNL development program. In these tests, LLW had a bulk ionic concentration similar to that of tap water (specific conductance of 200 to 300 μmho/cm). A large inventory of decontaminated and demineralized water is being accumulated by treating low-level waste and by retaining the water so treated in development experiments. This water will subsequently be adjusted to simulate closed-circuit water-recycle conditions (contaminated water of low bulk ionic content) in micro-pilot plant tests.

The flowsheet used for treating LLW includes zeta-potential-controlled (ZP) flocculation-clarification, cation-anion exchange, and sorption by activated carbon (Fig. 3.1). For LLW similar to tap water, 20 to 30 ppm of alum, as $Al_2(SO_4)_3$, and 0.5 ppm of activated SiO_2 was sufficient to neutralize the negative ZP of the suspended solids in the waste (from its original -14 to -17 mv to +2.5 mv) and obtain optimum clarification. Demineralization capacity (0.2% of ionic breakthrough as measured by specific conductance) with separate cation (Dowex 50W) and anion (Dowex 1) exchange columns was about 400 bed volumes (BV) of clarified LLW (total

Table 11. Effects of Variations in the Water-Recycle Process Flowsheet When ORNL LLW Is Used.

A. Changes in the Properties of the Water as it is Processed.

	ORNL Low-Level Waste					Flocculated Water			Demineralized Product Water	
	pH	Specific Conductance (μmho/cm)	Total Hardness (ppm $CaCO_3$)	Nitrate (ppm NO_3^-)	Zeta Potential (mv)	Alum Added (ppm $Al_2(SO_4)_3$)	pH	Zeta Potential (mv)	Specific Conductance (μmho/cm)	Vol. Product Water Per Vol. Cation Resin
Run 6, Normal Waste[a]	7.4	280	130	15	-12.8	20	ND[c]	+2.5	0.67	400
Run 12, High Nitrate Waste[a]	4.9	427	123	264	-15.8	27 to 64	4.4 to 4.7	-7.6 to -2.5	0.90	230
Run 13, Normal Waste,[b] Act. Carb. after cation exchange	8.0	316	123	10	-13.2	37	7.1	+2.7	1.0	270

B. Overall Decontamination Factors.

	^{137}Cs	^{90}Sr	^{60}Co	^{106}Ru	^{144}Ce	Total Rare Earths	^{125}Sb	^{95}Zr-Nb	^{131}I
Run 6, Normal Waste[a]	2600	6300	12,000	610	330	11,000	300	160	430
Run 12, High Nitrate Waste[a]	1000	5500	350	500	110	5,200	250	75	50
Run 13, Normal Waste,[b] Act. Carb. after cation exchange	1000	3000	100	500	70	2,000	250	40	>30[d]

[a]System: Alum-activated silica flocculation-clarification, cation-anion exchange, activated carbon.

[b]System: Alum-activated silica flocculation-clarification, cation exchange, activated carbon, anion exchange, activated carbon.

[c]Not determined.

[d]Decontaminated to background.

ORNL DWG. 65-10699

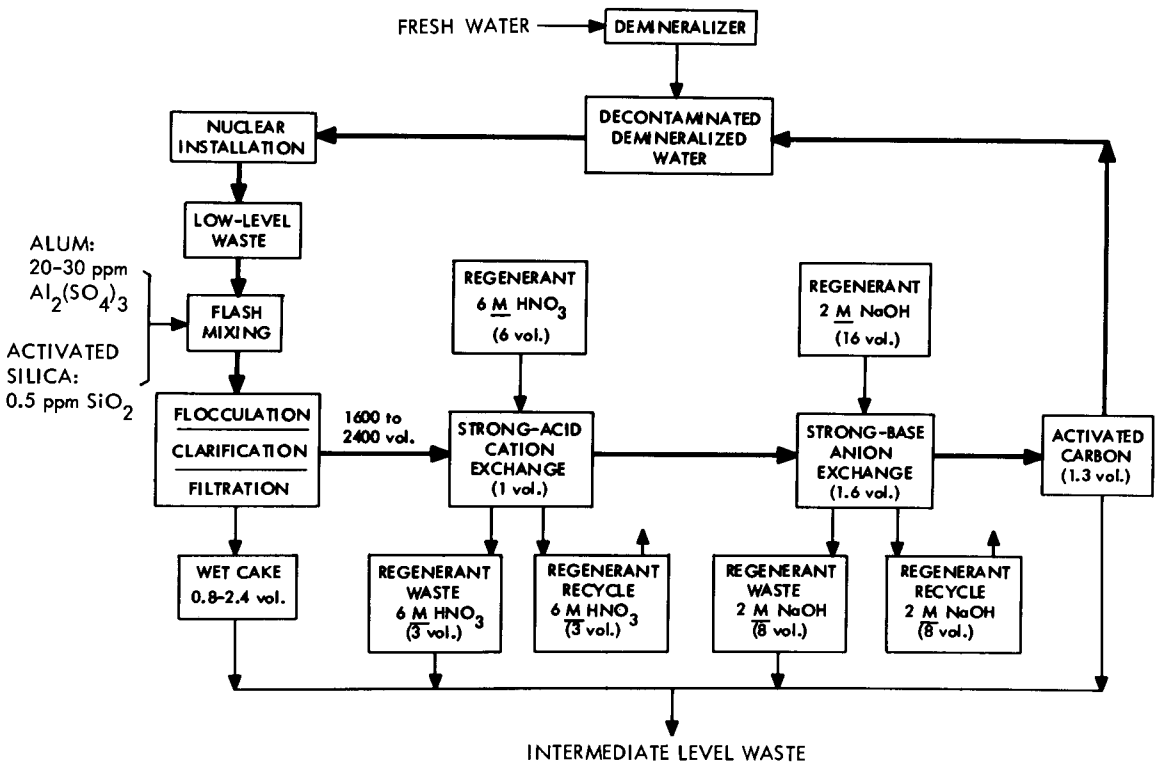

Fig. 3.1 Flowsheet for the Water-Recycle Process.

hardness of 100 to 130 ppm as $CaCO_3$) per volume of cation resin. Bituminous-coal-based activated carbon* removed a significant additional amount of ^{60}Co remaining after ion exchange.

When operating conditions deviate from normal (for example, run 6), high overall DF's for some radionuclides are more difficult to achieve (Table 11). For example, in run 12, the pH and specific conductance of LLW were 4.9 and 427 umho/cm, respectively, due to an abnormal twenty-fold increase in nitrate concentration to 260 ppm. The low pH prevented complete neutralization of the negative ZP charge on the waste colloids even though up to 3 times the normal amount of alum was added. Poor alum-activated silica flocculation resulted in poor upflow clarifier operation and a 35-fold decrease in the overall DF for ^{60}Co (Table 11). Obviously, the pH of this LLW should have been adjusted to 7 to 8 prior to adding the coagulants. The higher concentrations of NO_3^- and SO_4^{2-} also contributed to an early breakthrough in the demineralization step.

Another variation in the flowsheet was the insertion of an additional activated-carbon column into the system, between cation and anion exchange (run 13). This column sorbed ^{106}Ru from the cation exchange effluent (pH 2.5 to 3.0), but the total ^{106}Ru taken out was the same as without this column (run 6); the overall DF for ^{106}Ru was not improved. However, a greater than hundredfold decrease in the overall DF for ^{60}Co was noted. These data suggest that the chemistry of the ^{60}Co remaining after cation exchange treatment was altered by contact with the activated carbon and that activated-carbon treatment should come only after ion exchange.

Gross-beta decontamination is at least twofold greater than Dowex 1 anion resin than with Dowex 21K.

Regeneration and reuse of the activated-carbon column which follows anion exchange is a possible alternative to the disposal of the exhausted material. Elution with 2.75 bed volumes of 1 M HNO_3 reduced the sorbed ^{60}Co activity a hundredfold. There was some gassing in the column.

---

*Type CAL (12 x 40 mesh), made by Pittsburgh Activated Carbon Company, Pittsburgh, Pennsylvania.

4. ENGINEERING, ECONOMICS, AND SAFETY EVALUATIONS

4.1 The Cost of Perpetual Tank Storage

J. O. Blomeke E. J. Frederick R. Salmon E. D. Arnold

A study of the costs of perpetual storage of power-reactor fuel-processing wastes in tanks has been completed and published as ORNL-2873. In this study, the economics are examined for three representative types of financing: government ownership, private ownership, and a combination of government and private ownership. The case of government ownership includes only depreciation and interest on the investment capital; whereas, for private ownership, costs reflect a 15% return on equity as well as allowances for depreciation, insurance, taxes, and interest. In the third case, private ownership is assumed during a 20-yr period of waste accumulation, after which the government assumes responsibility for perpetual care of the tank farm. In each case, it is assumed that a permanent tax-free fund is established during the filling period of such size that the annual tax-free interest will be sufficient to provide for the periodic replacement of tanks and for the annual operating expense of the facility.

The tank farms were designed for storing high-radioactivity-level wastes in both acid and alkaline forms, and in tanks ranging in capacity from 200,000 to 5,000,000 gal. Capital costs were estimated for each case and then used in a computer code to estimate total costs for each method of financing as a function of tank size, tank lifetime, and fission product concentration in the waste. The basis of this study and the conceptual design of the tank farms were summarized in the previous semiannual report;[11] the final results are summarized below.

4.1.1 Raffinate Wastes

For the raffinate wastes, the initial capital expenditures varied from 8 to 16 million dollars, and the total over the 20-year period of waste accumulation ranged from 22 to 61 million dollars. The annual operating expenses ranged from 0.3 to 0.4 million dollars during the first year, to 0.5 to 2.0 million dollars during the twentieth year.

The size of the permanent fund needed for "perpetual care" ranged from 22 to 72 million dollars; and annual payments of 0.7 to 2.6 million dollars are required to establish this fund. The total costs of perpetual storage of acid raffinate waste, in mills per kwhr of electricity generated, is plotted in Fig. 4.1 against tank capacity for tank lifetimes of 25, 50, and 75 years for the three cases of financing. Minima occur at a tank capacity of about 1 million gallons in all cases. These minima range from 0.0165 mill/kwhr to 0.0184 mill/kwhr for case 1, from 0.0235 to 0.0253 mill/kwhr for case 2, and from 0.0251 to 0.0272 mill/kwhr for case 3. Total costs for alkaline waste storage were generally higher than the equivalent costs for acid storage (Fig. 4.2). For alkaline wastes, the optimum tank capacity is about 2.5 million gallons, and the minimum total costs are from 0 to 15% higher than those for acid wastes.

One of the least certain aspects of the basis used for this study is the degree of fission product concentration that can be tolerated during storage. The concentrations adopted are based on a careful consideration of Savannah River and Hanford experience and are believed to be as high as practical for wastes of this type. To obtain an indication of the effect of fission product concentration on costs, a second set of costs was computed assuming that the wastes were reduced in volume to half those of the original design basis. In this instance, acid Purex and Thorex wastes are stored at 50 and 100 gal per ton of fuel, respectively, and alkaline Purex and Thorex wastes are stored at 300 and 600 gal per ton. This reduction in volumes caused a decrease of between 15 and 30% in total costs. The optimum tank size for acid waste storage remained about 1 million gallons, whereas the optimum size for alkaline waste storage dropped from about 2.5 million to 1.5 million gallons.

4.1.2 Cladding Wastes

The costs of cladding-waste storage were compiled independently of those for the raffinates. The initial capital cost in all cases was 3.5 million dollars, and the total cost over 20 years was 52 million.

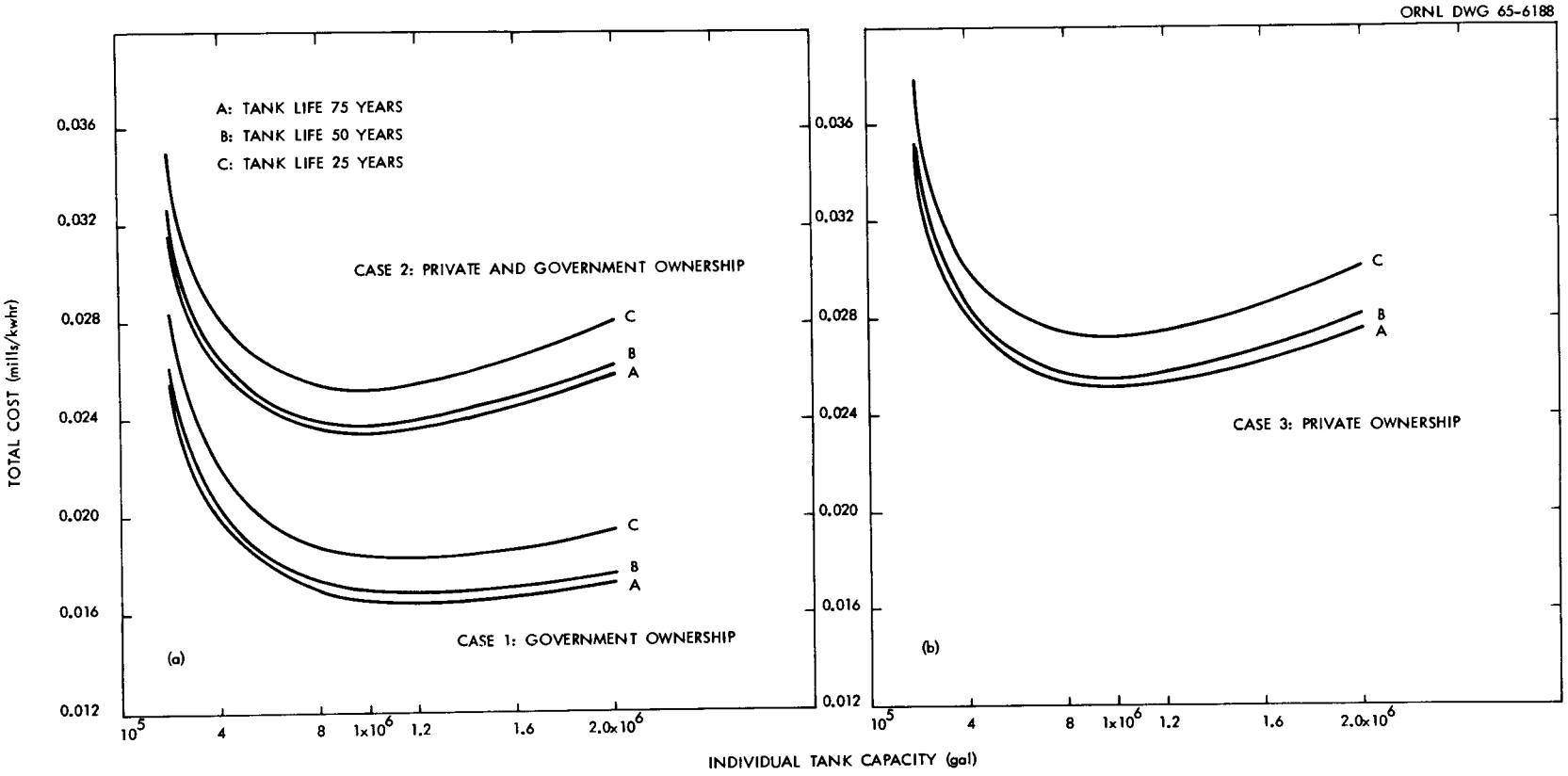

Fig. 4.1 Cost of Acid Waste Storage as a Function of Tank Capacity, Tank Life, and Method of Financing for (a) Case 1, Government Ownership; Case 2, Private and Government Ownership; and (b) Case 3, Private Ownership.

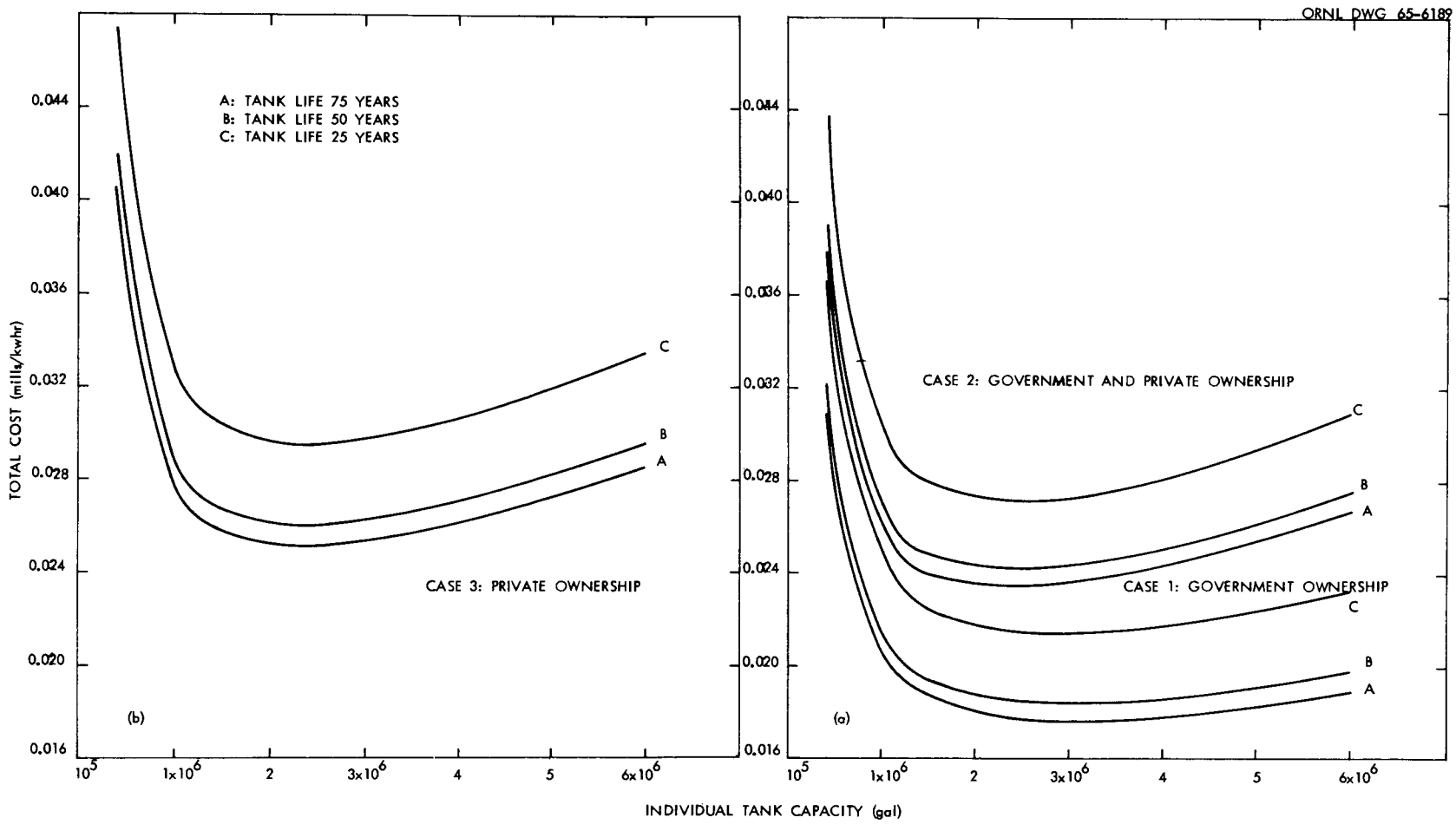

Fig. 4.2 Cost of Alkaline Waste Storage as a Function of Tank Capacity, Tank Life, and Method of Financing for (a) Case 1, Government Ownership; Case 2, Private Government Ownership; and (b) Case 3, Private Ownership.

The annual operating expenses ranged from 19 to 89 thousand dollars for the first year to 82 and 980 thousand for the twentieth year. The permanent fund varied from 17 to 78 million dollars, and required annual deposits of from 0.6 to 2.8 million dollars. Total costs ranged from 0.0215 mill per kwhr for tanks of 75-yr life with government ownership, to 0.0398 mill per kwhr for tanks of 25-yr life with private ownership. The total costs of cladding-waste storage, which are in every instance greater than the comparable costs for raffinate storage, are consequences of their larger volumes.

4.2 A Safety Analysis of Tank Storage

J. O. Blomeke L. C. Emerson

A safety analysis of tank storage of high-level power reactor fuel processing wastes has been undertaken, using the same basis as was adopted for the economic studies of waste management. A hypothetical tank farm is assumed to be located on the ORNL reservation, thus permitting a more detailed study to be made of the movement of accidentally released radionuclides by virtue of an existing thorough knowledge of the local environment. Tanks of Savannah River design with about 1 million gallons capacity are assumed, and when newly filled, contain between 4 and 7 billion curies of fission product activity, depending on whether the wastes are stored as alkaline or acid solutions. Maximum heat generation rates range from about 40 to 70 million Btu/hr.

We believe the most likely mechanism of a major release would be the loss of cooling. The worst possible time for this to occur would be when the tank was newly filled and the heat evolution rate was at its peak. In this event, the wastes would heat themselves to boiling in 10 to 20 hr. An additional 115 hr would be required for evaporation of the acid waste to dryness, and 240 hr would be required to evaporate the alkaline waste to dryness. It is estimated that decomposition of the inert and fission product salts would require 10 hr and 17 hr in the case of acid and alkaline wastes, respectively; and from 24 to 47 hr would be needed for thermal decomposition of the concrete vaults. Assuming continued containment of the fission products at this time,

it is estimated that the maximum in-tank temperature would reach several thousand °F at the end of an additional hour.

Based on these considerations, two incidents are postulated (Table 12). In the first one, it is assumed that cooling is interrupted for a time sufficient for the wastes to self-heat to boiling, and that they boil for 10 hr with both the condenser and the filter out of service. Releases from an acid and an alkaline waste tank are as shown. This type of incident might be such as could be incurred by sabotage of the surface-located cooling and ventilation facilities.

Table 12. Postulated Incidents

	Activity Released to Atmosphere	
	Acid Waste	Alkaline Waste
1. Self-boiling for 10 hr without condenser and filter.	300 curies/min Ru 10^3 curies/min FP's (720,000 curies)	300 curies/min FP's (180,000 curies)
2. Permanent loss of cooling.	90% of Ru, Cs, and Te; 5% other FP's — over 168 hr (1.1×10^9 curies)	50% of Ru; 25% of Cs and Te; 1% other FP's — over 300 hr (1.5×10^8 curies)

The second postulated incident assumes permanent loss of cooling as might result from an explosion of radiolytic hydrogen in the tank. Hydrogen is produced in these tanks at such rates that if the ventilation system failed, the lower explosive limit of 4% H_2 in air would be reached in only 1-1/2 to 3 hr; and our analyses indicate that quantities could accumulate which could explode with force sufficient to rupture the tank and concrete encasement. In this event, if no effective remedial action were taken, atmospheric releases of a major magnitude would be encountered over the ensuing 168 to 300 hr.

Assuming that the fission products (FP's) associate with the normal dust particles in the air, and choosing a typical particle size (i.e., deposition rate), the gamma exposure rate, in r/hr, at the ground from the FP's deposited by fallout, is shown in Fig. 4.3 as a function of the distance downwind from an acid waste tank. This is for incident 1 under conditions of rainfall and dry weather, at night. Here, it is assumed that the activity does not lie directly on the surface but is distributed exponentially throughout the topmost layers as in weapons fallout. Figure 4.4 shows similar curves for incident 2. The ground exposure rates for incident 2 are about 5000 times greater than those for incident 1.

Figure 4.5 shows the ground-level concentration (uc/cm^3) at various distances downwind following the first incident, and the resulting exposure to the lungs from breathing the contamination over the duration of the incident. These dose equivalents are the result of integration over the first year.

Figure 4.6 gives the same information for incident 2. These results are a thousand times higher than those shown in Fig. 4.5.

Similar analyses of incidents 1 and 2 for the case of alkaline waste gave results from 1/5 to 1/2 those of acid wastes.

A third source of exposure to the surrounding population is that which would result from direct radiation from the passing radioactive cloud. This has been found to be only a few percent of that from the two sources already treated and consequently is considered to be of negligible importance.

Another phase of this study, which is still in progress, is a consideration of a large-scale release of activity to the geological environment, and the resultant contamination of the ground and surface waters.[12] From a consideration of all known exposure pathways, and the corrective measures necessary, we expect to estimate the extent of liabilities incurred by these releases.

ORNL DWG 65-3086

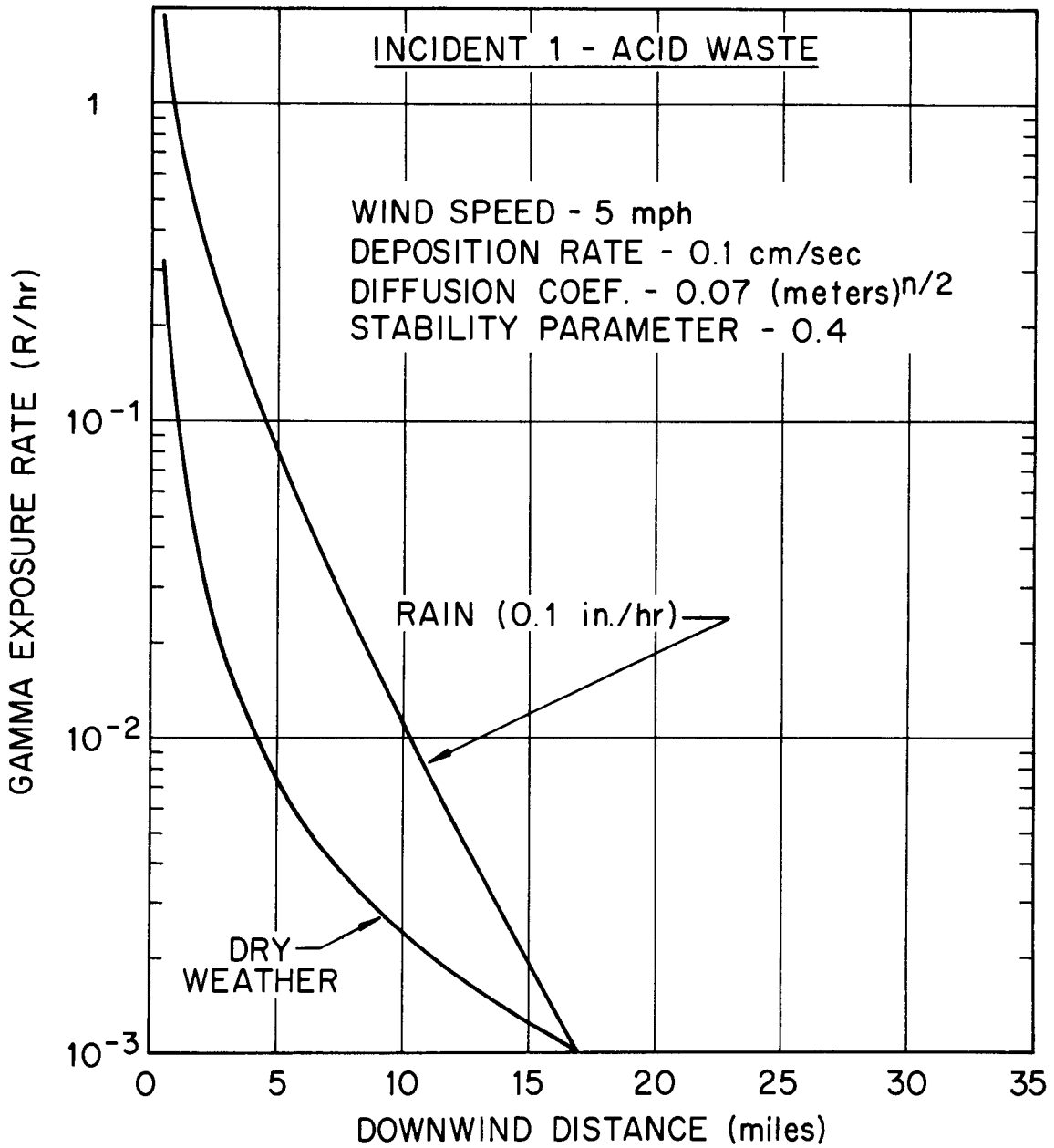

Fig. 4.3 Ground-Level Exposure Rate as a Function of Distance Downwind from an Acid Waste Tank Following Temporary Loss of Cooling.

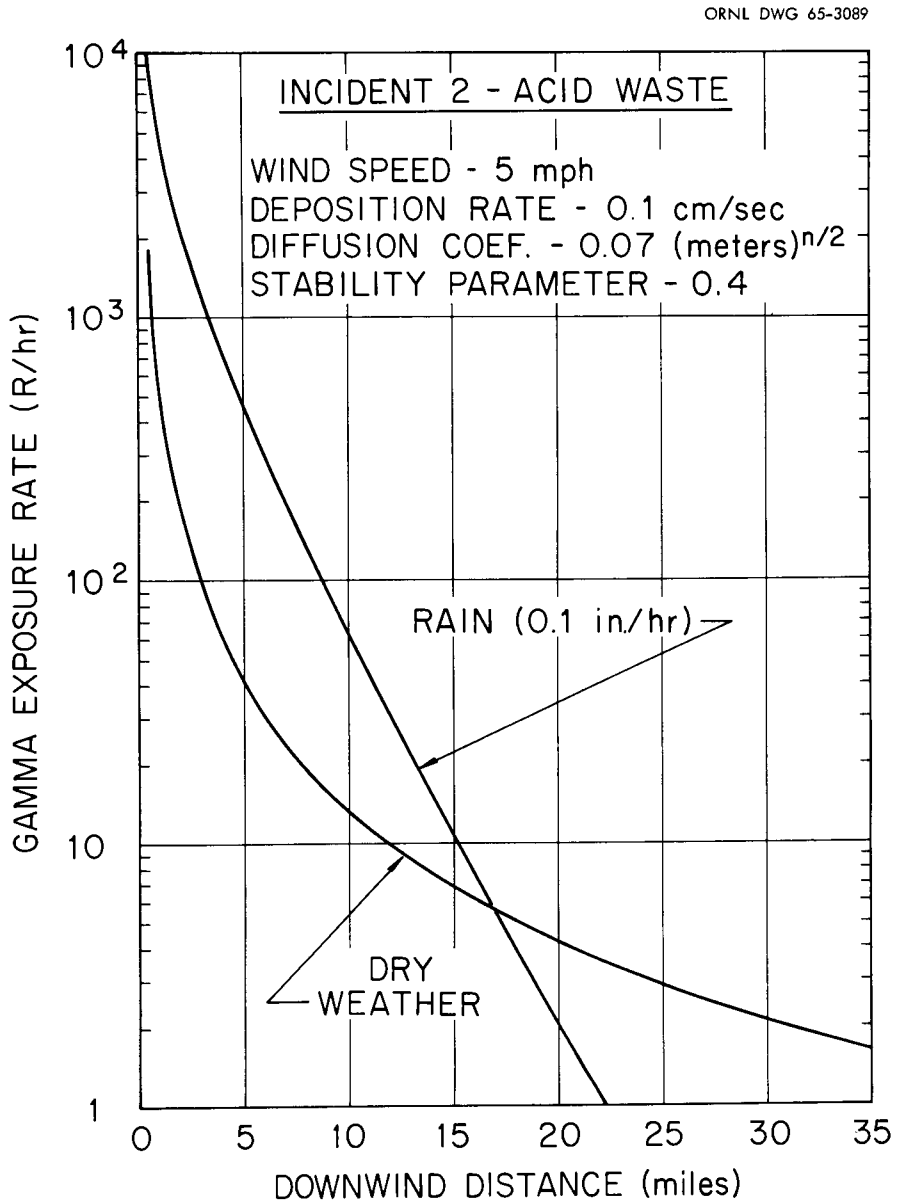

Fig. 4.4 Ground-Level Exposure Rate as a Function of Distance Downwind from an Acid Waste Tank Following Permanent Loss of Cooling.

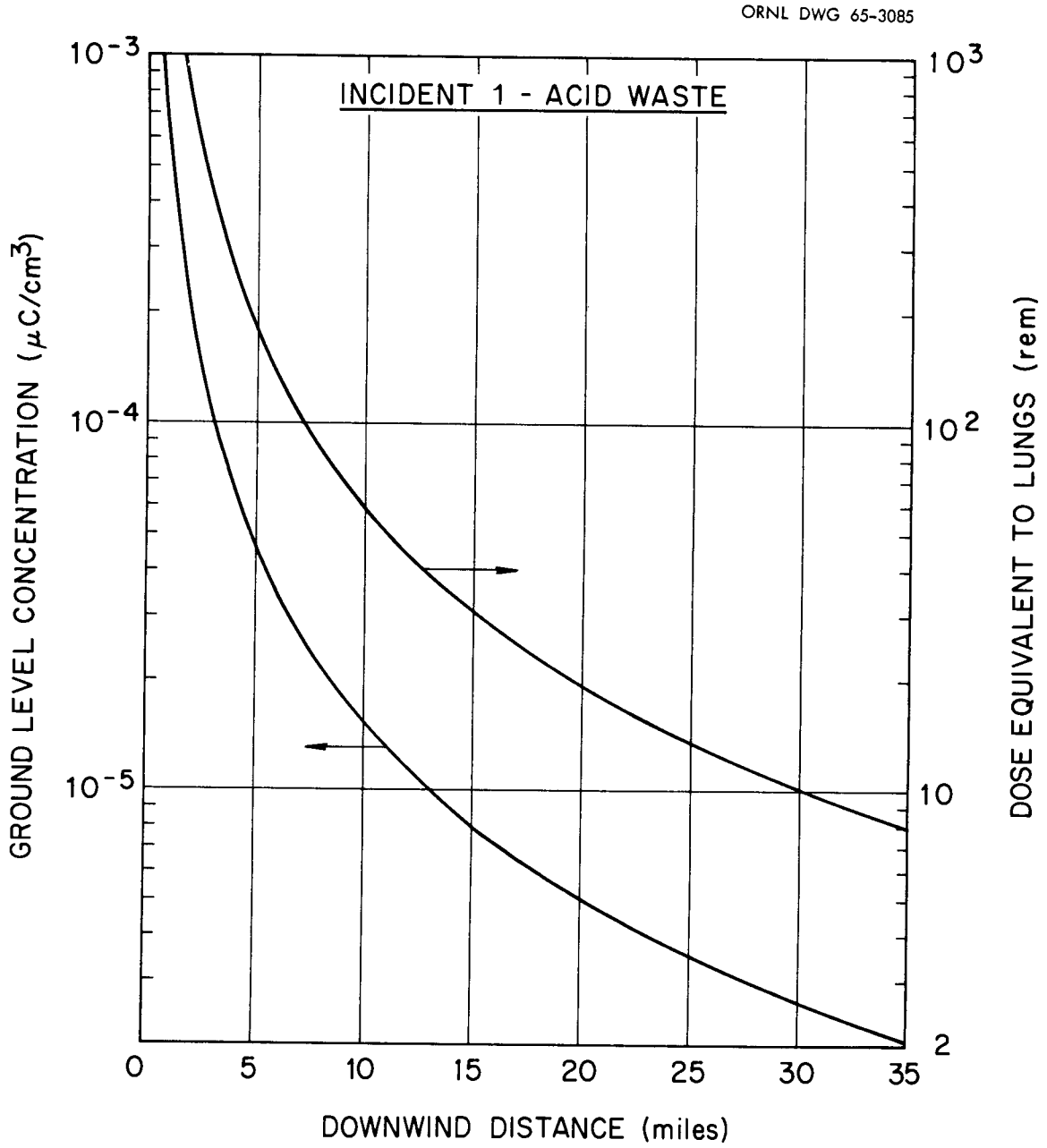

Fig. 4.5 Ground-Level Concentration as a Function of Distance Downwind from an Acid Waste Tank Following Temporary Loss of Cooling.

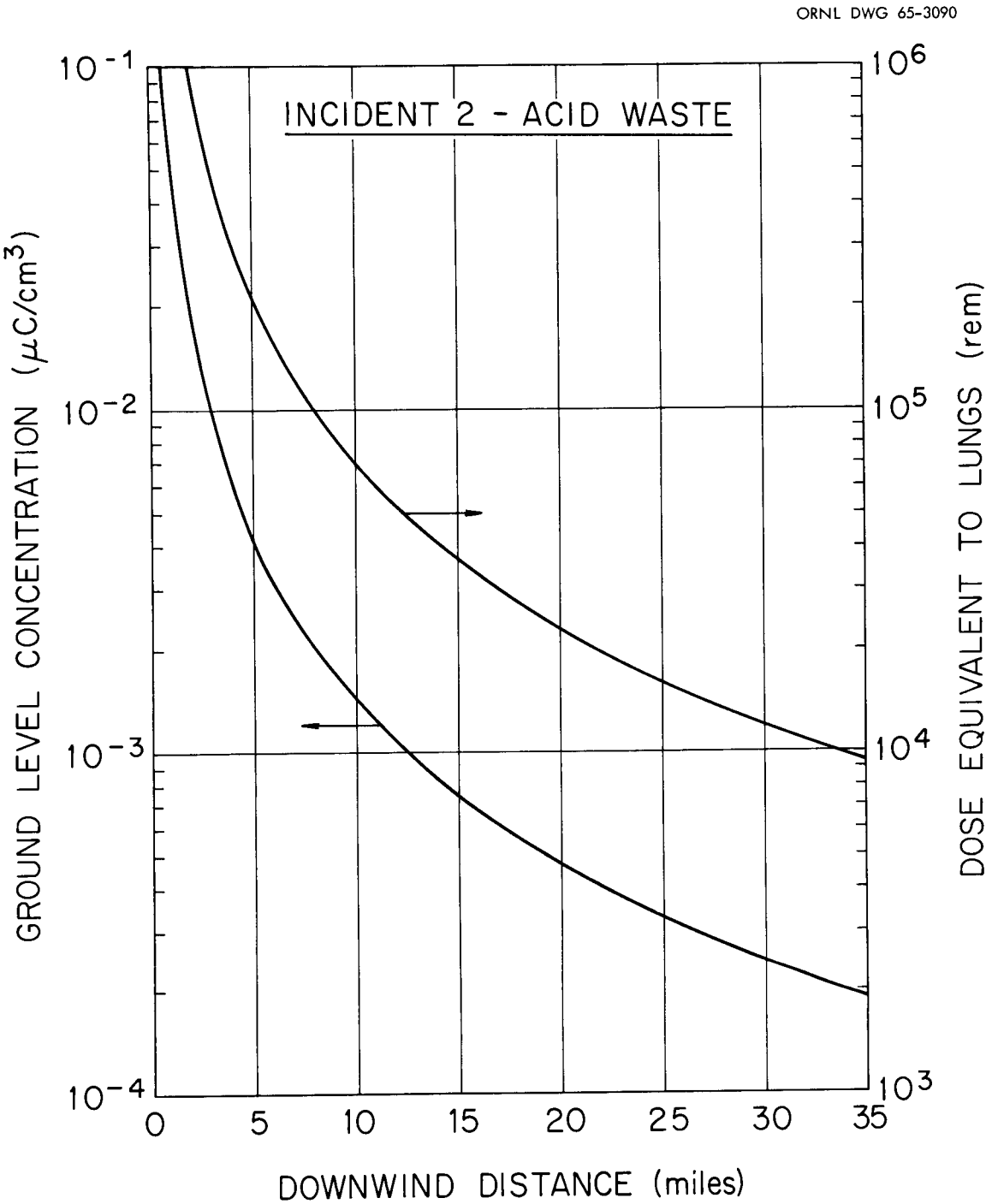

Fig. 4.6 Ground-Level Concentration as a Function of Distance Downwind from an Acid Waste Tank Following Permanent Loss of Cooling.

5. DISPOSAL BY HYDROFRACTURING

5.1 Objectives

The seventh injection in the series of tests with radioactive waste was done (1) to determine the ease with which an injection can be made into the slot used in a previous injection, (2) to evaluate the performance of the mass flowmeter, and (3) to obtain data useful in comparing field mixing of the slurry with laboratory mixing by measuring bleed-back of water from the grout. The waste solution had about 1.25 times the concentration of dissolved salts in normal ORNL waste. The activity of the waste solution in the underground tanks average 0.08 curie/gal, mostly due to ^{137}Cs. About 50 curies of ^{60}Co were added to the waste to distinguish it from that used in injection 6 when cores are recovered.

5.2 Plant Modification and Preparation

Tsuneo Tamura
R. C. Sexton[a]
Wallace de Laguna[b]
E. G. Struxness
F. S. Brinkley
H. O. Weeren[c]

5.2.1 Plant Modifications

Following injection 6 considerable concern was expressed by the Halliburton representative about the lumps that had been found in the solid mix. It was theorized that they had been formed by water condensed from the air during blending and aeration. To avoid their formation, a different blower was obtained. It was capable of supplying 450 cfm of air at 30 psig rather than 100 psig. However, it was found that the clumps had formed prior to blending (Sect. 5.2.2).

One of the heads of the injection pump was replaced. The pump was repacked, and new Chicksan fittings were installed on the high-pressure discharge. The sump tub was found to contain set cement (cement that had entered dry and had later become wet). Caked cement was also found

---

[a]Plant and Equipment Division.

[b]Leave of absence.

[c]Chemical Technology Division.

in the tub drain line. The cement was chipped and scraped out of the tub and drain lines, and hydrochloric acid solution was circulated through the system to complete the cleaning.

The concrete waste pit had been filled with cement in the cleanup operations of injection 6. Another pit was made and the suction and drain lines rerouted to the new pit. The suction line from the waste pit to the waste pump was plugged with cement, and this line was replaced. Bin 4 contained solids left from injection 6; all bins and "P" tanks were inspected and cleaned before use in injection 7.

The top of the wellhead cell was removed to simplify decontamination. The cell and the cell top were decontaminated, and the grating on the bottom side of the cell top was covered with welded metal sheets to make any future decontamination easier. The cell top was replaced and the cell was repainted.

5.2.2 Solids Blending

Blending was started on August 2, 1965. The contents of two trucks were blended and stored in bin 1. The third truck could not be fully unloaded because of many large clumps in the bottom. The source of the clumps was traced to its origin, and the blending was suspended until fresh material could be obtained. A screen was made and mounted on the truck for straining out any lumps during delivery.

Blending operations were resumed, and the blended solids were stored in bin 2. However, the clumps were found during delivery of solids, and blending had to be suspended again. Laboratory tests of samples of blended solids from bins 1 and 2 showed evidence of "flash setting", which was not encountered earlier when bagged samples were used. Further tests showed that the synthetic waste stored in the waste pit could be used with this blend without flash setting, and these solids were reserved for use with the synthetic waste. A new mix (second mix) to be used with actual ORNL waste was formulated, and there was no flash setting.

Blending was resumed after 10 days; no further difficulty was encountered, and bins 3 and 4 and the "P" tanks were charged with the new mix. A total of 587,000 lb of solids were stored.

5.3 Injection

Tsuneo Tamura E. G. Struxness
R. C. Sexton F. S. Brinkley
Wallace de Laguna H. O. Weeren

To ensure that the slot used in injection 6 would be capable of accepting fluid, the well was pressurized to 1600 psi, and a minimum of water was used to open the formation and ensure an adequate pumping rate. The injection took place on August 16. As planned, a water-solids mix was injected for the first 20 min to determine that the mass flowmeter was functioning properly. Injection of waste was started after this initial test.

It was soon established that the mass flowmeter readings were too high. Knowing the weight of solids in bin 3 (second mix) and the volume of waste pumped, it was calculated that the mix ratio had been 6 lb/gal instead of the desired 7 lb/gal. A similar error was noted after bin 4 (second mix) was empty. It was later suspected that the high reading was caused by a buildup of solids on the mass flowmeter.

Since the densometer and mud-balance reading had indicated that the solid:solution ratio was too low, the flow of solids was increased. However, the change was made when the waste solution being disposed was the synthetic waste 0.3 times the usual ORNL concentration, and the solids had been designed for a tank waste of 1.25-fold concentration. The lower salt concentration of the waste was caused by further dilution of the waste standing in the waste pit when the volume decreased through seepage. The increase in solids to this solution caused the slurry to be too viscous. This slurry could not be handled by the pumps, hence, the injection was halted, and the slurry was flushed out with water.

The injection was restarted by using a lower solids:liquid ratio for the remaining solids in bin 3, which were the original "P" tank solids (second mix). Although there was some suspicion that the solids in bin 1 (first mix) contained clumps, which might cause flow stoppage, no stoppage occurred. After bin 1, the solids of bin 2 (first mix) were used. Based on the rate of solids consumption and the amount of solids stored in the bin, it was planned to complete the injection by

using water and solids during the last 15 min. The use of water at the end serves to decontaminate the lines and the well. It required 54 min instead of 15 min to use up all the solids, which suggests again that the solids:liquid ratio was below that desired. The injection well was overflushed with water and valved shut rather than plugged; this was done to enable measurement of phase separation by bleed-back measurements.

5.4 Analysis of Data

Tsuneo Tamura
R. C. Sexton
Wallace de Laguna
E. G. Struxness
F. S. Brinkley
H. O. Weeren

Figure 5.1 shows the liquid volume pumped during the injection as measured by waste storage tank volumes and the flow totalizer. Since the tanks were directly calibrated and hence their reading more reliable, the data indicate that the totalizer was reading about 15% high.

Figure 5.2 is a plot of the solids flow rate based on the mass flowmeter readings, on calculations from the densometer readings, and the difference between the two. Comparison of these curves shows a gradually increasing difference for the first 90 min and a nearly constant difference thereafter, except for 30-min period when the mass flowmeter indicated very high flows and the densometer indicated lower than average flows. Integration of the mass flowmeter curve yields a value of 835,000 lb for the total weight of solids consumed; integration of the densometer curve yields a value of 635,000 lb (with no correction for the 3-min when consumption of solids was probably much higher than indicated). Since only 588,000 lb of solids were actually used, the accuracy of both curves is obviously poor.

It was noted during the injection that solids were building up on the mass meter and giving high readings. This would account for the difference in the mass-meter reading and the densometer. The mass-meter curve was therefore corrected by subtracting a fixed quantity from each reading over 90 min and a proportional quantity below 90 min. The amount subtracted was also chosen so that an integration of the corrected curve would give 588,000 lb of solids. With this corrected curve, the solid:

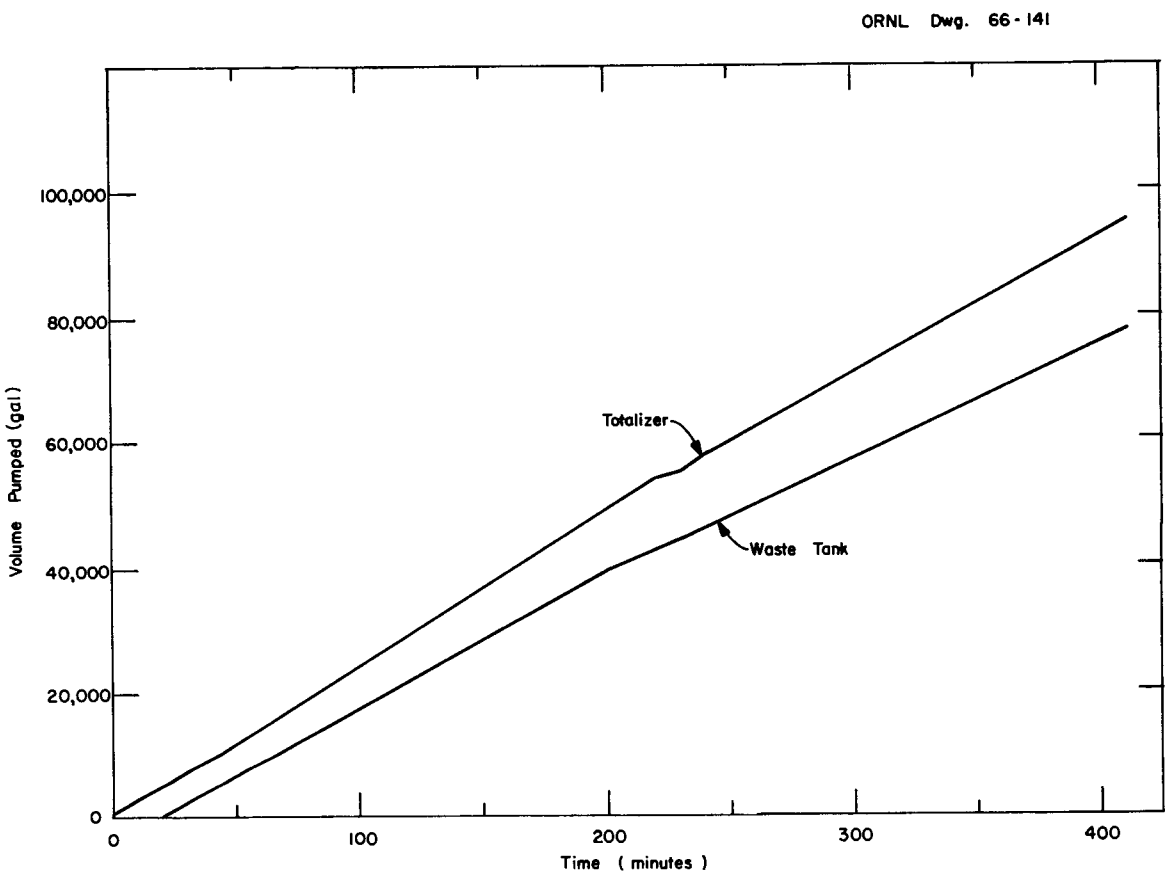

Fig. 5.1 Volume of Waste Pumped According to Readings Taken from the Waste Tank and from the Totalizer.

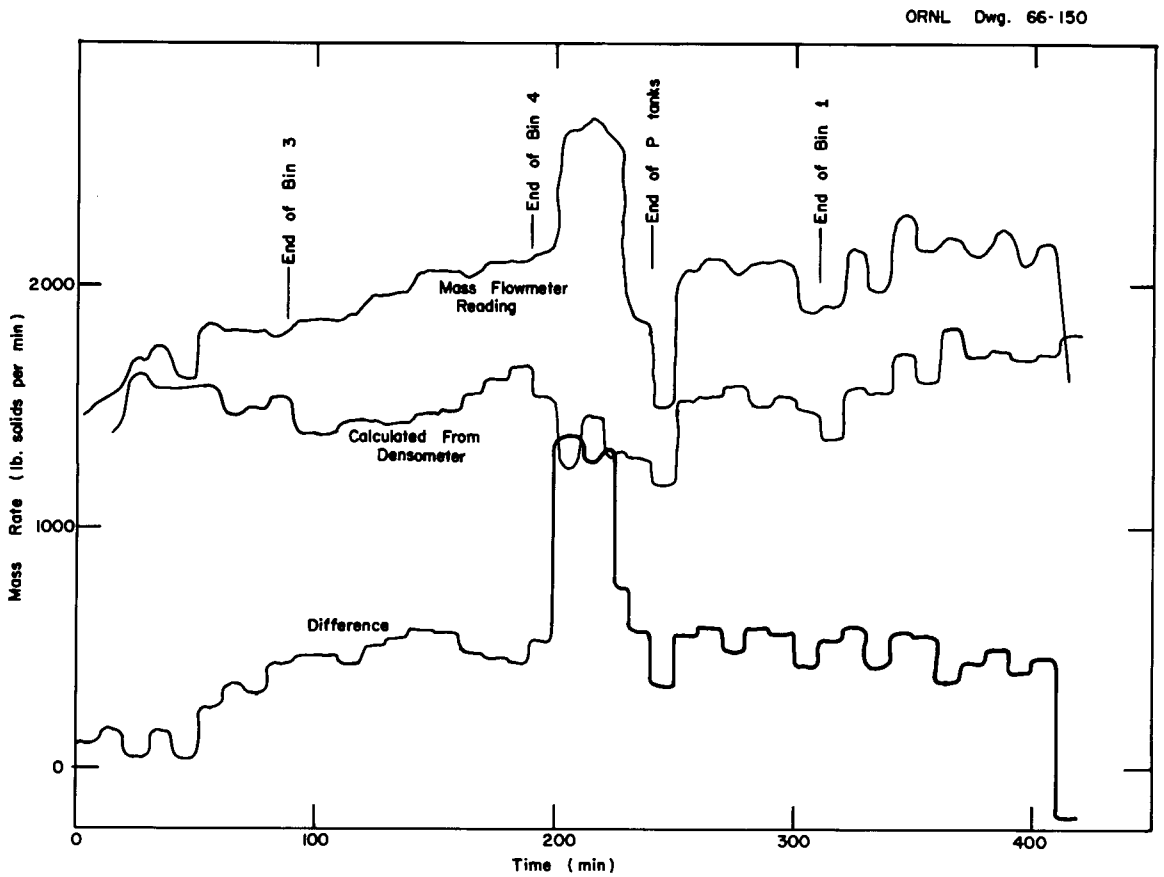

Fig. 5.2 Rate of Solids Feed Based on Mass Flowmeter Reading and Calculated from Densimeter Reading. The difference of the two readings are also shown.

liquid mix ratio was calculated, and the resultant curve is shown in Fig. 5.3. The desired mix ratio is also indicated in the figure. Note that except for a short period, the actual mix ratio was substantially below that desired. With most of the waste containing too little solids, it was suspected that phase separation would occur, and bleedback liquid has been measured during the first 3-1/2 months. These results show that a new mix formulation must be designed to show less phase separation, even with a 10% error in solids:liquid proportioning. Studies are being made, and preliminary results show that formulations with minimal phase separation can be designed.

5.5 Mechanical Effects of Hydrofracturing on Nearby Rocks

W. C. McClain

The effects on the surrounding and overlying rocks caused by injecting grout sheets into the ground at depth are now being studied. This examination seeks to provide information on the optimum sheet spacing and on the maximum number of sheets possible before the overburden fails, resulting in a release of grout to the surface. Better understanding of this subject will also be valuable in the determination of site-selection criteria for other areas.

The situation can be examined theoretically by assuming that the injection of material underground is inversely analogous to removing underground material. Concepts from mining-rock mechanics are then applicable to the problem.

A theoretical analysis developed by Salamon,[13] by which displacements and strains at all points in the rock mass can be calculated, is particularly amenable to the hydrofracture case. The solution involves the evaluation, by computer techniques, of the generalized equation,

$$Q = 1/\pi \iint_A S_z(\xi,\eta)\ f(r^2,\ z,H)\ d\xi\ d\eta\ ,$$

where

Q = the desired orthogonal deformational component, such as vertical movement, horizontal strain, or shear strain in a specified plane;

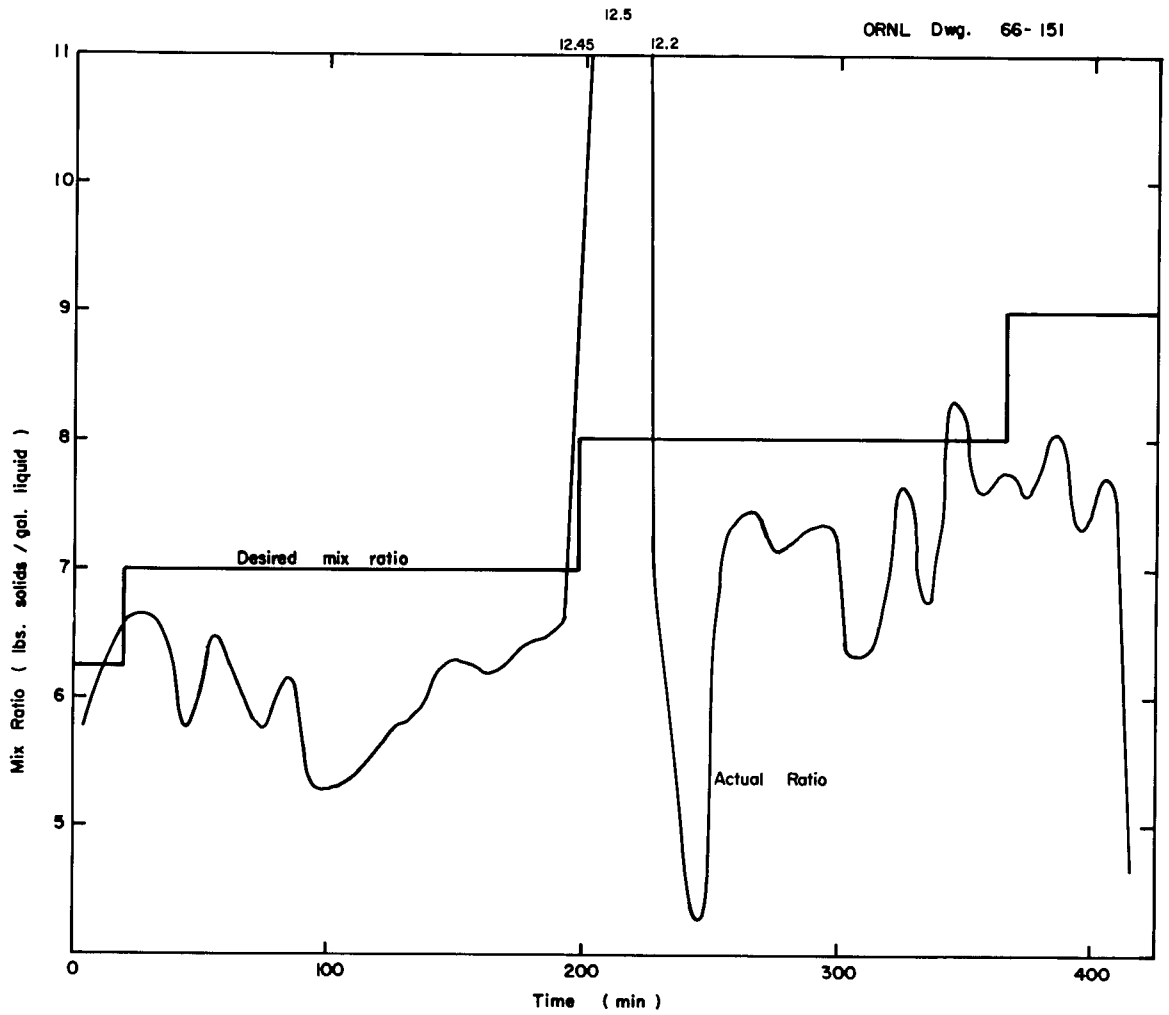

Fig. 5.3 Comparison of the Desired Mix Ratio and the Actual Ratio in Injection 7.

$S_z(\xi,\eta)$ = geometrical expression of the disturbance, in this case, the shape of the injected grout sheet;

$f(r^2Z,H)$ = a functional expression based on (1) the applicable deformational components, (2) the position of the point for which the solution is being made, and (3) the properties of the mathematical model being utilized;

$\iint_A d\xi\, d\eta$ = an integration over the area of the horizontal grout sheet.

The data from the shale-fracturing plant were compared with results of this theoretical evaluation for a number of mathematical models (homogeneous isotropic, homogeneous transversly isotropic, frictionless laminated and multimembrane) approximating the properties of the actual site. Based on the comparisons, a number of conclusions were drawn, contributing to the understanding of the hydrofracture phenomena.

Some of the more important of these conclusions are:

1. For injections similar to those at the shale-fracturing site (1000 ft depth, grout sheet of some few hundreds of feet in areal extent), the maximum surface uplift represents only a small fraction (5 to 20%) of the thickness of the sheet but extends over several times the area.

2. The volume of surface uplift should be equivalent to the injected volume.

3. For a given shape of injected grout sheet of constant horizontal dimensions, the surface uplift is everywhere proportional to the thickness of the sheet.

4. For an ellipsoidally shaped injection of high eccentricity in plan view (ratio of horizontal axes = 1/5), the surface uplift is very nearly circular and does not reflect the eccentricity of the injection.

5. For an injection which is circular in plan and elliptical in section, a region of high tensional strain in the vertical direction exists at the tip of the ellipse, while the maximum shear strains occur above and below the flanks of the injection.

6. DISPOSAL IN NATURAL SALT FORMATIONS

6.1 Preparation for Project Salt Vault

W. J. Boegly, Jr.
R. L. Bradshaw
F. M. Empson
W. C. McClain
F. L. Parker
W. F. Schaffer, Jr.

6.1.1 Prototype Test

Phase IV of the Hole Liner Prototype Experiment was terminated on July 19, after 47 days of operation without off-gas purge. The new bottom section of the lower liner, made at ORNL (type 304L stainless steel) and attached by the Lyons Manufacturing Company, appeared to be in good condition, although there was a bright red coating on the bottom three inches. The off-gas system was operated for 45 min just before shutdown, producing about 50 ml of condensate.

6.1.2 Safety Analysis

A draft copy of the Safety Analysis for the operation of Project Salt Vault[14] was completed, and reviews were held with the ORNL Radiochemical Plant Review Committee[15] and the Kansas State Board of Health.

The maximum credible accident for Project Salt Vault is one in which the canister is dropped down the waste-charging shaft, resulting in the destruction of the canister and failure of the cladding on some of the fuel assembly plates. Since fuel meltdown is not possible, it is assumed that 0.1% of the iodine and 100% of the rare gases contained in 19 fuel plates (each ETR assembly is composed of 19 plates) is released to the shaft. Because air flow is restricted in the shaft during transfers, and the material released is not vented until the waste-shaft fan is turned on, optimum meterological conditions can be selected prior to release. Even if this were not the case, and the activity from the fuel assembly were released during an inversion condition, the following would occur: Released ^{131}I would result in restrictions on mild production on land within a downwind distance of 1050 m, and at a distance of 100 m from the waste shaft an inhalation dose to the thyroid of 1.6 rems would be received; the ^{85}Kr and ^{131m}Xe released would result

in submersion exposures to an individual standing 100 m from the source of 42 and 16 millirems, respectively. Since milk production within 1050 m is negligible, and since it is possible to exclude workers from an area 100 m from the waste shaft, the consequences of a maximum credible accident can be minimized.

6.1.3 Equipment Installation

Procurement and installation of the waste-shaft fan has been completed. The fan will normally draw 5000 cfm of air up the shaft from the experimental area, but in an emergency the air flow can be reversed.

The hoist for handling the canisters has three speeds: 100, 33, and 1.6 ft/min. In normal operation, the slow speeds are used when the canister is being raised or lowered from the shipping carrier. The high speed is used for most of the canister travel in the shaft. The hoist is equipped with standard mine-safety auxiliaries, such as independent dual brakes, slip clutch, and a depth indicator. The capacity of the hoist (2000 lb) is sufficient to handle 12-in. calciner pots and to remove people from the mine in the case of an emergency in the main hoisting shaft.

Figure 6.1 shows room 1 (main radioactive array) during the time that the experimental equipment was being installed. The tops of the hole liners may be seen in this figure, along with the trenches containing heater, thermocouple, and off-gas lines. The large white box on the wall contains the off-gas system flowmeters. In the upper right corner of the picture may be seen the end of the main power-control panel.

6.1.4 Preoperational Tests

A number of operations were performed with empty fuel-assembly canisters to test the procedures, and minor procedural changes followed.

Early in October, two canisters were loaded with 500 curies each of ^{60}Co and shipped to Lyons in the shipping carrier. A fan-shaped beam was found to emanate from one section of the carrier (apparently due to

Fig. 6.1 Room 1, Main Radioactive Array of Waste Storage Canisters.

a gap in the lead shielding), necessitating the addition of an auxiliary shielding ring. The canisters were lowered into the mine, placed in the array holes, and removed a number of times to obtain handling experience with radioactive canisters and to evaluate the shielding calculations. It was also found that a "scatter" shield was needed inside the shot-retainer tubes in the hole liners.

All experimental equipment, such as the off-gas system, fission-product leak-detection system, etc., was put through a shakedown test before startup. The chief difficulty encountered was failure of the "Electrofilm" heaters on the off-gas-system tubes in the upper sections of the hold liners. During the shakedown tests, three of the seven heaters in the electrical array and two of the heaters in the radioactive array failed. There was no apparent reason for this since the units were operating below their rated temperature. Three units were repaired and two were replaced. No additional trouble was encountered with the operation of the electrical-array off-gas heaters, but by the second week after startup, all seven (including the replacements) of the units in the radioactive array had failed. Since there has been no indication of a water problem in these arrays, there are no plans to make any further replacements. However, it will be necessary to obtain more reliable units for installation of the array in the old mine floor, since water problems do exist there.

6.2 Startup of Project Salt Vault

R. L. Bradshaw
F. M. Empson
W. J. Boegly, Jr.
W. F. Schaffer, Jr.
F. L. Parker
W. C. McClain

6.2.1 ETR Fuel Assemblies

The 14 fuel assemblies from the Engineering Test Reactor cycle 73 were canned, the cans leak-tested, decontaminated, and loaded into the shipping carrier at the NRTS in Idaho without any major difficulties. Radiolysis of the coolant (ethylene glycol and water) presented a problem, which was solved by using plain water and installing a demineralizer in the cooling system.

The irradiation history of each of the fuel assemblies was taken into account in calculating the fission-product decay heat, and the assemblies were paired so that the total heat content of each canister would be about the same. The calculated heat generation rate as a function of time is shown in Fig. 6.2. The rates for five of the canisters follow this curve almost exactly, while the other two deviate by less than 10% (lower). Note that on November 18, the heat generation per canister was about 520. On November 1 (the original target date), the heat generation rate would have been about 630 w, compared with the 750 w calculated under the assumptions of the original feasibility study. The total fission-product activity in the seven canisters as of November 18 is calculated to have been about one million curies.

6.2.2 Startup

In order that the peak salt temperature may be raised to the vicinity of 200°C within the duration of the test (2 years) and with the limited number of heat sources, auxiliary heaters are attached to the hole liners. To simplify operation and analysis of data, a fixed power input was chosen. All holes are to be operated with a power input of 1500 w.

On November 15, the electrical (control) array and the main-radioactive-array heaters were turned on at 1500 w each. The heaters were operated two days before the first canister was installed so that the relationships between the temperatures at the prime points of comparison in the arrays could be established. The prime comparison point is the one at the vertical center-plane of the canisters but 1-1/2 ft from the central axis of the canister. Then, as each radioactive canister was placed, the electrical power was cut back so that the sum of the fission product power and electrical power was still 1500 w. Later, as the fission products decay, the electrical power will be increased periodically in accordance with Fig. 6.2.

On November 17-19, all seven of the fuel-assembly canisters were lowered into the mine and placed in the floor. Only one of the seven caused any difficulty. This canister could not be lowered out of the shipping carrier and finally had to be forced out by means of a steel

ORNL Dwg. 66-132

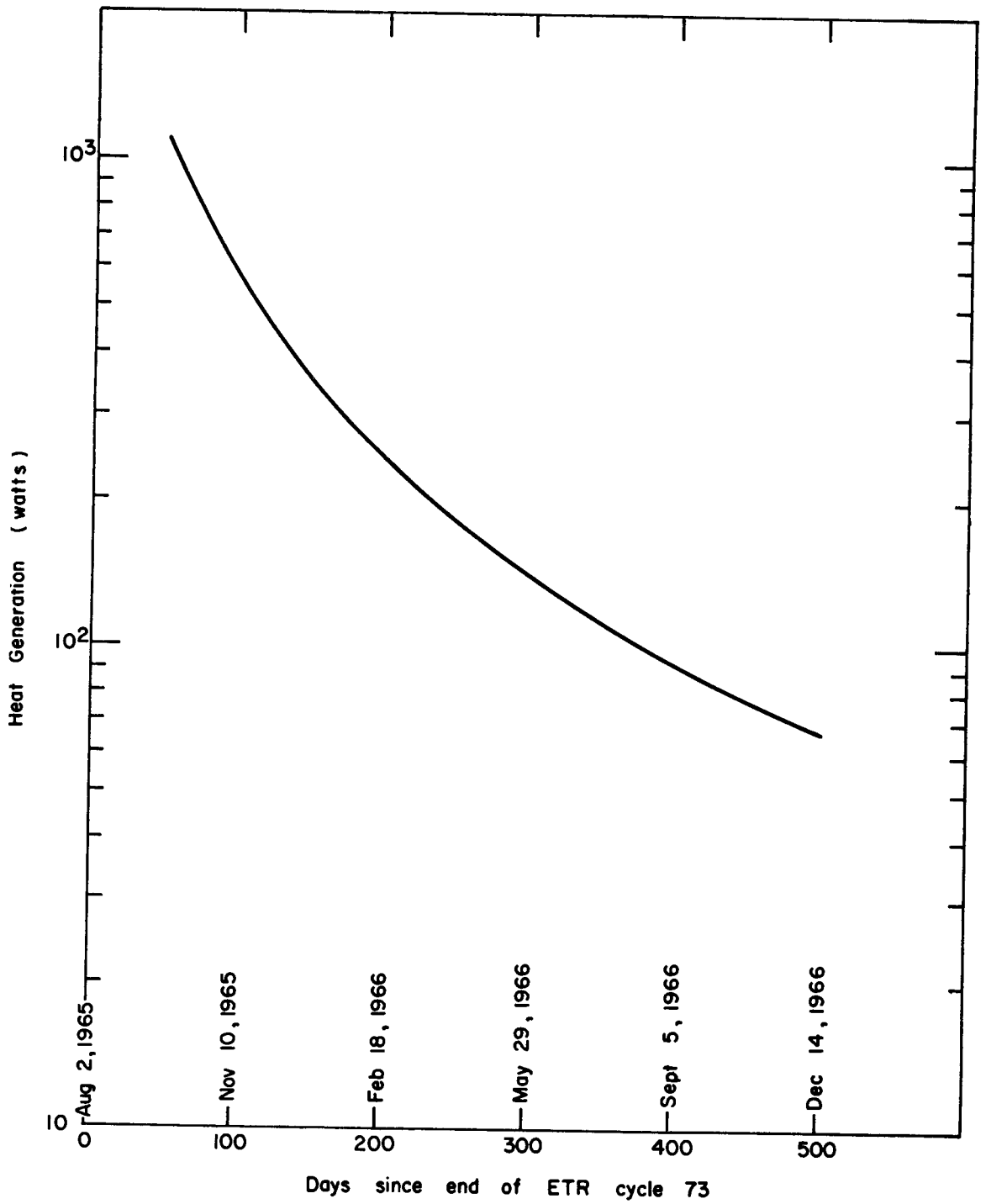

Fig. 6.2 Heat Generation Rate for All Canisters Except 2 and 4.

rod inserted through the cable port. No trouble was encountered in placing the can in the hole liner (tolerances are greater than in the carrier). A piece of tape was seen to be stuck to the top and side of the canister shield plug and may have caused the trouble.

The maximum radiation dosage received by any of those on the project during the entire loading period was 200 mr. Radiation levels immediately above the array holes (after installation of the scatter shields) are generally less than 10 mr/hr, and unlimited access is allowable everywhere except immediately over the holes.

6.2.3 Preliminary Results

Salt-Dose Measurements.--During the first week of operation, the dose rates in the air annulus between the hole liner and the salt and at various depths into the salt were measured with the specially developed chemical and glass-rod dosimeters. The results with the two types of dosimeter were in reasonable agreement with each other and with the theoretically calculated dose rates. The chief difference is that the peak dose rate appears to be at the surface of the salt, whereas the calculations showed the peak occurring at around 2 cm into the salt. The measured dose rate at the surface of the salt was about 5×10^4 rads/hr.

Temperature Rises.--Figure 6.3 shows the temperature-rise curves at the prime comparison point for the center and one peripheral hole. Data for both the electrical and radioactive arrays are shown, along with the theoretical curves calculated by using the 20°C thermal properties of salt. As may be seen from this figure, temperatures in both the electrical and radioactive arrays are satisfactorily close (both before and after placing of the canisters) to each other and to the theoretical calculations. As indicated in this figure, most temperatures, including the fuel element temperatures, are running somewhat lower than calculated. Fuel element temperatures range from about 225 to 265°C.

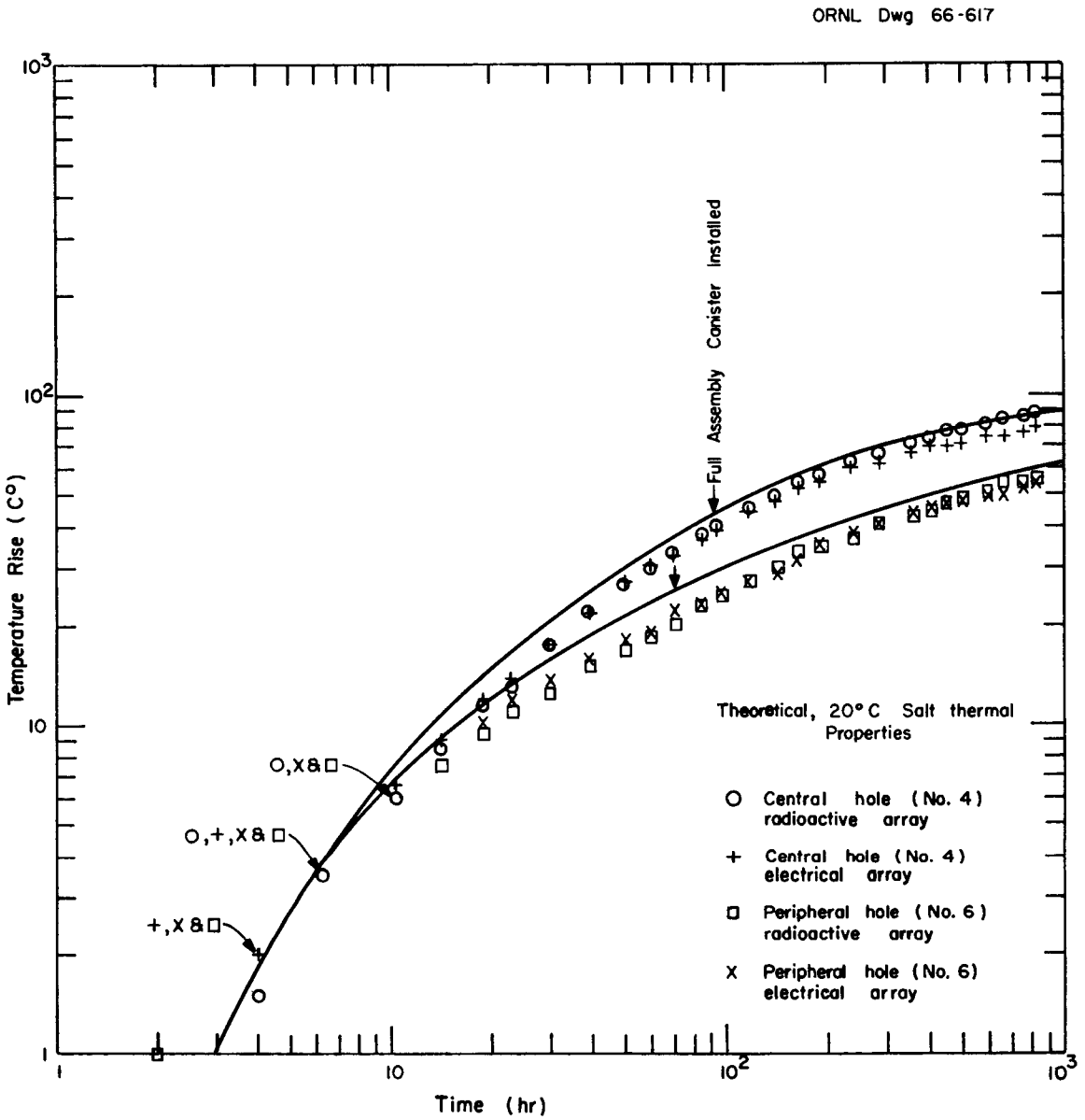

Fig. 6.3 Temperature Rises at 1-1/2 ft from Centers of Array Holes.

Rheological Measurements.--Figure 6.4 shows the floor-uplift profile along the north-south and east-west axes of room 1 (radioactive array) as of December 30, 1965, along with the time plot of the uplift in the center of the array. The results for room 4 are very nearly the same. As may be seen in Figure 6.4, the pillars (edges at 16-1/2 ft on the north-south plot) produce a restraining effect on the thermal expansion of the salt. As a consequence, the edges of the adjacent pillars are experiencing an increased stress (as if the overburden load had been increased), which has resulted in an increased transverse expansion rate in the pillars. In turn, this increased horizontal expansion has resulted in an increased thrust on the roof slab (about 2 ft thick), producing an accelerated rate of sag or separation from the formation above. The magnitudes of roof movement are small and do not constitute a hazard at the present time. As yet little or no temperature rise has occurred under (or in) the pillars themselves, and thus the increased pillar and roof movements are due only to transfer of thermal stress from the floor in the middle of the room.

To date, no significant differences in behavior between the two arrays have been observed, even though the peak salt dose had passed 10^7 rads by early December. In addition, no chlorine has been detected in the off-gas from the hole annulus.

6.3 Pillar-Model Studies

T. F. Lomenick

6.3.1 Effects of Shale Partings

Previous tests on scale-model specimens of rock-salt mine pillars have shown the effects of temperature, compressive loads, and time on cavity closure.[16] Lithologic changes in the salt column can also markedly affect the deformation of mine pillars. Even though some salt deposits, such as salt domes, are practically all salt, most bedded deposits contain lithologic discontinuities, or rock salt interbedded with layers of dolomite, shale, anhydrite, and other materials. For instance, the 300-ft-thick salt sequence at Lyons, Kansas, is only about

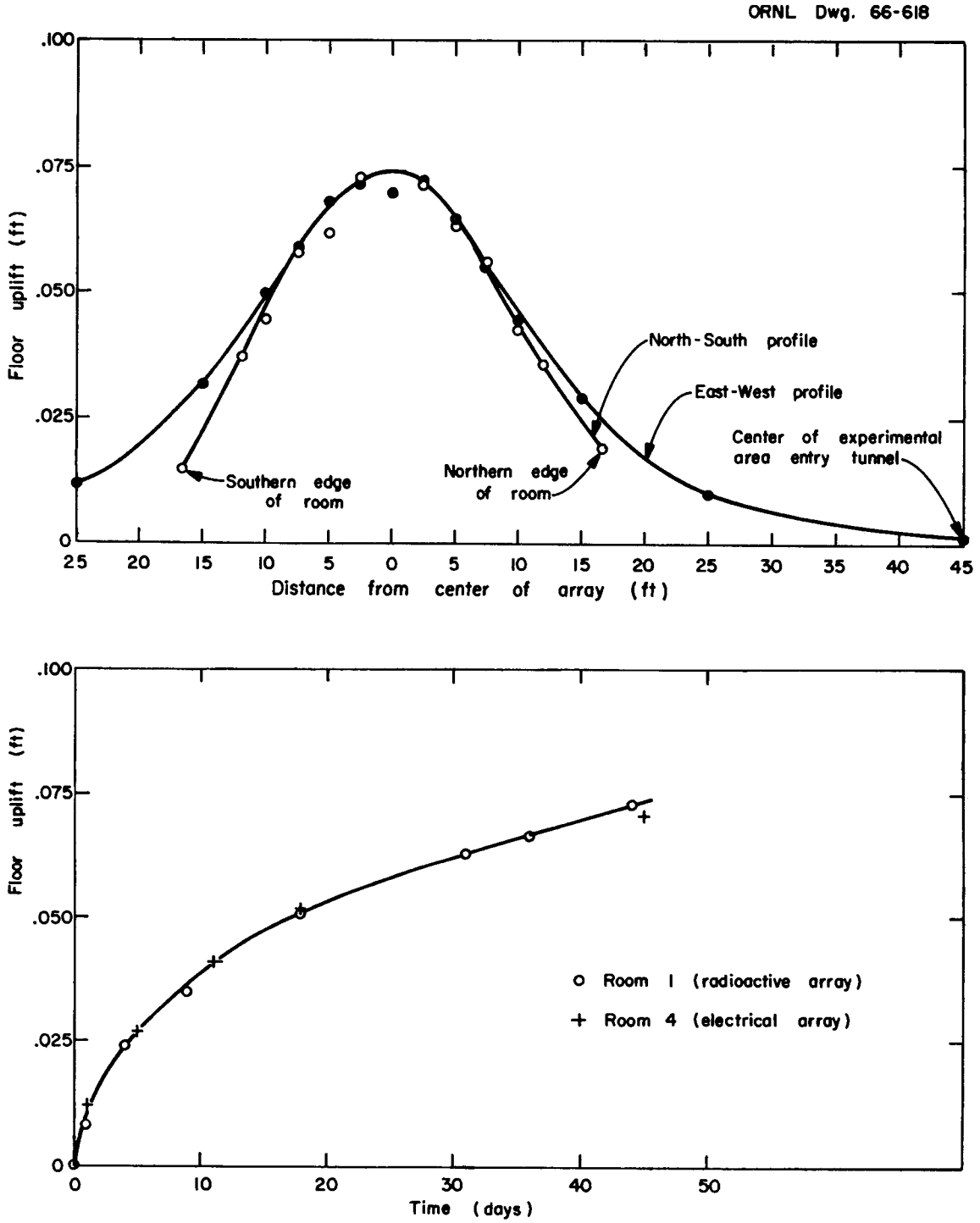

Fig. 6.4 Floor-Uplift Data.

60% NaCl with the other 40% being mostly shale and anhydrite.[17] In many cases these other materials may form a part of the roof, floor, or even the pillars in a mine and thus enter into the deformation of the openings. Shale layers (sometimes called "partings") are common in bedded salt deposits, and in many cases the salt is mined or falls to these layers since they form planes of weakness. The presence of these shale partings, even though they are quite thin, can have a significant effect on the rate of cavity deformation, depending on whether the shale is at the top and bottom of the pillar or in the center of it. This is shown in Fig. 6.5, where deformation curves are presented for model salt pillars that have been deformed (a) without any simulated shale partings, (b) with simulated shale partings at the top and bottom of a pillar, and (c) with a simulated shale parting in the center of the pillar. Thin sheets of Teflon lubricated with grease and graphite serve as friction reducers and thus simulate shale partings. (Analysis of data and observations from the Kansas mines indicates that the shale partings do have a lubricating effect, but it does not appear that they have so marked an effect as do the Teflon sheets. Therefore, the actual effects to be expected in a mine would lie somewhere between the two extremes shown in Fig. 6.5). For the model having no simulated shale partings, and for the model where the shale parting is in the center of the pillar, the deformational curves are almost identical, both showing about 0.03 in. or 3% deformation after 140 hr of testing. However, for the model with friction reducers at the top and bottom of the pillar, note that the deformation proceeds initially at a very fast rate before beginning to decrease with time. The model appears to then deform at a constant rate for a short time and then at an increasing rate that results in sudden failure after less than 130 hr. It is also of interest that for models with no simulated shale partings, sudden or catastrophic pillar failure could not be induced even under stresses as high as 14,000 psi.

The accelerated deformation rate of the models, when simulated shale partings occur at the top and bottom of the pillars, apparently results from the more or less independent deformation of the pillar from the roof and floor under these conditions. When there are no partings at

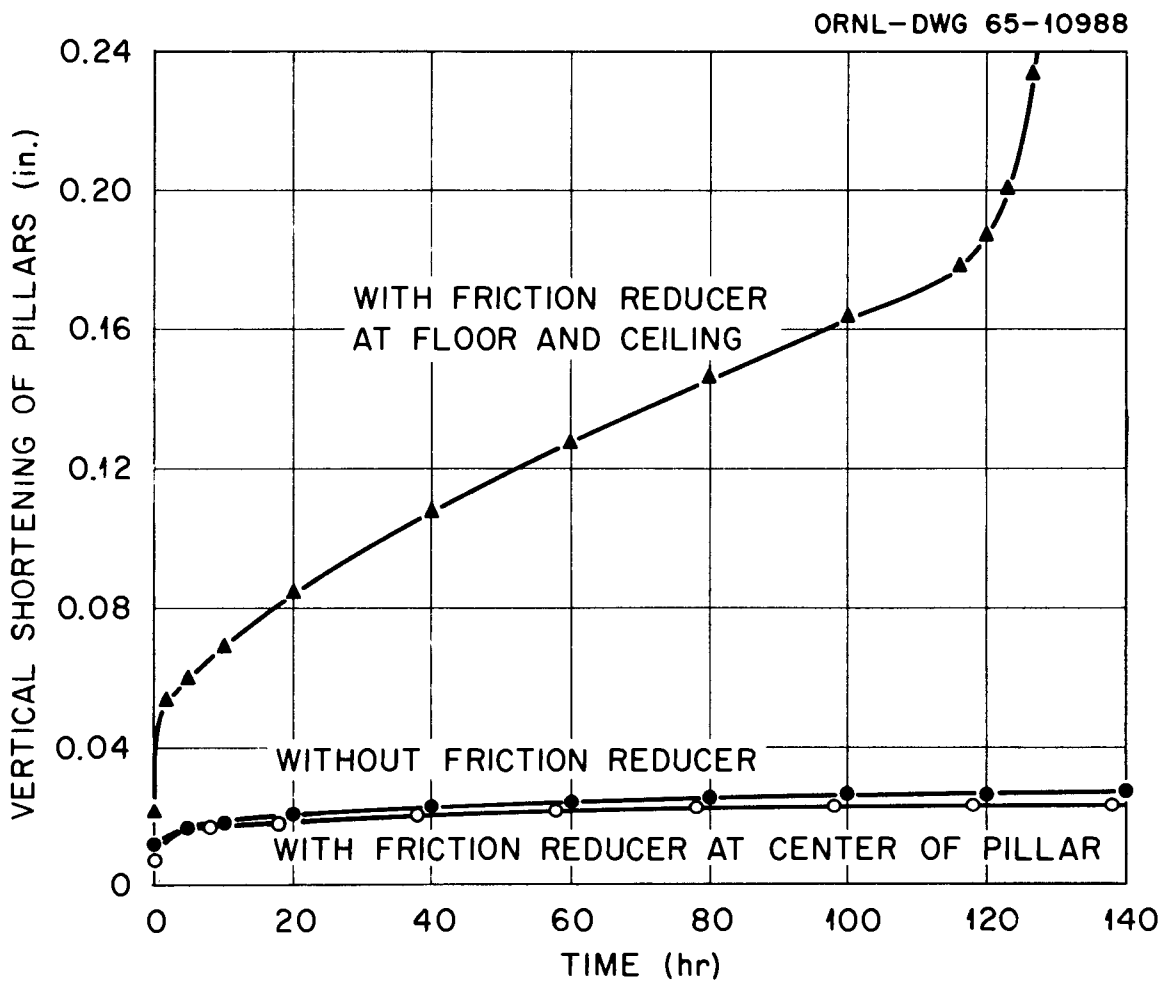

Fig. 6.5 Deformation of Model Rock-Salt Pillars at 4000 psi.

the top and bottom of the pillar, or even if the parting is in the center of the pillar, there is an interlocking effect of salt crystals from the pillar to the roof and floor which serves to allow the pillar, roof, and floor to deform more or less as a single unit. However, when partings exist between the pillar and the roof and floor, they serve as effective friction reducers, which consequently allow the pillar to deform more independently of the roof and floor, since horizontal confining pressures in the roof and floor are not transmitted into the pillar.

6.3.2 Deformational Behavior

Although the exact mechanisms of deformation within salt pillars are not fully understood at present, some generalizations as to movement have been formulated through observations of deformed specimens. Figure 6.6 shows cross-sectional views of two model pillars that have been cut vertically in half after deformation. Before deformation, the pillars were 4 in. in diameter and 1 in. high. In these specimens an attempt was made to define the principal movement through observing the relation of the pillar and the material above and below it after deformation. The dark horizontal lines seen in the salt specimens are 1/8-in.-diam holes that were bored horizontally through the top and bottom of the pillar and filled with colored salt before the specimens were deformed. In the model, deformed at 22.5°C, it is seen that the pillar is only slightly more than 4 in. in diameter. However, a considerable amount of loose salt from the outermost portion of the pillar had accumulated in the surrounding cavity opening but was subsequently removed. The cross-sectional view shows that the pillar did not deform independently of the roof and floor but that all three parts of the model entered into the closure of the cavity. Note especially how the roof and floor have flowed into the cavity opening. The most resistance to deformation in the models is believed to be found in the center portion of the pillar (due to confining pressure) and immediately above and below the pillar in the roof and floor. Thus, movement here is at a minimum. This is shown in the photograph by the greater distance between

PHOTO 81465

Fig. 6.6 Cross Sections of Model Pillars Deformed at 22.5 and 100°C.

the lines in the center portion of the pillar than at the edge of the pillar. Toward the outside of the pillar, there is less resistance to deformation; thus, salt from the pillars tends to move horizontally into the opening while material from above and below also moves in to fill the cavity.

In the model pillar, deformed at 100°C, the overall deformational pattern is similar to that for the sample tested at room temperature, but instead of the outermost portion of the pillar deforming through spalling, it stayed intact and deformed more plastically. The pillar diameter in this case increased from 4 in. to 4-1/2 in. as a result of the deformation.

In addition to these tests, model pillar tests have been performed on salt from mines at Hutchinson, Kansas; Retsof, New York; Detroit, Michigan; and Grand Saline, Texas. The Kansas salt is from a bedded deposit of Permian age, while the New York and Michigan salts are bedded and of Silurian age. The Grand Saline salt is a dome deposit. In general, there appear to be only slight differences in the deformational behavior of the salt from the mines at Lyons, Hutchinson, Detroit, and Grand Saline. For the Retsof salt, there is initially a much greater rate of deformation upon application of load at room temperature than for salt from the other places. However, after the initial deformation, the Retsof salt then deforms much slower. The reasons for these differences are not known at the present time.

7. SOIL STUDIES

7.1 Desorption of Cesium-137 from Clays and Soils

Tsuneo Tamura and O. H. Myers

The decrease with time in the amount of radiocesium leached when sodium acetate solution was used had been observed earlier with several reference clay minerals.[18] Since only NaOAc had been used and other possible factors had not been eliminated from consideration, it was decided to investigate this desorption more fully. The first factor

to be considered was the influence of anions other than acetate since it is known to cause expansion of the lattice of certain clay minerals.[19] Tests showed similar behavior of the radiocesium when NaCl solution was used, thus eliminating acetate as the cause. To test the influence of other cations, leaching was measured using the chloride salts of K, Ca, Mg, and Li. In these tests, only the A_p and B_2 horizons of the Captina soil were selected for study and for comparison with the reference clays. Figure 7.1 gives the results obtained for the A_p horizon. A decrease is noted with lithium, sodium, and possibly magnesium ions, but not with calcium or potassium ions.

When standard clay minerals were used in similar tests, NaOAc desorbed radiocesium continuously and more efficiently from the kaolinite and montmorillonite (Wyoming bentonite) samples. Muscovite, biotite, and illite behaved in general like the A_p and B_2 of the Captina. Figure 7.2 shows the response of illite obtained under the same conditions noted for the Captina A_p horizon, as shown in Fig. 7.1. Note the similarity in response; the maximum observed with NaCl in the A_p horizon was absent in the B_2, suggesting the influence of organic matter in the upper horizon. Compared with results of earlier tests, the maxima of desorption for these tests occurred at a shorter contact time for these two horizons.

The similarity in response between illite and the Captina samples shows that illite in soils plays an important role in the sorption of radiocesium. Even in the kaolinitic Fullerton soil, the response reported earlier suggests the presence of illite in the subsoil. X-ray diffraction diagrams confirm that illite (10.1 A) is indeed present in the Fullerton soil. The limited amount, however, reduces its influence in this soil. That illite in soil is an important mineral in cesium adsorption was noted early in Frederickson and his co-workers,[20] and also by Schulz _et al_.[21]

The data in Figs. 7.1 and 7.2 suggest that the order of desorption effectiveness is: K > Ca > Na > Li > Mg. Hence, if adsorption of radiocesium were to occur in the presence of these competitive ions,

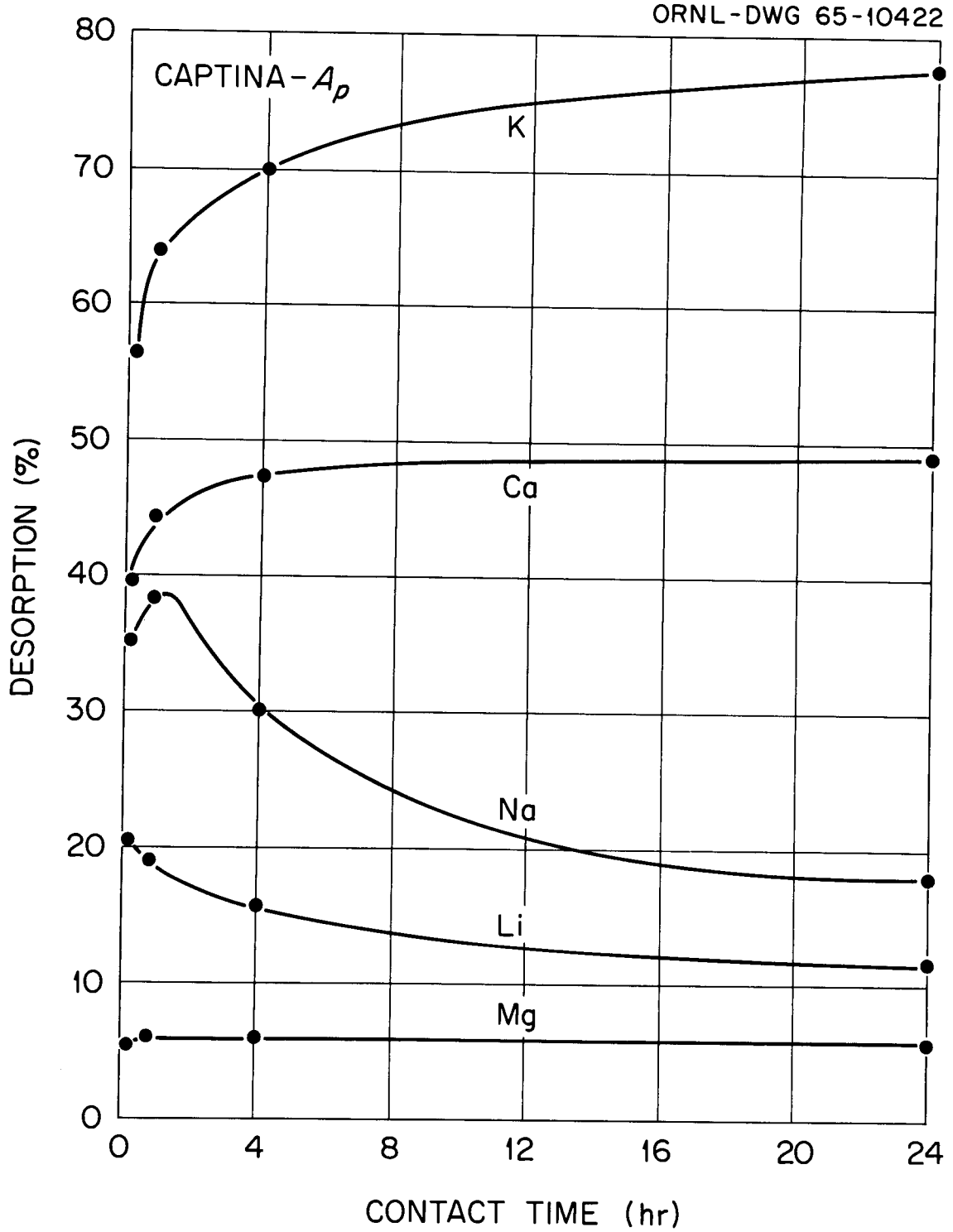

Fig. 7.1 Desorption of Carrier-Free Radiocesium from the A_p Horizon of the Captina Soil by Several Chloride Salts.

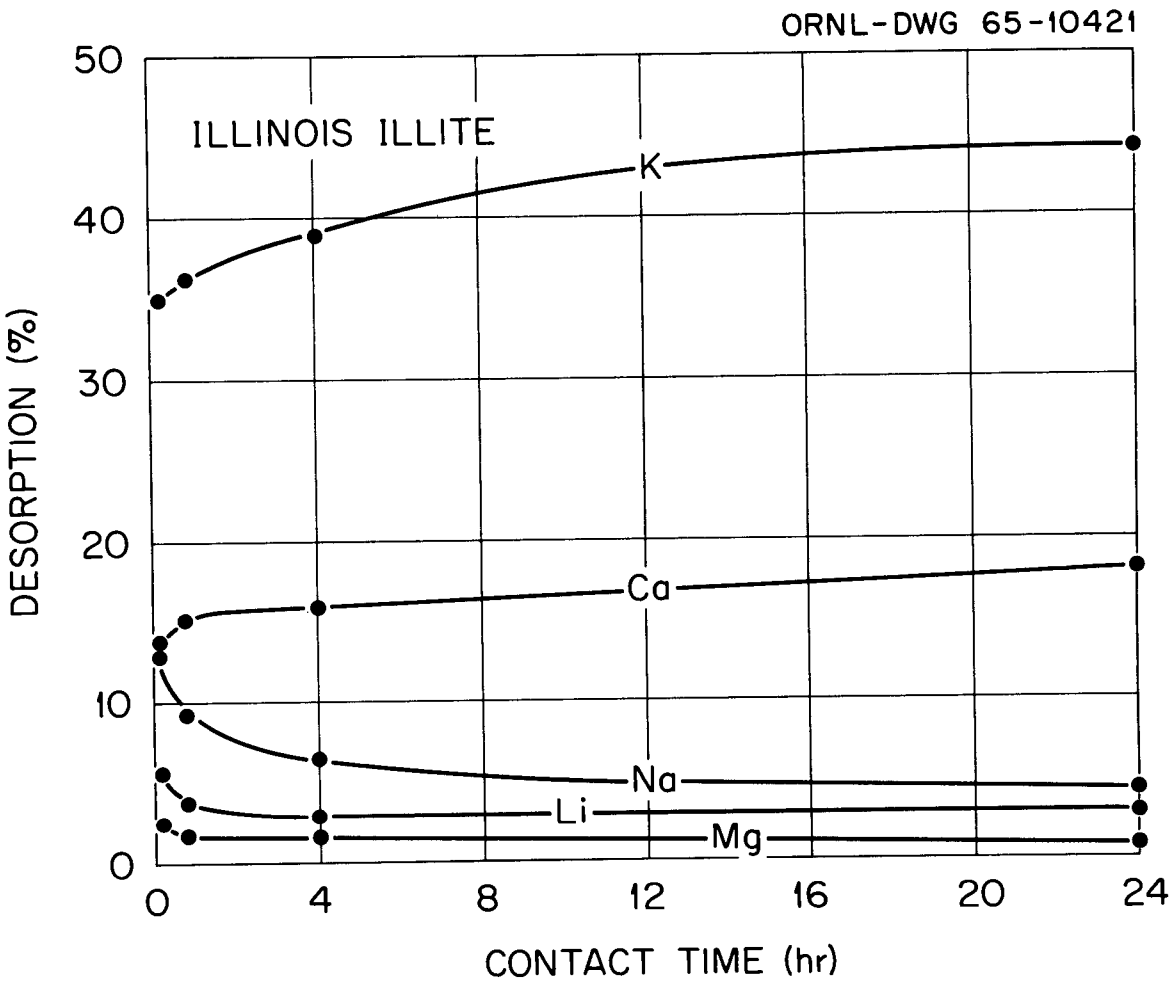

Fig. 7.2 Desorption of Carrier-Free Radiocesium from Illinois Illite by Several Chloride Salts.

more radiocesium, for example, should be adsorbed from a calcium solution than from an equivalent solution of potassium. Tests were made to corroborate this suggestion, and the results are shown in Table 13. The data show that the most effective competitor for radiocesium in tracer levels (2-6 x 10^{-5} mg per 0.1 g of clay) is potassium, followed by calcium, sodium, and magnesium. Hence, the same competitive order followed in desorption (Fig. 7.2) leads to the inference that the observed response is due to ion competition.

If the adsorption-desorption reactions are rapidly reversible, the data in Fig. 7.2 and Table 13 do not support each other. For potassium, one would have expected 96% of the radiocesium to be desorbed, according to the data in Table 13; instead 44% is desorbed (Fig. 7.2). Similarly, with calcium, 50% desorption is expected from the data in Table 13, but 18% is observed. This seeming anomaly may be explained by considering the nearly irreversible adsorption of radiocesium by minerals such as illite.

Table 13. Adsorption of Carrier-Free Radiocesium by Illinois Illite in 0.5 N Solutions of Selected Salts

Adsorption expressed in percent and as distribution coefficient, K_d; 50 cc of solution per 0.1 g of clay

Contact Time	KCl		$CaCl_2$		NaCl		$MgCl_2$	
	%	K_d	%	K_d	%	K_d	%	K_d
1	4.24	22	43.12	379	85.80	3020	98.17	26,820
24	3.40	18	49.11	482	91.12	5130	98.47	32,180
118	4.28	22	52.41	551	98.07	6720	98.78	40,480

The amount of radiocesium fixed irreversibly may be estimated from the response with potassium. From Fig. 7.2 it is seen that 44% is desorbed after 24 hr, leaving 56% on the clay. This 56% represents both irreversibly fixed cesium and cesium in equilibrium under 0.5 N KCl; the latter amounts to 1.5% based on the adsorption K_d for 24 hr, as

in Table 13; thus 54.5% of the cesium on the clay is fixed. Using this value as the amount of cesium not taking part in the desorption reaction with salts, one can calculate the expected desorption with the calcium, sodium, and magnesium salts. Thus, initially as much as 45.5% of the cesium could be desorbed (100% - 54.5% = 45.5%), of which nearly half (49%) would be resorbed in the 0.5 N calcium solution, as shown in Table 13. This should leave 23.2% in solution; the observed value is 18.5%. Similar calculations show that 4.5% and 0.7% of the cesium should remain in solution from the sodium and magnesium solutions after 24 hr, respectively. The observed values are 4.5% and 1.0%, as seen in Fig. 7.2 Hence, the difference in the observed desorption and adsorption of radiocesium is due to fixation in the mineral.

7.2 Movement of Cesium-137 by Runoff, Erosion, and Infiltration

A. S. Rogowski
E. R. Eastwood
Tsuneo Tamura
O. H. Myers

Rainfall for the 1964 to 1965 study period amounted to 53.1 in., and the annual erosion-index (EI) value was 329. The EI value is higher than the long-term average value for the area (210) and has the reoccurrence probability of about once every 15 to 20 years. On the basis of one year's data, the erodibility factor[a] for Captina soil was computed to be 0.40, and the appropriate cover factor[b] for the tall meadow plot was found to be 0.004. Other pertinent erosion parameters that were measured and obtained experimentally are given in Table 14. Large numbers of weeds with woody stems, along with heavy fertilization of plot 3, account for the large amount of plant material in 1965 on the vegetation-covered plots 2 and 3.

In Table 15 ^{137}Cs loss parameters are given. The distribution coefficient K_d for the A_p horizon of Captina soil was calculated to be 27,400 cc/g from field data and can be compared with the 30,000 cc/g value obtained in the laboratory. On the basis of ^{137}Cs concentration in the eroded solid and liquid runoff, the K_d values and the depth of penetration into the soil, the concentration in the soil, and the

[a]Erodibility factor = soil loss in tons per acre per unit of erosion index.

[b]Cover factor = (soil loss from vegetation-covered plot)/(soil loss from identical bare-soil plot).

Table 14. Erosion Parameters on Captina Soil for 1 Year of Experimentation

Parameter	Units	Plot 1, Bare Soil	Plot 2, Clipped Meadow	Plot 3, Tall Meadow
Slope	%	3.1	4.6	13.7
Slope length	m	2.2	2.0	2.0
Vegetation 1964	g/m^2	0	384	492
Vegetation 1965	g/m^2	0	2337	4611
Average runoff of water	%	53	39	19
Average infiltration	%	47	61	81
Soil loss[a]	g/m^2	2023	206	72

[a]To convert to tons per acre, multiply by 4.47×10^{-3}.

percentage contribution by the leach from vegetation and erosion were calculated. The fraction of ^{137}Cs fixed on the soil was taken as the difference between the percentage of radionuclide leached off the vegetation and estimated vegetation leach contribution to the runoff. Lower leach contribution and lower fixation on the soil of the clipped-meadow plot could be indicative of the physical impedance and retention of radiocesium by the overlying litter. The shallower estimated depth of penetration of the vegetation plots compared with a bare-soil plot could also reflect intermediate fixation in the litter material or in the topmost soil layer high in decaying organic matter.

In Table 16, the ^{137}Cs loss by erosion is given by season. It can be readily seen that highest loss occurred during the winter and spring months of 1964-65 on all plots, amounting to 77% for plot 1, 78% for plot 2, and very nearly 100% for plot 3. More than four-fifths and more than one-half of the cesium loss in the tall-meadow and clipped-meadow plots, respectively, were due to the five high-energy and -intensity rains that occurred during the winter and early spring seasons. The same five rains accounted for only one-third of ^{137}Cs loss on the bare soil plot. The equation, given previously, showing the relationship between soil loss and cesium loss was modified to read:

Table 15. Cesium-137 Loss Parameters on Captina Soil for 1 Year of Experimentation

Parameter	Units	Plot 1, Bare Soil	Plot 2, Clipped Meadow	Plot 3, Tall Meadow
Specific activity (eroded solids)	μc/g	0.14	0.86	0.86
Specific activity (runoff liquid)	$\mu c/cc \times 10^{-6}$	5.0	9.6	13.2
Depth of penetration[a]	cm	0.51	0.16	0.21
Concentration in soil	μc/g	0.12	0.39	0.29
Leach contribution to runoff[b]	%	--	55	66
Erosion contribution to runoff[c]	%	100	45	34
Fraction of leach fixed on soil[d]	%	--	89	95
Amount eroded	$\mu c/m^2$	277	177	62
Amount applied	$\mu c/m^2$	903	937	925
Percent eroded	%	30.7	18.9	6.7

[a]Estimated downward movement into the profile during the first year.

[b]Estimated percentage of ^{137}Cs carried away by runoff during the first year, that was leached from vegetation.

[c]Estimated percentage of ^{137}Cs lost that was actively eroded from the soil surface during the first year.

[d]Estimated percentage of ^{137}Cs leached from vegetation that was subsequently fixed on the soil during the first year of experimentation.

$$y = A(x/b)^m \qquad 0 < y < 100 \qquad x > 16 ,$$

where y is the cumulative percentage of cesium lost; x is the cumulative soil loss in g/m^2, and A has the values of 0.40, 0.69, and 0.37; and m has the values of 0.59, 0.62, and 0.68 for plots 1, 2, and 3, respectively. The correlation index, or R^2, values that are measures of fit of the equation were better than 90% for plot 1 and better than 98% for plots 2 and 3.

Table 16. Cesium-137 Loss by Erosion, Expressed as Percentage of that Applied for 1 Year of Experimentation[a]

Season	Plot 1, Bare Soil		Plot 2, Clipped Meadow		Plot 3, Tall Meadow	
	% of Applied	% of Eroded	% of Applied	% of Eroded	% of Applied	% of Eroded
Fall	4.0	13.1	4.1	21.6	0.01	0.1
Winter 1964-65	12.5	40.8	9.4	49.7	3.7	55.1
Spring 1965	11.1	36.3	5.4	28.5	3.0	44.7
Summer 1965	2.9	9.5	0.05	0.2	0.01	0.1
Fall 1965	0.1	0.3	0.00	0.0	0.00	0.0
Total loss	30.7	100	18.9	100	6.7	100

[a]Initially 903 $\mu c/m^2$ of ^{137}Cs was applied to plot 1, 937 $\mu c/m^2$ to plot 2, and 925 $\mu c/m^2$ to plot 3, on October 20, 1964.

In Table 17, loss of cesium by leaching of the vegetation is given. Following the spray application, all the ^{137}Cs was first found on the vegetation in the vegetation-covered plots. During the first month and after 6% of total rain, about 20% had leached off the vegetation; in 5 months and after 40% of total rain, about 75% had leached; and in 1 year, 95%. The slight increase noted in the litter of the clipped meadow after 153 days was probably due to sampling error. New 1965 vegetation contained less than 1×10^{-10} μc of radionuclide per gram, indicating that no significant uptake of cesium occurred during the 1965 growing season. Lack of uptake is probable due to the shallow penetration of the applied cesium into the profile, as shown in Table 15.

8. BEHAVIOR OF RADIONUCLIDES IN THE GROUND

D. G. Jacobs Y. E. Kim O. M. Sealand

8.1 Nonequilibrium Ion Exchange

A computer program was written to describe the transient behavior of radionuclides in the ground when the transporting solution is of a different concentration than the original ground water. The program

Table 17. Leaching Loss of ^{137}Cs from Vegetation for 1 Year of Experimentation

Time[a] (days)	Rain (in.)	Percentage Remaining on Vegetation[b]			
		Clipped Meadow		Tall Meadow	
		Plant	Litter	Plant	Litter
38	3.3	82.8	80.4	76.3	--[c]
71	7.8	30.1	25.3	46.7	--
153	20.2	23.9	28.4	25.8	--
356	53.1	0[d]	6.0[e]	0	5.3

[a]Time in days after October 20, 1964, date of application.

[b]Initially, all the applied ^{137}Cs was on the vegetation on the vegetation-covered plots. The concentration of ^{137}Cs was 2.95 μc/g of plant material on clipped-meadow plot, and 2.29 μc/g of plant material on tall-meadow plot.

[c]No litter present in 1964 vegetation.

[d]New 1965 vegetation contained less than 1×10^{-10} μc per gram of ^{137}Cs of plant material, indicating that no significant uptake of ^{137}Cs occurred during 1965 growing season.

[e]Values given for litter on both plots reflect the nonleached amounts of ^{137}Cs still on the 1964 vegetation.

is based on Gueckauf's model[22] for the passage of a wide band of solute through a chromatographic column, modified for changes in the adsorptive capacity due to changes in the total electrolyte concentration.

Figure 8.1 shows theoretical curves for a 1- x 1-1/2 x 12-in. core of Berea sandstone. The core is presaturated with 0.001 N $CaCL_2$ to represent ground water. Then radiostrontium is introduced in 0.05 N $CaCl_2$; the volume injected corresponds to 200%, 100%, etc. of the volume required to reach 50% breakthrough in a system containing only 0.05 N $CaCl_2$. Following the introduction of the tracer, leaching is done with 0.001 N $CaCl_2$ to correspond to the return of the original conditions.

Preliminary data show that the curves have the correct properties. The computer program is being modified to process the data and to fit the best curves, using K_d and the theoretical plate height as adjustable variables in the fitting process.

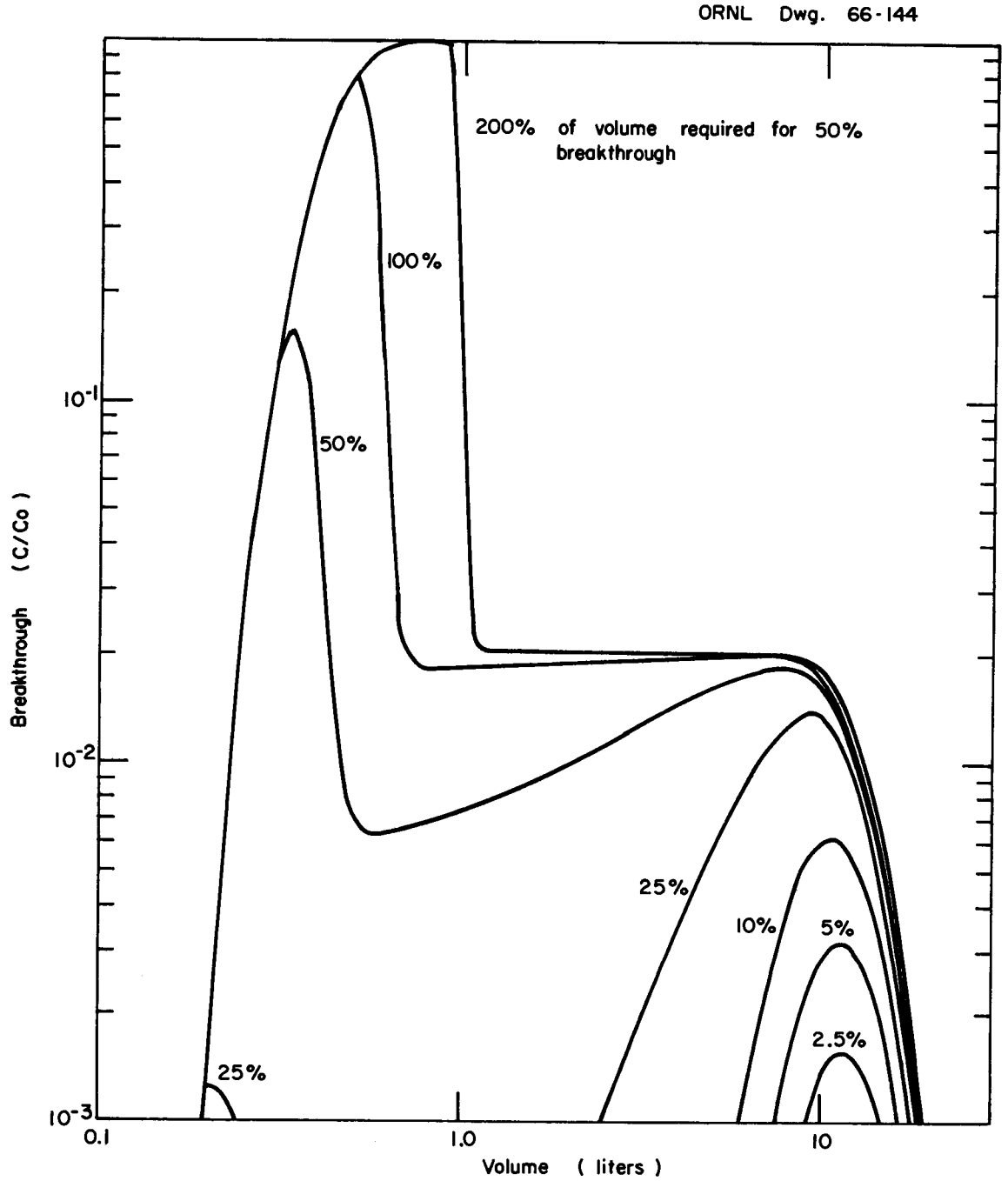

Fig. 8.1 Theoretical Curves for Passage of ^{85}Sr Through Berea Sandstone when Injected in 0.05 N $CaCl_2$ and Leached with 0.001 N $CaCl_2$.

8.2 Hydroxide Consumption by Conasauga Shale

In the vicinity of the intermediate waste trenches, small seeps have developed in which the pH of the seeping water has been gradually increasing. It was felt that the increase constituted a warning that only a small amount of the shale was being contacted by ground water moving from the trench to this seep and that a breakthrough of ^{90}Sr might be expected.

Samples of Conasauga shale were placed in solutions of different pH and allowed to stand overnight. The equilibrium pH was measured, and the consumption of hydroxyl ions was calculated. The results are shown in Fig. 8.2. The sorption of ^{85}Sr was also measured in each solution (Fig. 8.3). At pH 12 in 0.1 M Na, the K_d for ^{85}Sr is 143 ml/g and the K_d for hydroxyl ion is about 10 ml/g. This indicates that the strontium front leaving the waste trench would require about 14 times as long to reach the seep as did the hydroxyl-ion front. The severity of the problem will depend on the quantity of water carried through this seep.

9. DISPOSAL OF GASES INTO PERMEABLE FORMATIONS

D. G. Jacobs and O. M. Sealand

9.1 Estimation of the Behavior of Radionuclides Discharged to the Ground in a Gas

The fission product inventory was estimated for a reactor originally containing 5.82×10^{25} atoms of ^{235}U which had been operated for 1000 days at a neutron flux of 1.5×10^{13}. It was assumed that in an accident the fission products would be released as gases into a containment shell having a volume of 2.5×10^6 ft^3 (7.1×10^4 m^3). In the unrealistic case of complete fission product release as radioactive gases, the critical nuclide would be ^{90}Sr, and the critical organ would be bone. The initial concentration of radioactive contaminants in the containment shell would be about 2×10^{11} times the 40 hr/week occupational MPC_a (curve A, Fig. 9.1). Reduction in the level of hazard would correspond to decay of the ^{90}Sr.

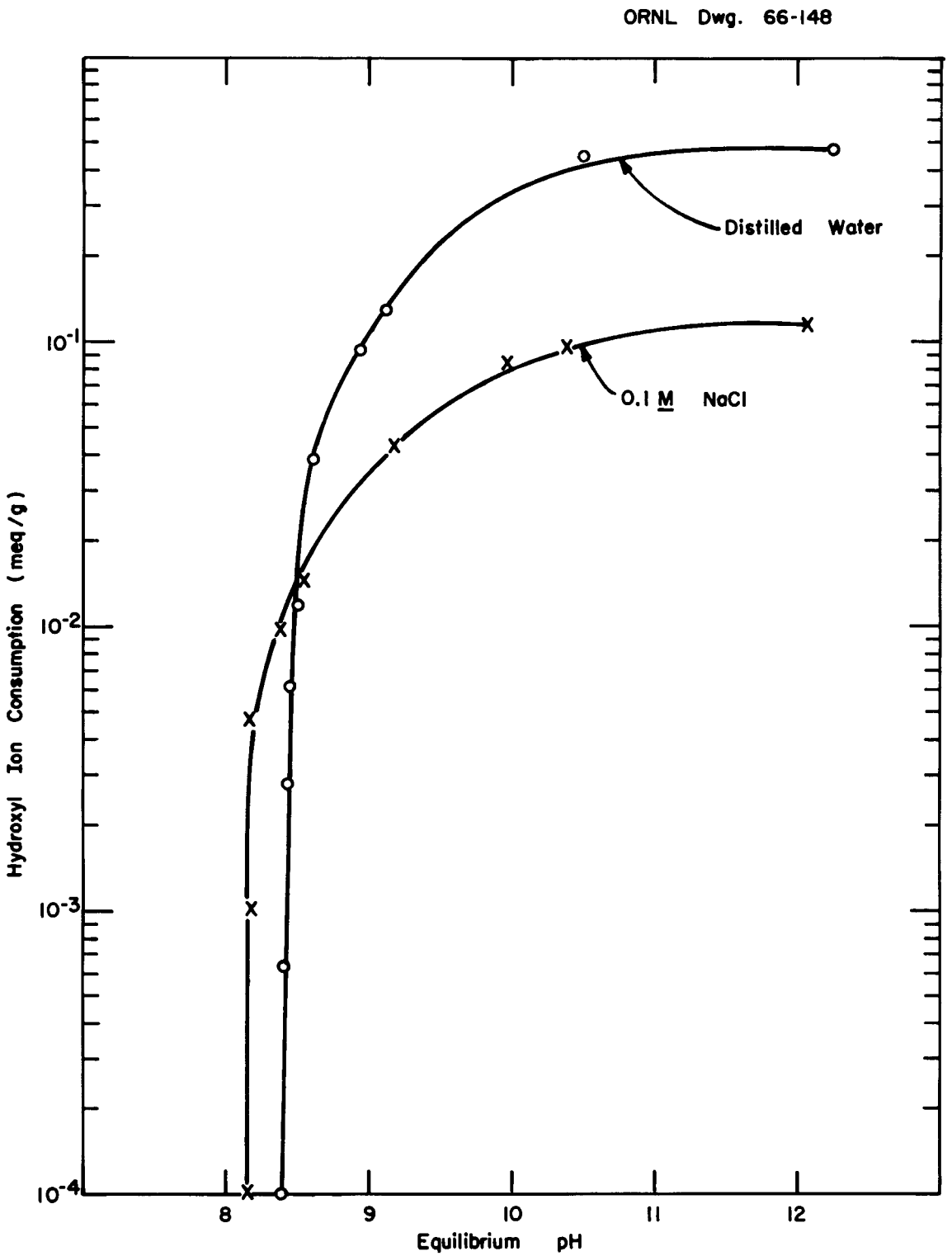

Fig. 8.2 Consumption of Hydroxyl Ions by Conasauga Shale.

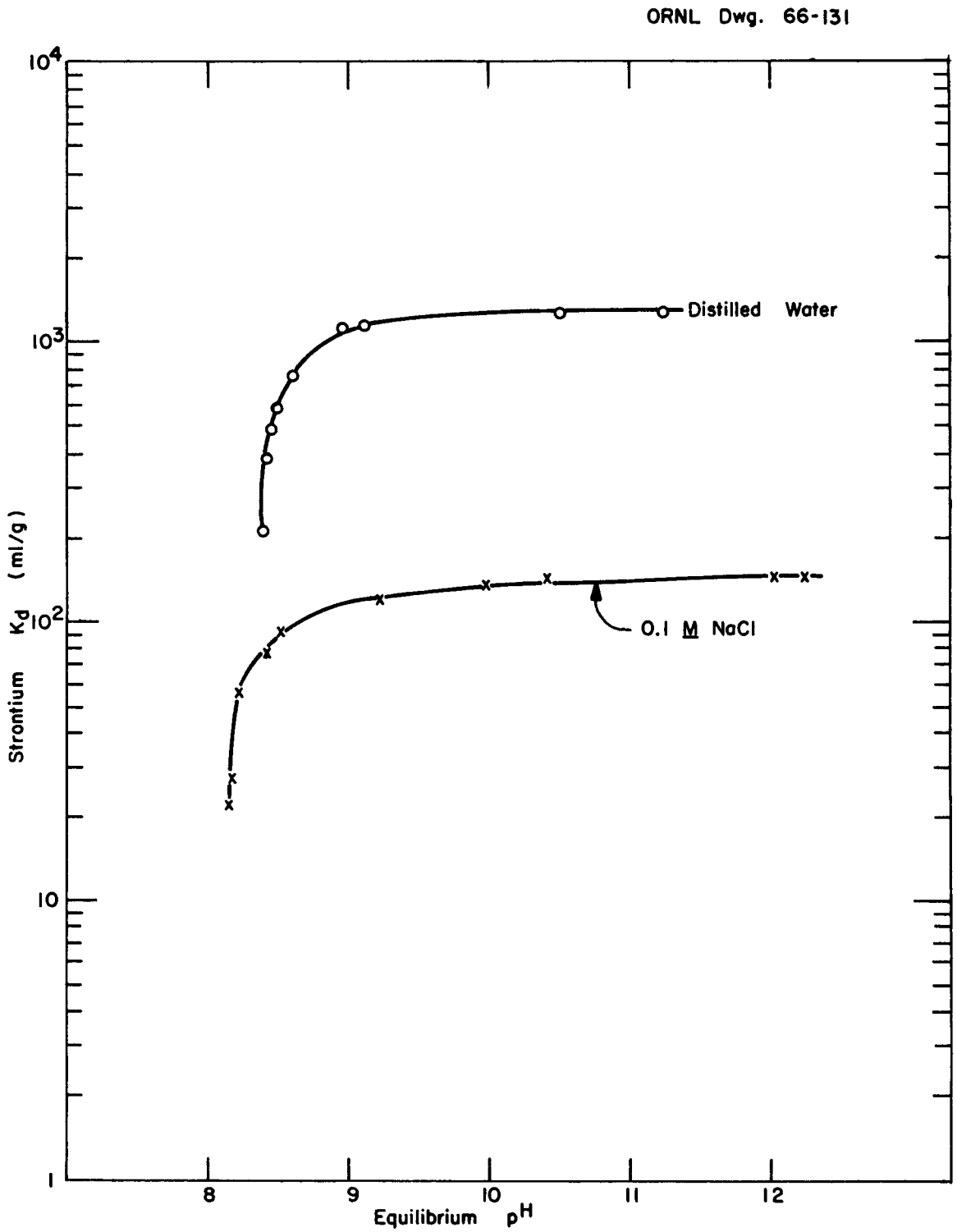

Fig. 8.3 Strontium Sorption by Conasauga Shale.

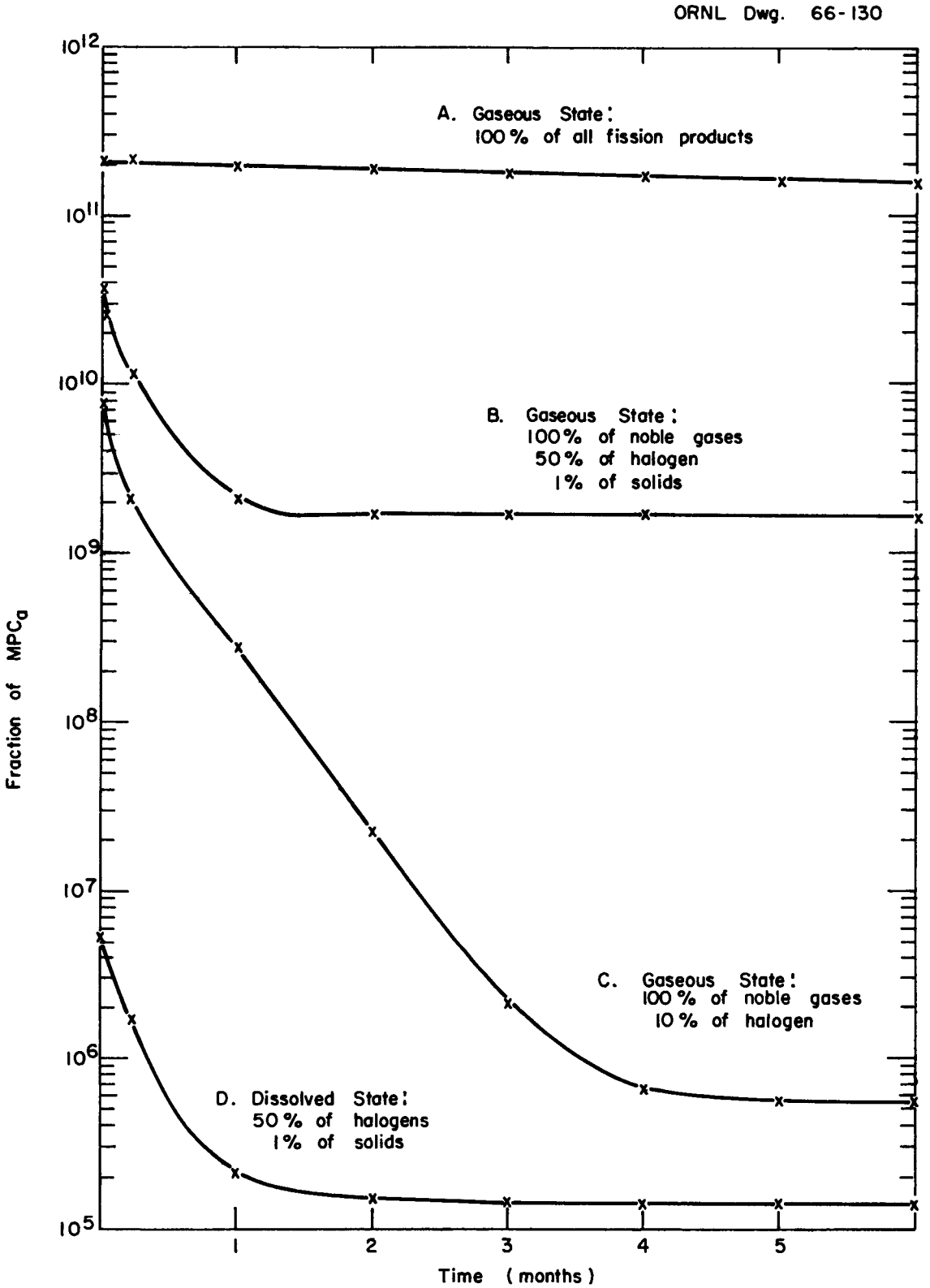

Fig. 9.1 Relative Hazard of Radionuclides Releases from a Reactor.

A more commonly accepted limit of release into the containment shell is: 100% of the noble gases, 50% of the halogens, 1% of the solids.[23] In this case, ^{131}I is the critical nuclide, and the thyroid is the critical organ for about the first month; thereafter ^{90}Sr is again the critical nuclide (curve B, Fig. 9.1). If the gases were pumped immediately from the containment shell into the ground, one would expect rather rapid condensation of the emitters that are normally solid. Part of the iodine would probably be in the form of methyl iodide and would remain gaseous. If we assume that 100% of the noble gases and 10% of the halogens remain in a gaseous state, ^{131}I is the critical element during the first four months. It decays leaving ^{85}Kr the limiting one thereafter (curve C, Fig. 9.1).

If a volume of ground water equal to the volume of the containment shell moves into the discharge zone and dissolves the released radionuclides, the hazard is even further reduced. This is due to two facts: A smaller volume of liquid is ingested than air is inhaled during a given time interval, and water is less mobile than air in a porous medium (by a factor of about 100). Most of the dissolved solid fission products could undergo ion exchange with the formation minerals and move at a much slower rate than the ground water.

For the purposes of calculations it was assumed that groundwater would flow at a rate of 1 ft/day and would be dispersed with a theoretical plate height of 50 ft. The delay factors due to ion exchange were assumed to be 100 ft strontium and most other elements, 200 for rare earths, 10,000 for cesium, and 10 for ruthenium. Table 18 lists the nuclides that would present the most serious contamination problems. The times given are the times required before radioactive decay plus dispersion and ion exchange in the formation reduces the concentration levels to permissible limits. The distance of migration is the maximum extent of longitudinal movement of a front at the permissible concentration before decay occurs. If the flow is radial, or if there is appreciable lateral dispersion, the extent of movement would be considerably reduced. Figure 9.2 shows the combined effects of ion exchange, dispersion, and radioactive decay on the lateral movement of ^{90}Sr by moving ground water.

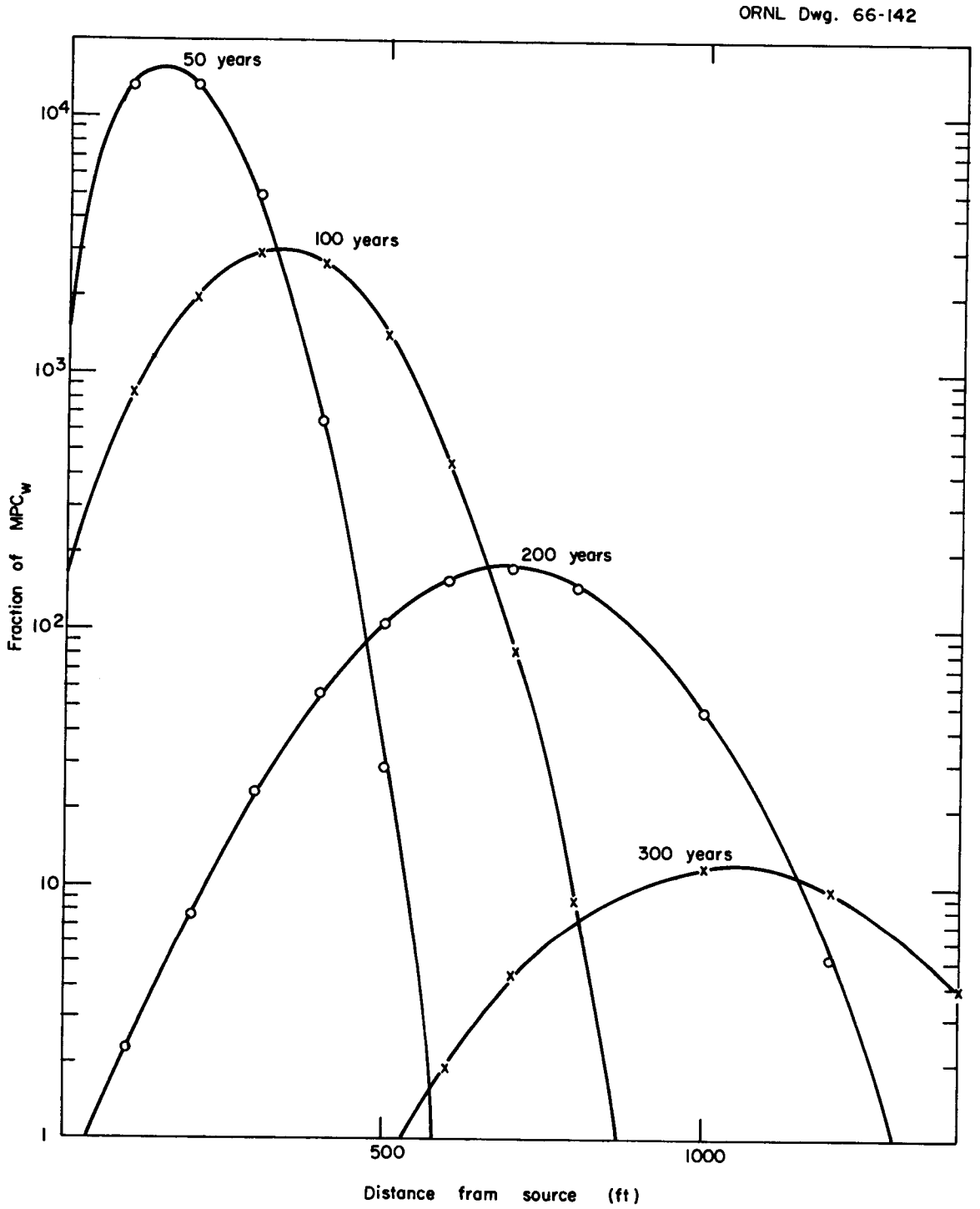

Fig. 9.2 The Lateral Movement of ^{90}Sr by Ground Water as Affected by Ion Exchange and Dispersion.

Table 18. Expected Extent of Movement of Fission Products in the Ground

Nuclide	Distance of Migration (ft)	Time Required for Decay and Dispersion to Permissible Levels (yr)
^{90}Sr	1600	380
^{90}Y	400	220
^{106}Ru	400	11
^{131}I	300	0.4
^{132}I	200	0.4

From the exercises we can conclude that the relative hazard due to release of airborne activity from a reactor incident could be markedly reduced by pumping the gases into the ground. The delay time afforded, especially for condensable radiation emitters, would greatly reduce the spread of contamination. Strontium would most likely present the most serious contamination of local ground water, if it were released to the extent of 1%, but its extent of movement would be about 1600 ft in an area where the groundwater moves at a mean velocity of 1 ft/day. The extent of vertical movement would be expected to be at least an order of magnitude lower, so no contamination of a second aquifer should occur.

9.2 Adsorption of Iodine by Minerals

A numerical error was found in the former calculations of the activation energy of desorption of iodine from Clinch River sediment. Subsequent calculations show that the corrected value for the activation energy for desorption ranges from 14.2 kcal/mole at a loading of 10^{-10} mole of I_2 per cm^2 to 54 kcal/mole at a loading of 10^{-11} mole of I_2 per cm^2. These values are consistent for a system containing condensed I_2 (energy of sublimation = 14.66 kcal/mole) plus some chemisorbed iodine on the mineral surfaces. Previously, it had been necessary

to postulate that some of the I_2 vapor had been converted to HI in order to account for the low values obtained for the activation energy.

A computer program is being written to determine the quantity of chemisorbed iodine and to refine the estimates of the energy required to desorb the two phases of iodine from the mineral surfaces.

It is difficult to compare the adsorption of iodine gas by different clays measured in individual nonflowing systems because the equilibrium concentration of iodine in the gas phase is likely to be different. An ordinary flow system also presents difficulties. Iodine was so readily adsorbed that nothing could be detected at the effluent end of a 1-1/2- x 12-in. core after several days of running. Therefore, an arrangement was devised whereby several clays could be tested in a single flow system. A 1-in.-thick glass column was used as the main reaction vessel (Fig. 9.3). The clay samples consisted of 1/8-in.-diam glass rods coated with a clay paste and then dried. Five samples could be placed on a rack that held the samples centered in the reaction vessel. At each end of the reaction vessel was placed a diffusion tube,[24] which consisted of 1 ft of silver-plated copper tubing, 1 ft of rubber hose, and 1 ft of charcoal-coated copper tubing. The diffusion tubes give a relative measure of the concentration of iodine at the two ends of the reaction vessel. The influent end was attached to a U-tube into which radioactive I_2 had been previously condensed. The effluent from the two diffusion tubes, the reaction vessel, and the U-tube could be regulated.

A run was made to test iodine sorption by Wyoming bentonite, illite, kaolinite, vermiculite, and Clinch River floodplain sediment at room temperature. The total input was 1140 μc. The recovery was 80% (Table 19). Based on the relative flow rates, one would have expected a total of 143 μc to have entered the first diffusion tube and 103 μc into the second. However, the concentration profile of iodine deposited in the diffusion tube indicated a loss of only about 2.5% of the amount entering each diffusion tube. The adsorption of iodine by the clays used in this run is seen to be closely related to their surface area (Table 20).

ORNL Dwg. 66-147

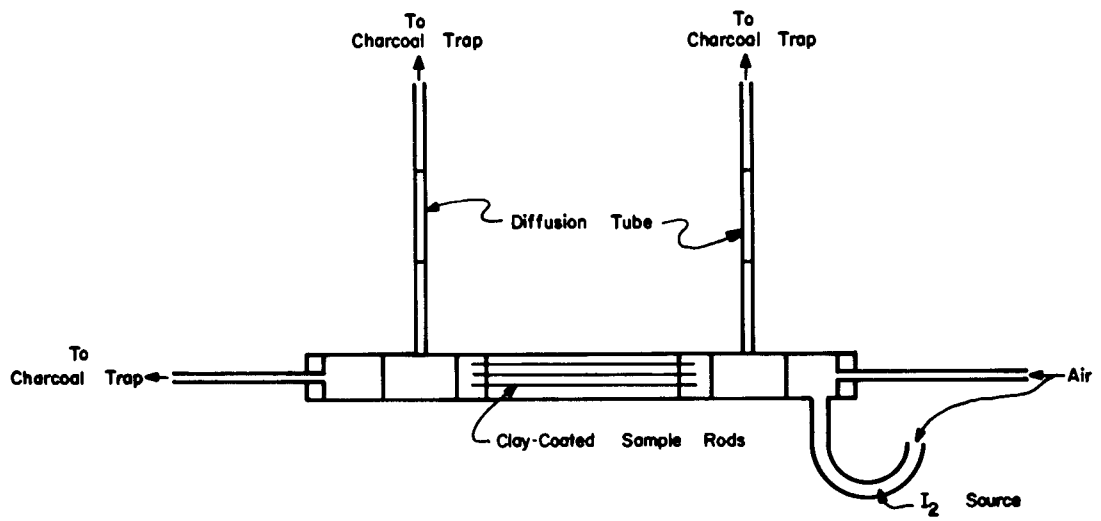

Fig. 9.3 Schematic of the System Used to Measure Iodine Sorption by Clays in a Flowing System.

Table 19. Mass Balance of Iodine in a Flowing Sorption Experiment

Total input	1140 μc
Amount in U-tube after the experiment	554
Total adsorbed by clays	150
Amount recovered in 1st diffusion tube	39
Amount recovered in 2nd diffusion tube	20
Total recovered	763 μc
Estimated Losses	
First diffusion tube	1 μc
Second diffusion tube	<1
Reaction vessel	150
Total accounted for	914 μc

Table 20. Sorption of Iodine by Clays in a Flow System

Clay	Iodine Adsorbed (μc/g)	Surface Area (m^2/g)	Iodine Adsorbed ($\mu c/m^2$)
Wyoming bentonite	34.4	64.2	0.54
Illite	31.9	58.4	0.55
Vermiculite	5.7	3.6	1.58
Kaolin	4.2	13.6	0.31
Clinch River flood-plain sediment	3.5	4.3	0.81

9.3 Nuclear Safety Pilot Plant Runs

A sorption pack containing two 115-g samples of Berea sandstone followed by three 18-g samples of charcoal was placed in the gaseous effluent line of Nuclear Safety Pilot Plant run 10. The activity levels of the released gas were too low to obtain satisfactory results, but the two samples of sandstone sorbed enough iodine to give 131 ± 31 and 88 ± 30 disintegrations of ^{131}I per minute, compared with 295 ± 44 for the first charcoal sample. No ^{85}Sr, ^{106}Ru, or ^{134}Cs was detected on any of the samples. On sandstone samples 1 and 2, 196 ± 90 and 102 ± 86 disintegrations of ^{144}Cs per minute were detected, but none was detected on the charcoal.

In run 11 the sorption pack contained, in order, Conasauga shale (62 g), Bo-4 Zonolite (28 g), exfoliated Zonolite (16 g), Berea sandstone (84 g), and two 18-g samples of charcoal. No ^{85}Sr, ^{134}Cs, or ^{106}Ru was detected on any of the samples. Iodine-131 and cerium-144 were sorbed as follows (Table 21):

Table 21. Sorption of Iodine and Cesium by Clays in NSPP Run 11

	^{131}I (dis/min) x 10^3	^{144}Ce (dis/min) x 10^3
Conasauga shale	540 ± 11	72 ± 9.8
BO-4 Zonolite	92 ± 2	12 ± 1.8
Exfoliated Zonolite	46 ± 1.1	4.1 ± 9.2
Berea sandstone	31 ± 0.7	4.4 ± 0.62
Charcoal	400 ± 5	34 ± 4.8
Charcoal	1.7 ± 0.15	0.32 ± 0.15

It has been suggested that the most important difference between run 10 and run 11 was a change in the furnace atmosphere from reducing conditions in run 10 to oxidizing conditions in run 11, causing HI release in run 10 and I_2 release in run 11.[25]

10. SAFETY EVALUATION

10.1 Clinch River Safety Studies

K. E. Cowser

Recent information on metabolic processes of children and adults permits a preliminary assessment of the importance of metabolic processes in estimating internal dose. In particular, Kulp and Rivera examined the effects of bone growth, rate of bone turnover, and the ratio of strontium to calcium in bone to that in diet on the retention of ^{90}Sr in the skeleton of man.[26,27] The difference equation for the model developed by Kulp (herein referred to as the age-dependent metabolic model) can be expressed as:

$$S_n = S_{n-1} - (f_n + \quad) S_{n-1} + K_n \frac{I_n C_n}{G_n} \left[f_n Ca_{n-1} + (Ca_n - Ca_{n-1}) \right],$$

where

S_n = pc ^{90}Sr skeleton burden at time n,

f_n = fractional bone turnover rate during the period from time n-1 to time n,

= ^{90}Sr radiological decay constant,

$K = \left(\frac{Sr}{Ca}\right)_{bone} \quad \left(\frac{Sr}{Ca}\right)_{diet}$,

I_n = fluid intake, liters/day,

C_n = ^{90}Sr concentration in water, pc/liter,

G_n = calcium intake, g/day,

Ca_n = calcium content of the skeleton, g.

The equation relates the loss and gain of ^{90}Sr during the period of interest, and is based on calcium metabolism. Calcium may enter and leave the skeleton each period. Bone turnover is defined as the quantity of calcium that enters and is excreted from the skeleton. The fractional

bone-turnover rate f is the bone-turnover rate divided by the quantity of calcium contained in the skeleton. Strontium-90 in the skeleton is lost as a result of bone turnover and radiological decay and is gained by bone remodeling and bone growth.

By recursive application of the difference equation, the skeleton burden can be determined. The dose rate is given by:

$$D_n = a \frac{S_n}{W_n} ,$$

where

D_n = dose rate, rems/yr,
W_n = mass of the skeleton at time n, kg,
a = a constant; for ^{90}Sr, 1.03×10^{-4} (rems/yr)/(pc/kg) .

These equations were coded for computer solution using intervals of one month during 0 to 2 years of age, three months during 2 to 24 years, and yearly intervals thereafter.[a]

Estimation of the dose received by the skeleton of males due to ingestion of Clinch River water were performed using the same values for fluid intake, and ^{90}Sr concentration in water and skeleton mass, that were previously employed with the adjusted ICRP model.[28] Values of daily calcium intake and calcium content of the body were taken from Albritton and Mitchell, respectively;[29,30] values of bone turnover rate and the observed ratio (K_n) were from Rivera.[2] Examples of the cumulative skeleton dose (1944 to 1963) to individuals of various ages are given in Table 22. For comparative purposes, the table also includes the skeleton dose calculated with the adjusted ICRP model. In all cases the age-dependent metabolic model yields a slightly larger estimate of total dose (an average of 15% for the individuals listed) than the adjusted ICRP model. Unquestionably, changes can be expected in the values of metabolic factors as new information becomes available.

---

[a]Calculations were performed by H. J. Fisher, U.S. Public Health Service, while working with the Internal Dose Estimation Section, Health Physics Division, ORNL.

Table 22. Dose (rems) Received by Skeleton of Males from Drinking Water

Cumulative dose from ingestion of Clinch River water for the period 1944 to 1963

Age at Start of Exposure	Age-Dependent Metabolic Model	Adjusted ICRP Model
0	2.2	1.7
5	2.4	2.3
9	3.1	2.6
14	3.3	2.9
19	3.3	2.8
25	2.9	2.6

11. REFERENCES

1. C. L. Fitzgerald, H. W. Godbee, M. H. Davis, and W. E. Clark, A Computer Code for Storing and Retrieving Data and Developing Improved Solids for Fixation of Highly Radioactive Wastes, ORNL-3824 (in press).

2. J. M. Holmes, R. E. Blanco, J. O. Blomeke, W. E. Clark, H. W. Godbee, C. W. Hancher, J. C. Suddath, and M. E. Whatley, Pot Calcination Process for Converting Highly Radioactive Wastes to Solids, "Symposium on Treatment and Storage of High-Level Radioactive Wastes," IAEA, Vienna, 1963, pp. 255-286.

3. H. W. Godbee and W. E. Clark, "Use of Phosphite and Hypophosphite to Fix Ruthenium from High-Activity Wastes in Solid Media," Ind. Eng. Chem. Product Research and Development 2, 157-62 (1963).

4. D. E. Ferguson, Chem. Technol. Div. Annl. Progr. Rept., May 31, 1965, ORNL-3830 (November 1965).

5. R. E. Blanco et al., Recent Developments in Treating Low and Intermediate-Level Radioactive Waste in the United States, TM-1289 (Dec. 1, 1965).

6. H. W. Godbee, E. J. Frederick, and N. S. S. Rajan, Incorporation of Intermediate-Level Radioactive Solutions and Slurries in Emulsified Asphalt, ORNL (in preparation).

7. J. H. Goode, Fixation of Intermediate Level Radioactive Waste in Asphalt: Hot-Cell Tests, TM-1343 (Nov. 18, 1965).

8. J. W. Gossett, Chemical Processing 28, 29 (October 1965).

9. D. E. Ferguson, Chem. Technol. Div. Annl. Progr. Rept., May 31, 1965, ORNL-3830 (November 1965).

10. R. E. Blanco et al., Recent Developments in Treating Low and Intermediate-Level Radioactive Waste in the United States, TM-1289 (Dec. 1, 1965).

11. F. L. Parker and R. E. Blanco, Waste Treatment and Disposal Semiannual Progress Report, July-December 1964, ORNL-TM-1081, pp. 104-12 (May 1965).

12. F. L. Parker and R. E. Blanco, Waste Treatment and Disposal Progress Report, May-October 1963, ORNL-TM-757, pp. 90-98 (April 1964).

13. M. G. D. Salamon, "Elastic Analysis of Displacements and Stresses Induced by the Mining of Sean or Reef Deposits," J. S. African Inst. Mining and Metallurgy 65 (4, 6, 10) (November 1963, Jan.-May 1964).

14. W. J. Boegly, Jr., Safety Analysis - Project Salt Vault, ORNL (in preparation).

15. P. N. Haubenreich, Review of Project Salt Vault - A Demonstration of the Disposal of High-Level Radioactive Solids in a Salt Mine, ORNL-CF 65-10-23 (Oct. 14, 1965).

16. F. L. Parker et al., Health Phys. Div. Annl. Progr. Rept. July 31, 1965, ORNL-3849, p. 16-18.

17. T. F. Lomenick, The Geology of a Portion of the Hutchinson Salt Member of the Wellington Formation in the Mine of the Carey Salt Company, Lyons, Kansas, ORNL-TM-597 (Sept. 3, 1963).

18. T. F. Lomenick and T. Tamura, Soil Sci. Soc. Amer. Proc. 29, 383-87 (1965).

19. K. Wada, Amer. Mineralogist 46, 79-85 (1961).

20. L. Frederickson et al., Proc. Second U.N. Intern. Cong. on Peaceful Uses of Atomic Energy 18, 449-70 (1958).

21. R. K. Schulz, R. Overstreet and I. Barshad, Soil Science 89, 16-27 (1960).

22. E. Gueckauf, Trans. Far. Society 60, 729 (1964).

23. J. J. Di Nunno, F. D. Anderson, R. E. Baker, and R. L. Waterfield, Calculation of Distance Factors for Power and Test Reactor Sites, TID-14844 (Mar. 23, 1962).

24. W. E. Browning, Jr., R. D. Ackley, and R. E. Adams, Nuclear Safety Program Semiannual Progress Report for Period Ending December 31, 1963, pp. 60-64, ORNL-3547 (1964).

25. Oak Ridge National Laboratory Status and Progress Report, October 1965, ORNL-3886, p. 18 (Nov. 4, 1965).

26. J. L. Kulp, "Radioactive Fallout from Nuclear Weapons Tests," Proc. of a Conf. held in Germantown, Md., November 15-17, 1961, TID-7632 p. 457 (1962).

27. J. Rivera and J. H. Harley, The HASL Bone Program 1961-1964, HASL-163, p. 7 (1965).

28. K. E. Cowser, "Clinch River Study: Hazards Analyses," in Waste Treatment and Disposal Progress Report for February-April 1963, ORNL-TM-603 (Dec. 16, 1963).

29. E. C. Albritton, Standard Values in Nutrition and Metabolism, W. B. Saunders Company, 1954.

30. H. H. Mitchel et al., "The Chemical Composition of the Adult Human Body and Its Bearing on the Biochemistry of Growth," J. Bio. Chem. 158, 625 (1945).

INTERNAL DISTRIBUTION

1. ORNL-Y-12 Technical Library Doc. Ref. Sec.
2-4. Central Research Library
5-14. Lab. Records
15. Lab. Records, ORNL-RC
16-17. R. E. Blanco
18. J. O. Blomeke
19. W. J. Boegly, Jr.
20. R. L. Bradshaw
21. J. C. Bresee
22. R. E. Brooksbank
23. F. N. Browder
24. K. B. Brown
25. P. H. Carrigan, Jr.
26. K. M. Chandra
27. W. E. Clark
28. K. E. Cowser
29. F. L. Culler
30. W. Davis, Jr.
31. W. de Laguna
32. F. M. Empson
33. D. E. Ferguson
34. E. J. Frederick
35. H. W. Godbee
36. H. E. Goeller
37. J. M. Googin
38. P. A. Haas
39. C. W. Hancher
40. C. E. Haynes
41. R. F. Hibbs
42. J. M. Holmes
43. D. G. Jacobs
44. W. H. Jordan
45. L. J. King
46. H. Kubota
47. T. F. Lomenick
48. H. G. MacPherson
49. W. C. McClain
50. K. Z. Morgan
51. R. J. Morton
52. E. L. Nicholson
53-54. F. L. Parker
55. J. J. Perona
56. R. M. Richardson
57. J. T. Roberts
58. M. J. Skinner
59-60. E. G. Struxness
61. J. C. Suddath
62. T. Tamura
63. J. W. Ullmann
64. M. E. Whatley

EXTERNAL DISTRIBUTION

65. E. L. Anderson, AEC, Wash.
66. W. G. Belter, AEC, Wash.
67. H. Bernard, AEC, Wash.
68. A. B. Joseph, AEC, Wash.
69. J. A. Lieberman, AEC, Wash.
70. W. H. Regan, AEC, Wash.
71. R. F. Reitemeier, AEC, Wash.
72. Vincent Schultz, AEC, Wash.
73. J. N. Wolfe, AEC, Wash.
74. H. M. Roth, AEC, ORO
75. C. S. Shoup, AEC, ORO
76. J. R. Horan, AEC, Idaho
77. K. K. Kennedy, AEC, Idaho
78. J. A. Buckham, PPC, Idaho Falls, Idaho
79. C. M. Slansky, PPC, Idaho Falls, Idaho
80. H. J. Carey, Jr., Carey Salt Co., Hutchinson, Kan.
81. C. W. Christenson, LASL
82. J. C. Frye, State Geological Sur. Div., Urbana, Ill.

83. W. B. Heroy, Sr., Geotechnical Corp., Dallas, Tex.
84. L. P. Hatch, BNL, Long Is., N.Y.
85. W. E. Winsche, BNL, Long Is., N.Y.
86. S. Lawroski, ANL
87. J. J. Weinstock, RAI, Long Is. City, N.Y.
88. E. W. Bloore, U.S. Army Nucl. Def. Lab., Edgewood Arsenal, Md.
89. D. B. Lombard, LRL
90. S. J. Reno, State Health Dept. Topeka, Kan.
91. Wes Lewis, NFS, West Valley, N.Y.
92. C. R. Cooley, BNWL, Richland, Wash.
93. E. R. Irish, BNWL, Richland, Wash.
94. A. M. Platt, BNWL, Richland, Wash.
95. G. Rey, BNWL, Richland, Wash.
96. G. J. Alkire, BNWL, Richland, Wash.
97. B. W. Mercer, BNWL, Richland, Wash.
98. L. F. Coleman, BNWL, Richland, Wash.
99. J. R. Eliason, BNWL, Richland, Wash.
100. L. H. Meyer, du Pont, SRL
101. R. M. Girdler, du Pont, SRL
102. Harvey Groh, du Pont, SRL
103. C. H. Ice, du Pont, SRL
104. C. M. Patterson, du Pont, SRL
105. W. B. Scott, du Pont, SRL
106. E. B. Sheldon, du Pont, SRL
107. D. S. Webster, du Pont, SRL
108. V. R. Thayer, du Pont, Wilmington, Dela.
109. R. L. Nace, USGS, Wash. D.C.
110. P. H. Jones, USGS, Wash. D.C.
111. C. P. Straub, USPHS, Cincinnati, Ohio
112. Dade Moeller, USPHS, Winchester, Mass.
113. W. J. Lacy, Of. of Civil Def., Wash. D.C.
114. J. E. Crawford, U.S. Bureau of Mines, Wash. D.C.
115. J. W. Watkins, U.S. Bureau of Mines, Wash. D.C.
116. H. Gladys Swope, U. of Wisc., Madison, Wisc.
117. P. A. Krenkel, Vanderbilt Univ., Nashville, Tenn.
118. E. F. Gloyna, Univ. of Texas, Austin, Texas
119. W. J. Kaufman, Univ. of Calif., Berkeley, Calif.
120. L. Silverman, Harvard Grad. Sch. of Public Health, Cambridge, Mass.
121. G. M. Fair, Harvard Univ., Cambridge, Mass.
122. H. A. Thomas, Jr., Harvard Univ., Cambridge, Mass.
123. John Geyer, Johns Hopkins Univ., Baltimore, Md.
124. W. A. Patrick, Johns Hopkins Univ., Baltimore, Md.
125. Abel Wolman, Johns Hopkins Univ., Baltimore, Md.
126. C. R. Naeser, George Washington Univ., Washington, D.C.
127. H. C. Thomas, U. of N.C., Chapel Hill, N.C.
128. H. H. Hess, Princeton Univ., Princeton, N.J.
129. W. H. Reas, GE, Vallecitos Lab., Calif.
130. Fred Herbert-Oettgen, Touramerica Div., The E. F. MacDonald Co., N.Y.
131. L. C. Watson, AECL, Chalk River, Can.
132. John Woolston, AECL, Chalk River, Can.
133. AECL, Chalk River, Can.; Attn: C. A. Mawson, I. L. Ophel

134. Librarian, AAEC, Res. Estb., Private Mail Bag, Sutherland, N.S.W., Australia; Attn: R. C. Cairns and L. Keher
135. AERE, Harwell, England; Attn: H. J. Dunster
136. AERE, Harwell, England; Attn: R. H. Burns, K. D. B. Johnson
137. AERE, Harwell, England; Attn: J. M. Fletcher
138. Peter Wace, AERE, Harwell, England.
139. Yehuda Feige, Min. of Def., AEC, Rehovoth, Israel
140. Jitender D. Sehgal, Bombay, India
141. Michio Ichikawa, Tokai-Refinery, At. Fuel Corp., Tokai-Mura, Ibraki-Ken, Japan
142. Atou Shimozato, Nucl. Reac. Des. Sect., Nucl. Power Plant Dept., Hitachi, Ltd., Hitachi Works, Hitachi-Shi, Ibaraki-Ken, Japan
143. Federico de Lora Soria, Grupo de Combustibles Irradiados, Junta de Energia Nucl., Div. de Mat., Ciudad Univ., Madrid-3, Spain
144. Baldomero Lopez Perez, Doctor en Quimica Ind., Centro de Energia Nucl., Juan Vigon, Ciudad Univ., Madrid-3, Spain
145. CEA, Saclay, France; Attn: A. Menoux, C. Gailledreau
146. CEA, Fontenay-aux-Roses, France; Attn: J. Sauteron
147. P. J. Regnaut, Centre d'Etudes Nucl., Fontenay-aux-Roses, France
148. C. J. Jouannaud, Plutonium Extraction Plant, Marcoule, France
149. Eurochemic, Mol, Belgium; Attn: R. Rometsch, T. J. Barendregt, F. Marcus
150-151. E. M. Shank, Eurochemic, Mol, Belgium
152. Centre d'Etude Nucleaire, Mol, Belgium; Attn: L. Baetsle
153. Centre d'Etude Nucleaire, Mol, Belgium; Attn: P. de Jonghe
154. Euratom, Casella Postale No. 1, Ispra, Italia; Attn: M. Lindner
155. F. Dumahel, Commissaire Boite Postale n° 149, Paris (15 eme), France
156. George Straimer, Rad. Protection Dept., Luisenstrasse 46, West Germany
157. Hubertus M. Holtzem, Rad. Protection Dept., 532 Bad Godesberg, W. Germany
158. Gerard M. K. Klinke, Const. Dept., Min. of Fed. Propert, Bad Godesberg, W. Germany
159. Helmut Krause, Decontamination Dept., Karlsruhe Nucl. Res. Center, 75 Karlsruhe, Siemensallee 83, W. Germany
160. Harold F. Ramdohr, Waste Storage Dept., Karlsruhe Nucl. Res. Center, Leopoldshafen/Bd. Max-Plandk-Str. 12, W. Germany
161. Hermann F. A. Borchert, Petrology, Mineralogy, and Economic Geology Dept., Mining Academy Clausthal, Siemensalle, W. Germany
162. Division of Research and Development, ORO
163-177. DTIE, AEC, OR